LEVEL II

②

AFWAL-TR-81-3051

SUPERPLASTIC ALUMINUM EVALUATION

Rockwell International Science Center
1049 Camino Dos Rios
Thousand Oaks, California 91360

June 1981

Final Report for Period 16 April 1979 – 31 December 1980

Approved for public release: distribution unlimited

FLIGHT DYNAMICS LABORATORY
AIR FORCE WRIGHT AERONAUTICAL LABORATORIES
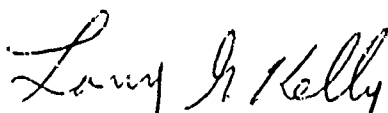AIR FORCE SYSTEMS COMMAND
WRIGHT-PATTERSON AIR FORCE BASE, OHIO 45433

NOTICE

When Government drawings, specifications, or other data are used for any purpose other than in connection with a definitely related Government procurement operation, the United States Government thereby incurs no responsibility nor any obligation whatsoever; and the fact that the government may have formulated, furnished, or in any way supplied the said drawings, specifications, or other data, is not to be regarded by implication or otherwise as in any manner licensing the holder or any other person or corporation, or conveying any rights or permission to manufacture use, or sell any patented invention that may in any way be related thereto.

This report has been reviewed by the Office of Public Affairs (ASD/PA) and is releaseable to the National Technical Information Service (NTIS). At NTIS, it will be available to the general public, including foreign nations.

This technical report has been reviewed and is approved for publication.

Larry G. Kelly, Chief
Structural Concepts Branch
Structures and Dynamics Division

FOR THE COMMANDER

Ralph L. Kuster, Jr., Colonel, USAF
Chief, Structures and Dynamics Division

"If your address has changed, if you wish to be removed from our mailing list, or if the addressee is no longer employed by your organization please notify AFWAL/FIBC , W-PAFB, OH 45433 to help us maintain a current mailing list".

Copies of this report should not be returned unless return is required by security considerations, contractual obligations, or notice on a specific document.

SECURITY CLASSIFICATION OF THIS PAGE *(When Data Entered)*

REPORT DOCUMENTATION PAGE	READ INSTRUCTIONS BEFORE COMPLETING FORM	
1. REPORT NUMBER AFWAL-TR-81-3051	2. GOVT ACCESSION NO. AD-A107760	3. RECIPIENT'S CATALOG NUMBER
4. TITLE *(and Subtitle)* Superplastic Aluminum Evaluation		5. TYPE OF REPORT & PERIOD COVERED Final Report 04/16/79 through 12/31/80
		6. PERFORMING ORG. REPORT NUMBER SC5214.34FR
7. AUTHOR(s) M.W. Mahoney C.W. Hamilton		8. CONTRACT OR GRANT NUMBER(s) F33615-79-C-3218
9. PERFORMING ORGANIZATION NAME AND ADDRESS Rockwell International Science Center 1049 Camino Dos Rios Thousand Oaks, CA 91360		10. PROGRAM ELEMENT, PROJECT, TASK AREA & WORK UNIT NUMBERS Prog Element 61101F,62201F Project 0100, 2401 Work Unit 24010339
11. CONTROLLING OFFICE NAME AND ADDRESS Flight Dynamics Laboratory (AFWAL/FIB) Air Force Wright Aeronautical Laboratories, AFSC Wright-Patterson AFB, OH 45433		12. REPORT DATE June 1981
		13. NUMBER OF PAGES 233
14. MONITORING AGENCY NAME & ADDRESS*(if different from Controlling Office)*		15. SECURITY CLASS. *(of this report)* Unclassified
		15a. DECLASSIFICATION/DOWNGRADING SCHEDULE

16. DISTRIBUTION STATEMENT *(of this Report)*

17. DISTRIBUTION STATEMENT *(of the abstract entered in Block 20, if different from Report)*

18. SUPPLEMENTARY NOTES

19. KEY WORDS *(Continue on reverse side if necessary and identify by block number)*

Superplasticity, Aluminum Alloys, Cavitation, Mechanical Properties, Forming Limits, Microstructure, Cost/Weight Advantages

20. ABSTRACT *(Continue on reverse side if necessary and identify by block number)*

With the development of a process to produce fine grain aluminum alloys, it is now possible to superplastically form (SPF) structural aircraft components. This document presents results from several important areas which are considered to be critical to providing a realistic assessment of the technical and economic potential for superplastic forming structures using a high strength 7475 aluminum alloy. Areas of study included (1) the evaluation of structural applications; (2) the determination of superplastic forming

DD FORM 1473 EDITION OF 1 NOV 65 IS OBSOLETE
1 JAN 73

SECURITY CLASSIFICATION OF THIS PAGE *(When Data Entered)*

limits; (3) a microstructural study of cavities formed during superplastic deformation; (4) the application of hydrostatic gas pressures to suppress cavitation, and (5) the effect of superplastic deformation on subsequent service properties.

Accession For		
NTIS GRA&I	X	
DTIC TAB	☐	
Unannounced	☐	
Justification		
By		
Distribution/		
Availability Codes		
Dist	Avail and/or Special	
A		

FOREWORD

This document presents final results determined under Air Force Contract No. F33615-79-C-3218, Project No. 2401, for a period of performance from 16 April 1979 through 31 December 1980. The program was conducted for the purpose of evaluating the potential for superplastic formed aerospace structures utilizing a commercial high-strength aluminum alloy, specially processed to develop a fine grain size. This program was administered under the technical direction of Mr. Larry Kelly of the Flight Dynamics Laboratory of AFWAL, Wright-Patterson Air Force Base, Ohio. The technical developments reported herein involved a team effort coordinated by the Rockwell International Science Center, and supported by the North American Aircraft Division of Rockwell International and the University of Delaware. The program manager was Dr. C.H. Hamilton and Principal Investigator was Mr. M.W. Mahoney.

The superplastic formability cavitation characteristics, and the use of hydrostatic pressure to suppress cavitation were conducted by a Science Center team including Dr. C.C. Bampton, Dr. A.K. Ghosh, and Dr. R. Raj in addition to the program manager and principal investigator. The structural design study was conducted by Mr. A.R. Del Mundo and Mr. F. McQuilkin of the North American Aircraft Division of Rockwell International. The influence of cavitation on service properties was conducted by Dr. C.C. Bampton (who at the time was post-doctoral appointee at University of Delaware) and under direction of Dr. J.W. Edington of the University of Delaware.

TABLE OF CONTENTS

TABLE OF CONTENTS

TABLE OF CONTENTS

LIST OF ILLUSTRATIONS

SECTION 2 EVALUATION OF STRUCTURAL APPLICATIONS OF SUPERPLASTIC FORMED HIGH STRENGTH ALUMINUM

SECTION 3 FORMING LIMITS FOR SUPERPLASTIC FORMED FINE GRAIN 7475 Al

LIST OF ILLUSTRATIONS

LIST OF ILLUSTRATIONS

SECTION 4   A MICROSTRUCTURAL STUDY OF CAVITIES FORMED DURING SUPERPLASTIC
DEFORMATION OF FINE GRAINED 7475 Al

LIST OF ILLUSTRATIONS

LIST OF ILLUSTRATIONS

SECTION 5 SUPPRESSION OF CAVITATION BY THE APPLICATION OF CONFINING
GAS PRESSURE DURING SUPERPLASTIC DEFORMATION OF FINE GRAINED 7475 Al

SECTION 6   THE EFFECTS OF SUPERPLASTIC DEFORMATION ON SUBSEQUENT
SERVICE PROPERTIES OF 7475 Al

LIST OF ILLUSTRATIONS

LIST OF TABLES

SUMMARY

The program reported herein was conducted (1) to determine if superplastic forming of high strength aluminum would offer potential benefits in structural applications for aerospace systems, and (2) to establish forming limits based on the development of cavitation during superplastic forming and its effect on subsequent mechanical properties. The latter characteristic was considered to be a primary obstacle facing the use of superplastic formed aluminum, and therefore the consideration of the potential for this new technology would necessarily include an assessment of cavitation.

For the design study, components selected for evaluation had mature production cost histories and well defined design requirements. Two such structural components were considered from the T-39 Saberliner aircraft which met these criteria. One of these, the nose fuselage frame, was found to offer potential cost savings of 36% and weight savings of 22% if superplastically formed.

The study addressing cavitation development during superplastic forming was conducted with the objective of establishing a "forming limit" approach to limit cavitation in formed structures. However, during the course of the program, a technique was conceived for suppressing cavitation entirely through the use of a low level of hydrostatic pressure easily developed by use of a back pressure during the forming process. The program was then extended to establish suitable forming parameters for this technique.

This report has been prepared as a series of independent reports presenting the respective developments of this program. A more detailed discussion summarizing each of these studies is presented below.

SECTION 2 EVALUATION OF STRUCTURAL APPLICATIONS OF SUPERPLASTIC HIGH STRENGTH ALUMINUM

A design trade study has been conducted to determine the feasibility of utilizing the superplastic forming (SPF) capability of aluminum alloys to produce unique, cost effective and efficient aircraft structures. Based on a preliminary evaluation of the potential payoff of SPF aluminum on both wing and fuselage components, the T-39 fuselage frame at Station 13 was selected for detailed design and analysis. Results of the study showed that a 22 percent weight savings and 36 percent cost savings would be realized by fabricating the bulkhead using SPF procedures rather than conventional assembly procedures.

SECTION 3 FORMING LIMITS FOR SUPERPLASTIC FORMED FINE GRAIN 7475 Al

A concept was pursued in this study to establish the limits of superplastic forming in terms of strain state based on the onset and/or development of cavitation, and for which design properties could be identified. The approach used was to establish the influence of strain state (uniaxial, plane strain, and balanced biaxial) on the inception and growth characteristics of cavitation, and correlate the extent of cavitation with

xx

tensile and fatigue properties. Based on these data, it was then possible to establish strain states for which little or no loss in properties are observed, and thereby define forming limits for superplastic forming this material. These results coupled with checks against strains developed in actual parts as well as predicted analytically, show that a wide range of structural parts can be superplastically formed within the constraints of the recommended forming limits.

SECTION 4 A MICROSTRUCTURAL STUDY OF CAVITIES FORMED DURING SUPERPLASTIC DEFORMATION OF FINE GRAINED 7475 Al

The observations suggest that, with the optimum superplastic deformation conditions, cavity nucleation, rather than cavity growth, is generally the rate determining step in the overall development of cavitation with strain. Cavities do not generally form at even the largest of the common single phase inclusion particles unless forming conditions are such as to significantly increase the flow stress. It appears that, as well as local stress concentrations, additional effects are required, such as temperature induced particle decohesion and internal gas evolution, in order that cavities may grow to stable sizes. Such conditions may exist at certain two phase inclusion particles in the 7475 Al alloy. Suitable modifications to the standard alloy processing may therefore be devised which result in even lower rates of cavitation at the optimum superplastic forming conditions.

SECTION 5   SUPPRESSION OF CAVITATION BY THE APPLICATION OF CONFINING GAS
PRESSURE DURING SUPERPLASTIC DEFORMATION OF FINE GRAINED 7475 Al

It has been shown that the application of hydrostatic gas pressures

during superplastic deformation of fine grained 7475 Al can entirely prevent

the intergranular cavitation normally encountered at atmospheric pressure. A

critical ratio of confining pressure to flow stress may be defined for each

superplastic forming condition above which virtually no cavitation occurs. In

low strain rate superplastic deformation conditions, where intergranular

cavitation plays a significant part in final tensile rupture, the superplastic

ductility may be improved by the application of confining pressures.

Similarly, the detrimental effects of large superplastic strains on service

properties may be reduced or eliminated by the application of suitable

confining pressures during the superplastic forming. In this case the

superplastically formed material may have the same design allowables as

conventional 7475 Al sheet.

SECTION 6   THE EFFECTS OF SUPERPLASTIC DEFORMATION ON SUBSEQUENT SERVICE
PROPERTIES OF 7475 Al

A preliminary investigation has been carried out to quantify the

effects of superplastic deformation on the major ambient temperature service

properties. It is shown that the properties most degraded, by the development

of cavitation after large superplastic strains, are those that depend on the

tensile overload stress (fracture stress). This affects, to varying extents,

xxii

ductility, tensile strength, fatigue life and stress corrosion life. The effects are not, however, generally significant below superplastic effective strains of about 0.8 to 0.9 (120-150% elongation) with the optimum forming conditions (T = 516°C, $\dot{\varepsilon}$ = 2 × 10^{-4} s^{-1}). Furthermore, since the fine grain processing has an initial beneficial effect on the ductility related properties compared to conventionally processed sheet, most superplastically formed components would suffer very little, if any, design penalties.

SECTION 1

INTRODUCTION

The benefits offered by the unique forming capability of a
superplastic metal have become increasingly clear as a result of numerous
programs involving titanium alloys. With titanium, it has been demonstrated
that significant cost and weight savings are possible where designs are
modified to utilize superplastic forming. It has been believed that similar
benefits should be possible with aluminum structures, but the unavailability
of a superplastic aluminum alloy suitable for structural application has
previously deterred serious studies of this benefit. Recently, a thermo-
mechanical process has been developed which produces a fine grain size and
resulting superplasticity in high strength aluminum alloys, and therefore now
permits an assessment of the potential for superplastic forming of aluminum
structures. A detailed evaluation of the superplastic properties of fine
grained 7475 Al alloy was conducted under contract with the U.S. Army Armament
Research and Development Command (ARRADCOM, Contract No. DAAK10-78-C-0424,
final report No. ARSCD-CR-8001), and provided the necessary foundation for
subsequent development in terms of design studies and evaluation of important
forming characteristics and service properties of the material. This program
was therefore initiated to address these issues.

In the course of the previously mentioned program conducted under
ARRADCOM sponsorship, it was found that fine grained aluminum alloys develop
voids, or cavities during superplastic deformation. While such cavitation was

1

apparently developing at high strain levels, it was considered that they may influence mechanical properties, and could therefore be a major obstacle to the full exploitation of this technology.

This program was conceived to address cavitation as a major issue, and a detailed study was conducted to characterize the development of the cavitation and its influence on material properties. The initial effort was directed toward establishing a "forming limit" based on the development of cavitation and suitable for fabrication of structural components. However, during the course of the program, a technique for suppressing cavitation was conceived which involved the use of a "back-pressure" to induce a hydrostatic compressive stress within the material. The program was then modified to permit development of a more thorough understanding of this method and to establish suitable forming parameters utilizing this technique.

The program reported herein addresses several key issues important to the successful exploitation of superplastic forming of aluminum; and for the purpose of clarity and completness, each of these studies is presented as an independent report but contained under this cover.

These studies are presented in Sections 2-6 and are as follows:

2.0 Evaluation of Structural Applications of Superplastic Formed High Strength Aluminum.

3.0 Forming Limits for Superplastic Formed Fine Grain 7475 Al.

4.0 A Microstructural Study of Cavities Formed During Superplastic Deformation of Fine Grained 7475 Al.

5.0 Suppression of Cavitation by the Application of Confining Gas Pressure During Superplastic Deformation of Fine Grained 7475 Al.

6.0 The Effects of Superplastic Deformation on Subsequent Service Properties of 7475 Al.

SECTION 2 EVALUATION OF STRUCTURAL APPLICATIONS OF SUPERPLASTIC FORMED HIGH STRENGTH ALUMINUM

A. R. Del Mundo and F. McQuilkin

Rockwell International

North American Aviation Division

Los Angeles, CA   90009

FOREWORD

The North American Aircraft Division (NAAD) of Rockwell International conducted a program to directly compare the applicability of superplastic forming of a high strength aluminum alloy on existing T-39/Sabreliner parts as a baseline.

The performance period for this program was from 28 May 1979 through January 1980. This program was sponsored by the Science Center of Rockwell International, Thousand Oaks, California under Air Force Contract No. F33615-79-C-3218, Project No. 2401.

SUMMARY

Rockwell International Corporation has conducted a trade study to determine the feasibility of utilizing the superplastic formability of a 7000 Series aluminum alloy to produce unique, cost effective and efficient structures.

Based on a preliminary evaluation of the potential payoff of using superplastic forming (SPF) for both wing and fuselage components, the fuselage frame at Station 13 of the T-39 Sabreliner was selected for detailed design and analysis.

Results of the study showed that a 22 percent weight savings and a 36 percent cost savings could be realized by replacing the conventionally formed frame with a frame fabricated using SPF procedures. A summary of this result is shown in Figure 1.

To verify the results of this study, it was recommended that a full-scale, limited production run of the Station 13 frames be fabricated and tested.

- BUILT UP ALUMINUM ASSEMBLY
  18 DETAIL PARTS

- 22 % WEIGHT SAVINGS
- 36 % COST SAVINGS

- SPF ALUMINUM ASSEMBLY
  5 DETAIL PARTS

Fig. 1   Comparison of the existing riveted, sheet metal frame and the proposed design of a replacement superplastically formed frame.

2.1 INTRODUCTION

2.1.1 Background

The field of aerospace technology is continually being pressured to develop innovative design concepts and fabrication techniques to produce more economical systems. Since aircraft structures represent a large fraction of cost and weight of the aircraft, major developments are being centered in this area. One of these techniques has been the superplastic forming (SPF) first developed by Rockwell International (NAAD). Until very recently this process was not possible with aluminum alloys because the alloy as presently manufactured did not possess superplastic properties. However, with the development of thermomechanical procedures that produce a fine grain structure in structural aluminum alloys, it is now possible to superplastically form aluminum aircraft components.

2.1.2 Objective

The objective of this program was to determine if the superplastic forming of high strength aluminum alloys would result in unique, cost effective and structurally efficient configurations. This objective was achieved by following the step by step interrelated program activities shown in Figure 2.
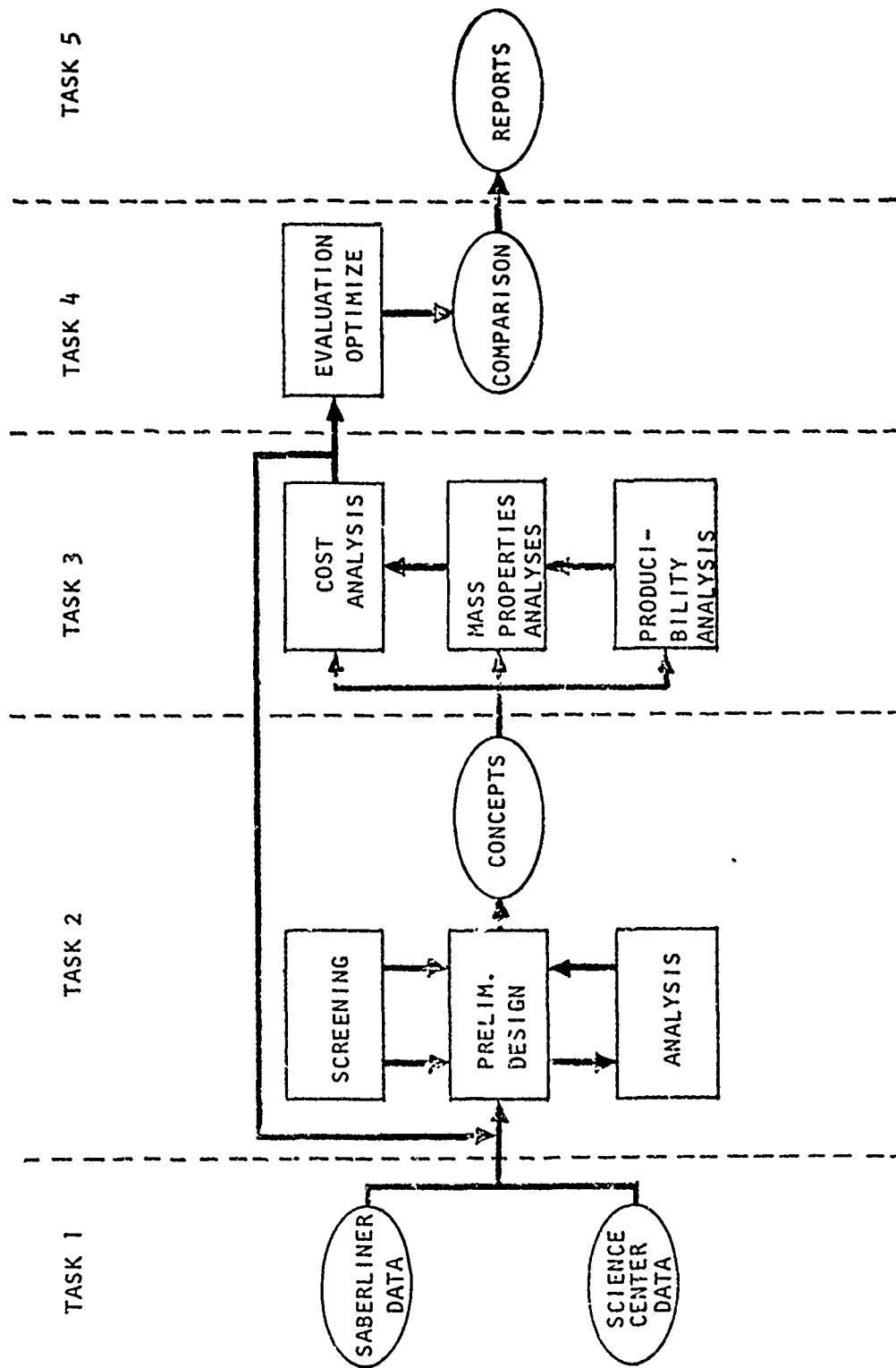
Fig. 2   Program task flow diagram.

12

2.2 DESIGN STUDY

The objective of this program was accomplished by selecting two existing conventional aluminum structures on the T-39 Sabreliner aircraft and redesigning each using SPF aluminum technology. The most promising of these parts was then selected for a more detailed study, considering strength, durability, weight, cost and producibility.

All necessary data for the establishment of structural design criteria were gathered to aid in the selection of the component for advanced aluminum alloy applications. The Sabreliner wing inboard leading edge rib (DWG 265-130201) was considered as a candidate wing component. The present baseline design uses a 7079-T611 aluminum forging. The new SPF replacement design would use superplastically formed 7475-T61. This new configuration was defined by a preliminary drawing (079-402) shown in Figure 3. It showed two sinewave web concepts and a beaded web.

The Sabreliner criteria for this component requires a 45 psi fuel pressure resulting from a crash condition which is critical for the proposed design. This pressure must be carried in beam bending between the top and bottom flange.

Considering a pin-ended beam, 1" wide with the web cross section shown in Figure 3, the margin of safety is zero using the .093 web thickness at 12.96 maximum height of the web. As the web decreases in height toward the nose, the web thickness needed for the 45 psi crash condition is decreased to .032 thick. Thus, the web thickness is tapered from .093 at the front spar to

13

SECTION C-C
CONCEPT C
(SEE WING WEB CONFIGURATIONS)

SECTION B-B
CONCEPT B
(BONDED WEB AND CAP)

SECTION A-A
CONCEPT A
(SEE WING WEB - CLOSED SIDE)

Fig.3   Proposed SPF configuration of the Sabreliner inboard leading edge rib.
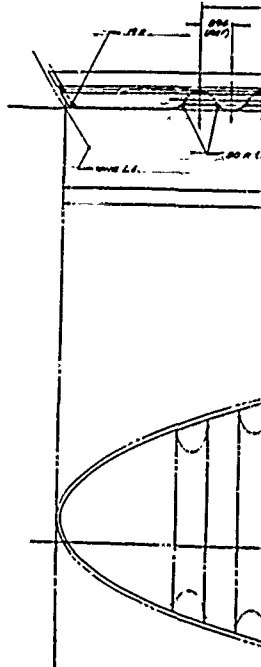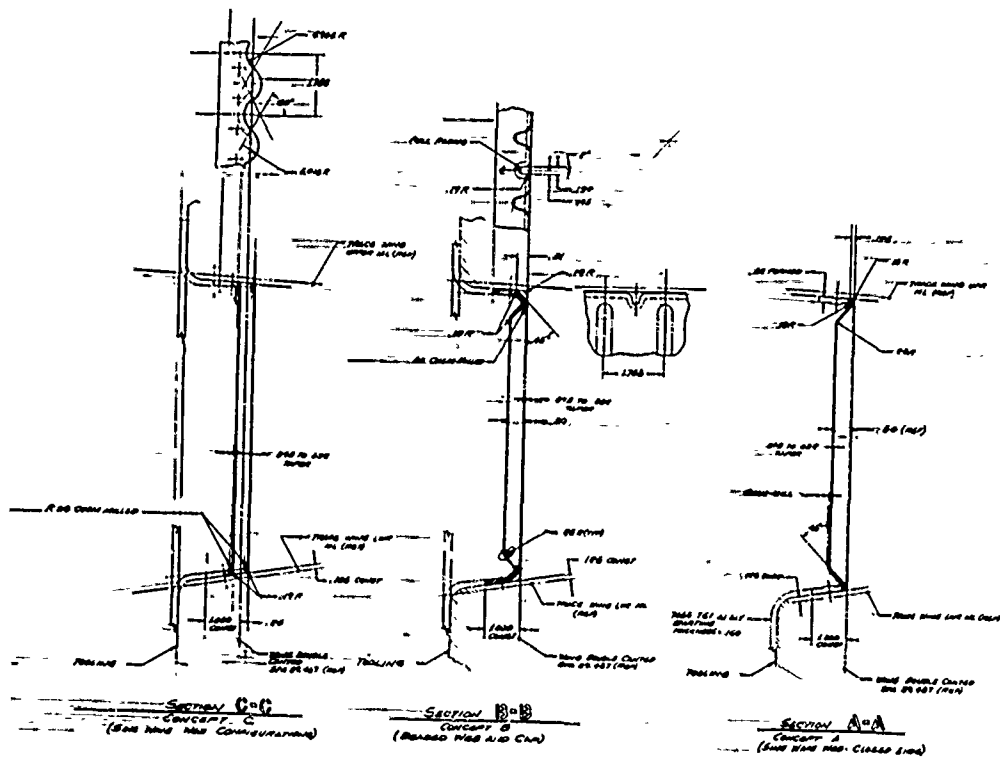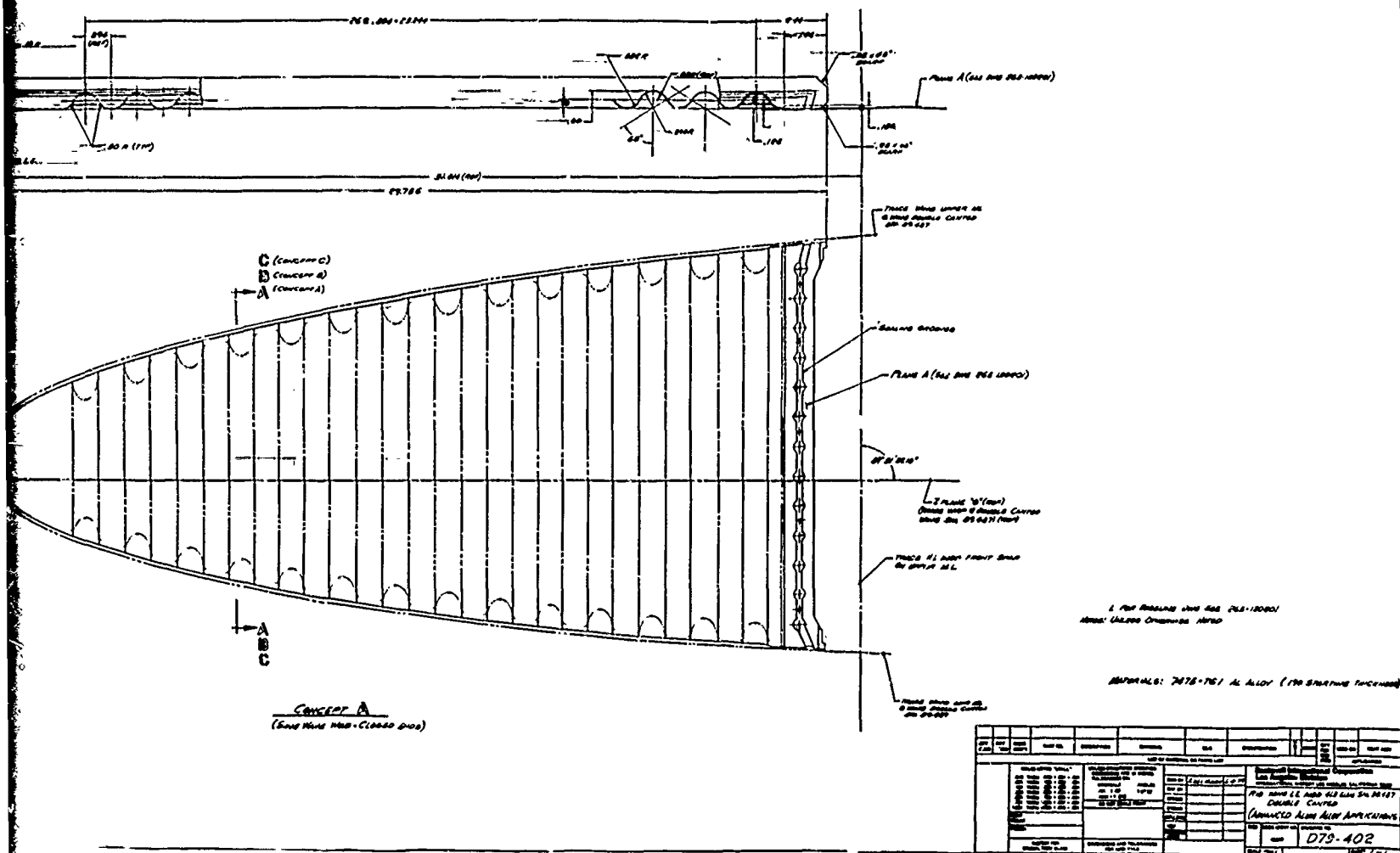
.032 thick at the nose of the rib. Based on these gages, the results of the weight analysis indicate a five percent weight savings as shown below:

$$\text{Web } (271) \left(\frac{.032 + .093}{2}\right) (1.21) (.101) \quad = \quad 2.06$$

$$\text{Pad } (1.44) (13.0) (.093) (.101) \quad\quad = \quad .176$$

$$\text{Lap } (1.00 \ (62) \ (.190) \ (.101) \quad\quad = \quad \underline{1.190}$$

$$\text{Total weight of SPF alum. rib} \quad = \quad 3.426$$

$$\text{Weight of the baseline rib} \quad\quad = \quad 3.60$$

The cost analysis, as shown in Table 1, indicates that the existing aluminum forged rib appeared to be more cost effective. Conversely, the long forging lead time could enhance the approach of superplastic forming if the material were readily available.

A similar study was conducted for the Sabreliner fuselage frame at station 13.00. The existing frame is made out of 18 sheet metal parts riveted together as shown in Figures 4 and 5. The proposed superplastically formed frame assembly (Figure 6) consists of an SPF frame and four clip angles. Since the mounting and attachments at longerons are unchanged, the frame was analyzed for the radar mounting loads on the web. The web of the proposed frame was stiffened by beads and formed depressions which replaced the back-up angles on the baseline configuration. The margin of safety of 1.91 in bending was obtained using a limit load of 10.09.

Using the sizing based on the stress analysis, the proposed frame was then analyzed for cost effectiveness and compared to the baseline. The

17
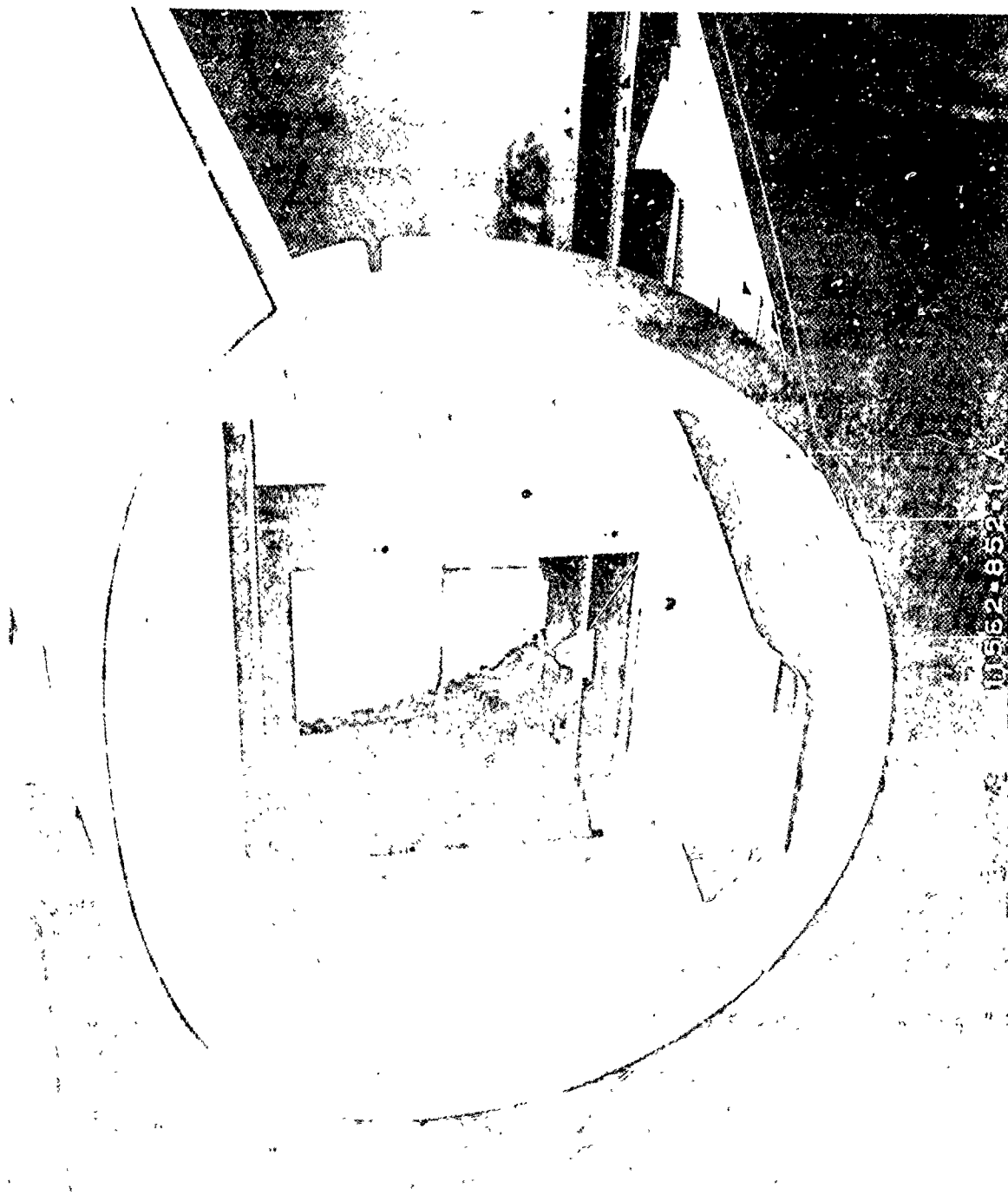
Fig. 4 Front view illustration of the existing sheet metal riveted frame.
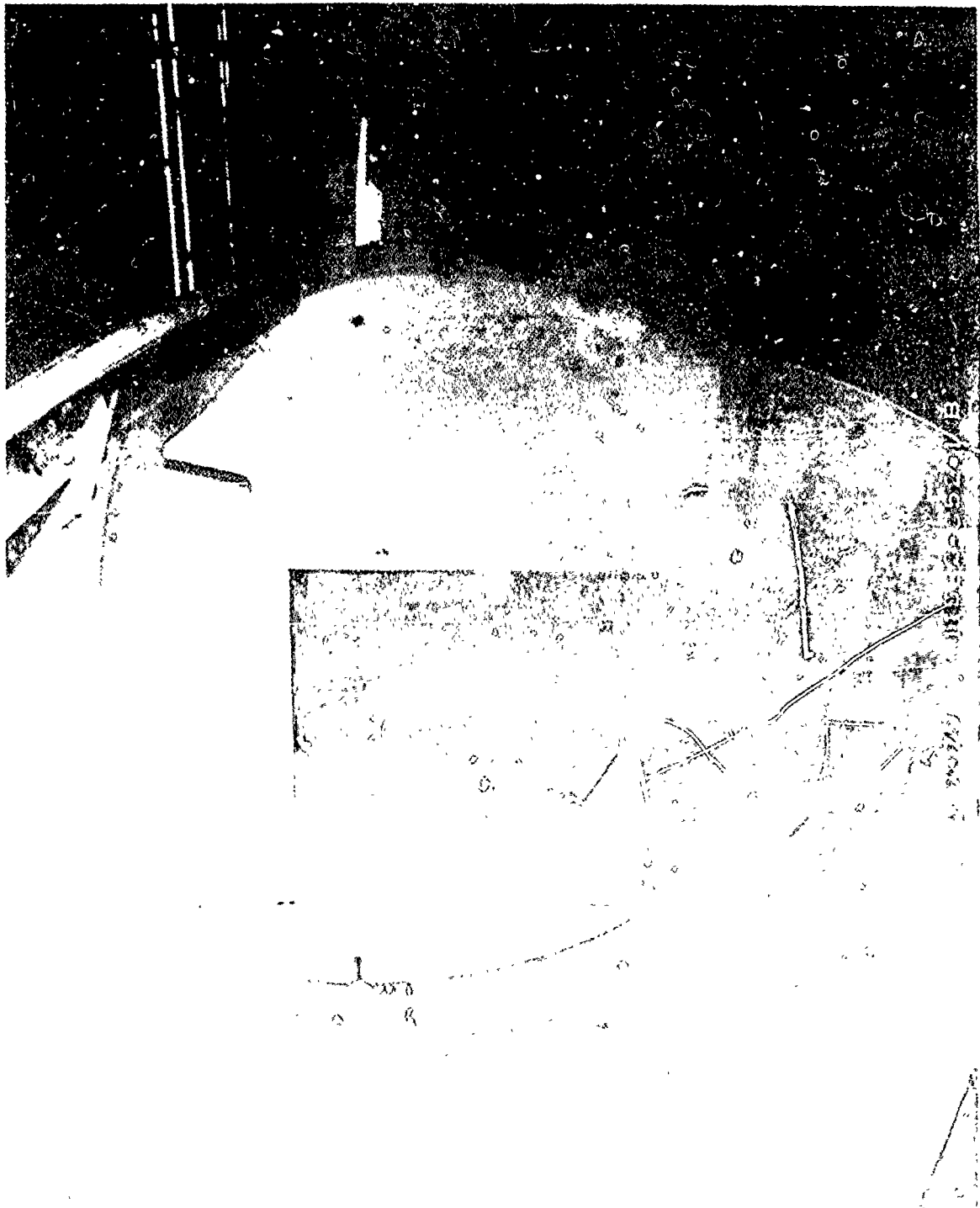
Fig. 5   Rear view illustration of the existing sheet metal riveted frame.

19

Section C-C

Section C-C

-011 ASSY
VIEW LOOKING FWD

Section B-B
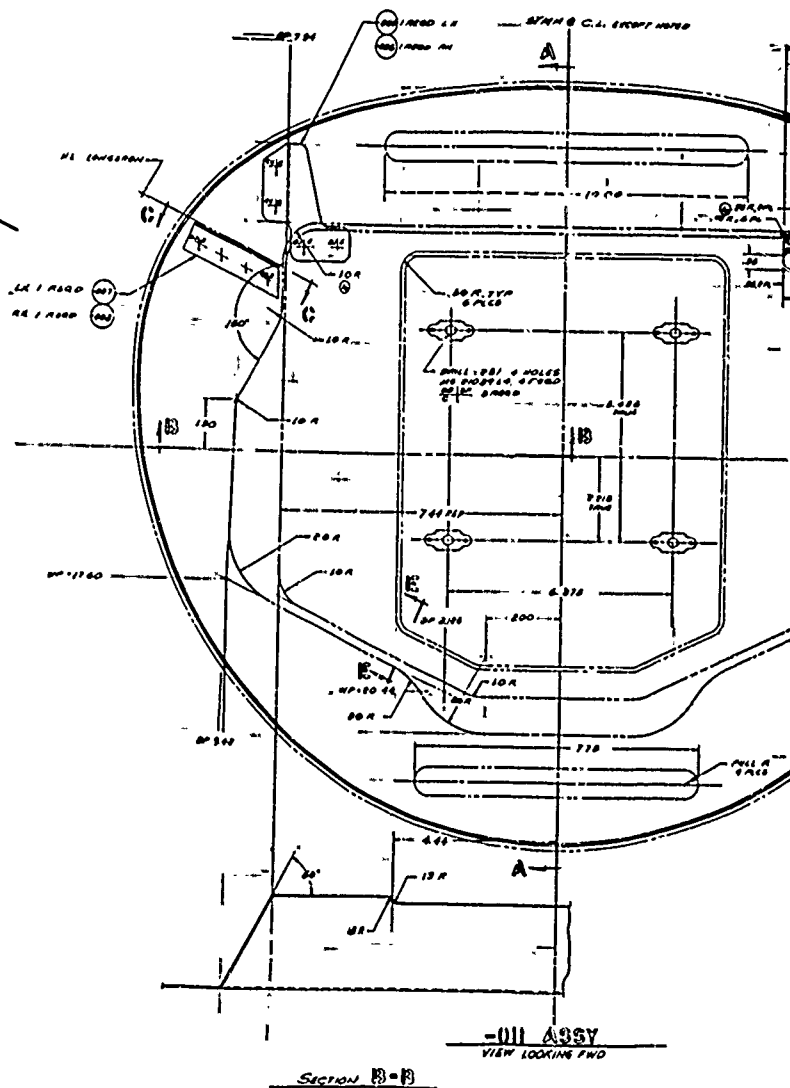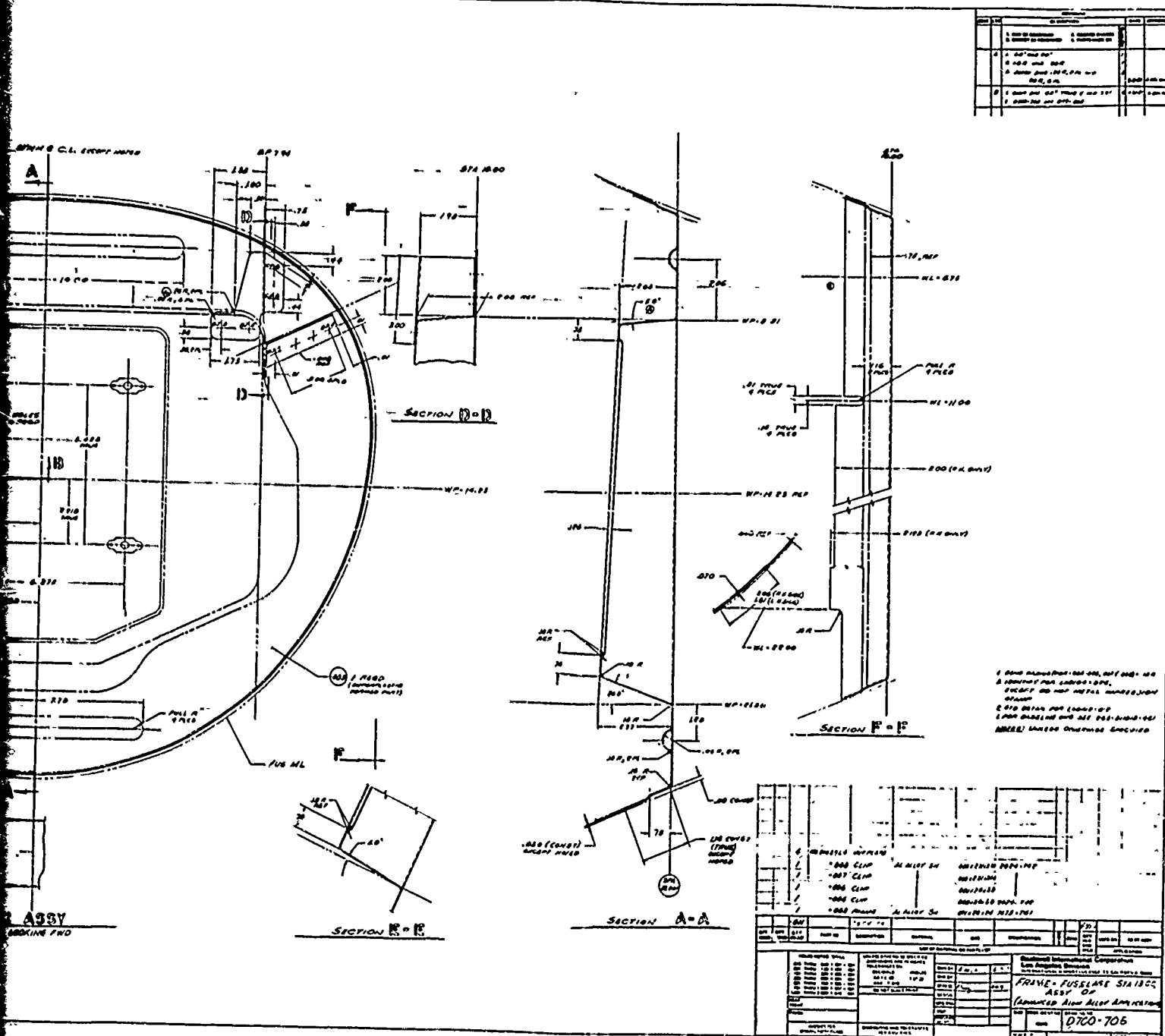
Fig. 6 Proposed SPF configuration
of the Sabreliner forward frame.

21

analysis as summarized in Table 2 indicated a 22 percent cost savings. The cost savings was attained primarily from reduced tooling costs and assembly time. The analysis also covered the fabrication of tooling and the detail part fabrication trimming and assembly. The rates and ratios used for the analysis were for FY 1979 for 500 components. A 36 percent weight savings was gained as detailed in Table 3.

The integration of the angle support with the web and the reduced number of detail parts contributes to a large fraction of the weight savings.

TABLE 1 COST ANALYSIS
MACHINED ALUMINUM FORGING[1] RIB
VS
SUPERPLASTIC FORMED RIB

	CONVENTIONAL FORGING	SUPERPLASTIC FORMED
FABRICATION HOURS	(7.02)	(8.57)
FABRICATION DOLLARS	$319	$390
TOOLING HOURS	(.83)	(2.65)
TOOLING DOLLARS	$ 33	$104
MATERIAL		
TOOLING	$ 35	$ 14
PRODUCTION	$ 89	$ 59
CHEM MILL.	----	$ 89
	$476[2]	$655[2]

[1] CUMULATIVE AVERAGE @ 500

[2] 1979 RATES AND RATIOS

TABLE 2 COST ANALYSIS

SHEET METAL FRAME [1]

VS

SUPERPLASTIC FORMED FRAME

	SHEET METAL	SUPERPLASTIC FORMED
FABRICATION HOURS	(16.0)	(9.7)
FABRICATION DOLLARS	$728	$441
TOOLING HOURS	(7.7)	(4.4)
TOOLING DOLLARS	$303	$173
MATERIAL		
TOOLING	$ 32	$ 17
PRODUCTION	$ 65	$ 36
CHEM MILL.	----	$ 47
	$1,128 [2]	$714 [2]

[1] CUMULATIVE AVERAGE AT 500

[2] 1979 RATES AND RATIOS

TABLE 3 WEIGHT ANALYSIS OF SHEET METAL FRAME VS SUPERPLASTIC FORMED FRAME

BASELINE

ANGLES	.96
FRAMES	.60
DOUBLERS	1.32
CAP	.16
STIFFENERS	.03
SHIMS	.05
SUPPORT	.69
CLIP ANGLES (COMMON)	____
	$3.81
HARDWARES	.17
TOTAL WEIGHT	3.98 LBS

SPF FRAME

WEB	2.26
FLANGE	.76
CLIPS	.08
TOTAL WEIGHT	3.10

2.3 CONCLUSIONS AND RECOMMENDATIONS

The results of this study indicate that the new high strength super-plastic aluminum alloy utilizing the SPF process is capable of producing unique, cost effective and efficient structures. The process enables the designer to produce a cost effective design of a complex part which otherwise would require fabrication by conventionally formed sheet metal components and riveted assembly.

Weight and cost advantages were gained primarily from fewer components in the assembly. The savings realized from reduced material requirements and the reduced manhours required to assemble a part also contributed to the cost savings. For the T-39 frame evaluated there was an anticipated cost savings of 36% and weight savings of 22%.

In view of the foregoing conclusions as supported by the analysis contained in this report, it is recommended that the following studies be implemented:

- Design refinement and in-depth analysis of the selected component
- Test specimens and a full size component of the selected design should be fabricated to verify the producibility, structural integrity, cost savings and weight savings calculated from this study. A total of ten to twelve parts should be fabricated in a production environment to demonstrate the advantages of

27

production techniques, such as hot loading, to high-rate fabrication.

SECTION 3   FORMING LIMITS FOR SUPERPLASTIC FORMED FINE GRAIN 7475 Al

M. W. Mahoney, C. H. Hamilton and A. K. Ghosh

Rockwell International Science Center
Thousand Oaks, CA   91360

ABSTRACT

A concept was pursued in this study to establish the limits of superplastic forming in terms of strain state based on the onset and/or development of cavitation, and for which design properties could be identified. The approach used was to establish the influence of strain state (uniaxial, plane strain, and balanced biaxial) on the inception and growth characteristics of cavitation, and correlate the extent of cavitation with tensile and fatigue properties. Based on these data, it was then possible to establish strain states for which little or no loss in properties are observed, and thereby define forming limits for superplastic forming this material. These results coupled with checks against strains developed in actual parts as well as predicted analytically, show that a wide range of structural parts can be superplastically formed within the constraints of the recommended forming limits.

3.1 INTRODUCTION

A thermomechanical process for developing a fine grain size in precipitation-hardenable aluminum alloys has been described in Refs. 1-3. This method consists of overaging the alloy to generate large precipitates, rolling to produce significant deformation around these precipitates and finally recrystallizing to produce a fine grain size. Using this thermo-mechanical process, grain sizes of the order of 10 to 15 μm have been achieved in the high strength Al-Zn-Mg alloys (7000 Series). It has been shown that the development of this fine grain size and relatively equiaxed grain morphology permits substantial superplastic deformation.[4] However, in view of the commercial interest in superplastic forming of aluminum alloys it is important to recognize that cavitation can occur during superplastic flow at elevated temperatures.

Ghosh and Hamilton observed cavitation in a 7075 Al alloy after superplastic deformation and concluded that cavitation rate (1) increased with increasing temperature, (2) increased with larger grain sizes and (3) showed a maximum at an intermediate strain rate of 1.76×10^{-4} s^{-1}.[4] The work pre-sented in this report extends these efforts to include the fracture tough 7475 alloy and evaluates the effect of stress state on cavitation rate during gas pressure forming of highly strained parts. Based on these results, a forming limit diagram is presented which predicts the design penalty associated with different levels of cavitation.

33

3.2 MATERIALS

All tests herein were performed using a conventional composition of 7475 aluminum. The composition limits for this alloy are comparable to 7075 and are shown in Table 1. Per procedures discussed in Ref. 1-3, this material was thermomechanically processed to sheet $\sim$ 2.5 mm thick resulting in a grain size of $\sim$ .14 μm in the rolling direction and $\sim$ 8 μm in the transverse directions. Microstructure of the thermomechanically processed sheet as compared to as-received plate is shown in Fig. 1.
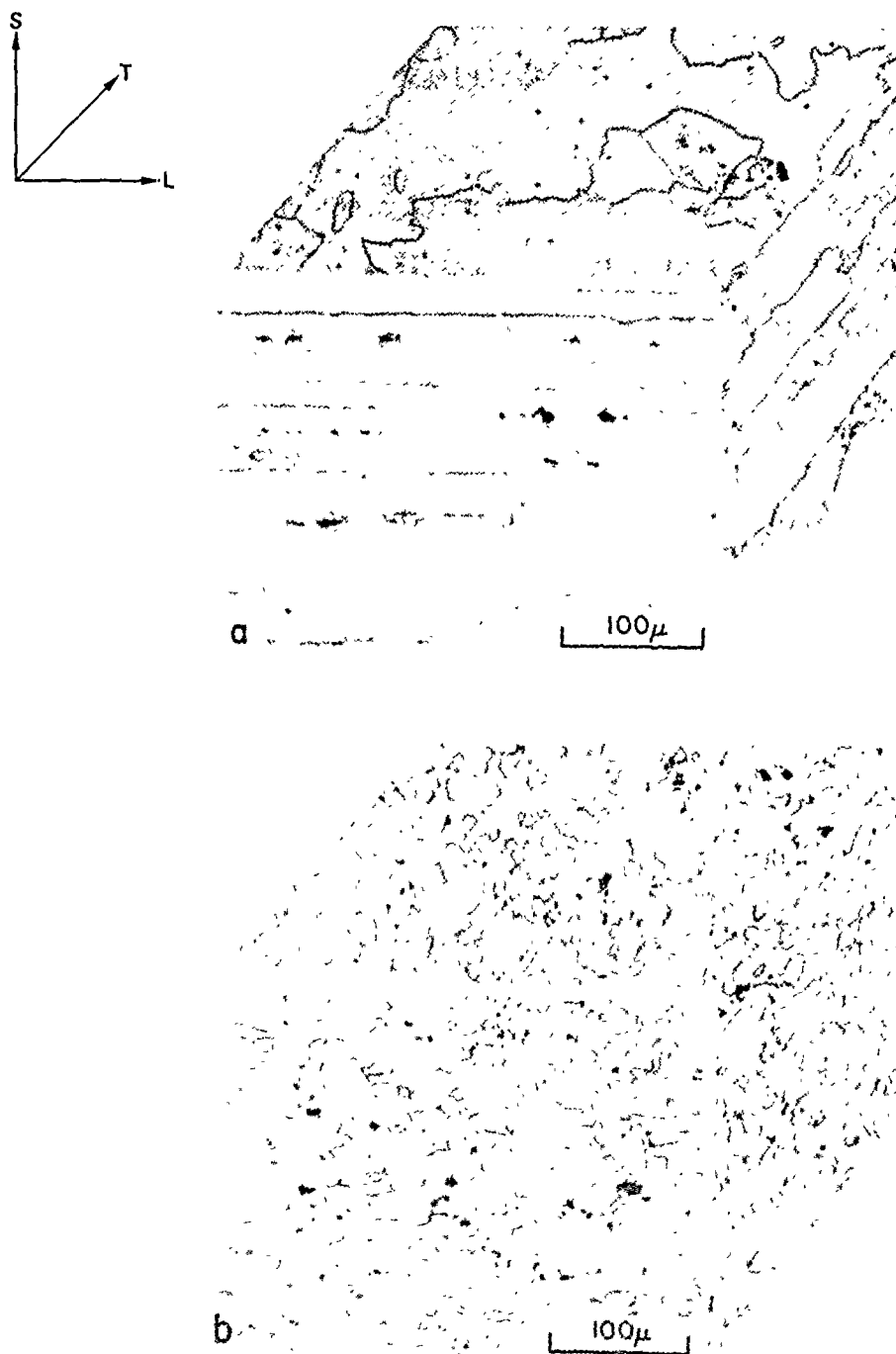
Fig. 1 (a) As-received 7475 aluminum, (b) thermomechanically processed 7475 aluminum (10-14 µm grain size). L indicates longitudinal direction; T indicates long transverse direction, and S indicates short transverse direction.

36

3.3 EXPERIMENTAL PROCEDURES

3.3.1 Tensile Tests

Evaluation of potential superplasticity was conducted by determining flow stress over a strain rate range of 10^{-5} to 2×10^{-2} s^{-1} at temperatures of 499, 516 and $527^{o}C$ in a manner as originally proposed by Backofen et al.[5] Superplastic flow characteristics were determined by a step strain-rate test whereby strain rate was incrementally increased each time the load reached a maximum. From this kind of data, a measure of the strain-rate sensitivity of the flow stress is defined by the strain-rate sensitivity exponent, m, where: $m = \partial(\ln\ )/\partial(\ln\dot{\varepsilon})$ resulting from the relation $\sigma = K\dot{\varepsilon}^{m}$ where is the flow stress and $\dot{\varepsilon}$ is the strain rate.

Although there are several methods for determining m, one should not lose sight of the fact that m is simply a computed value describing the relationship between the flow stress and strain rate. Further, m is not a constant, but varies with strain rate and is thus descriptive of the strain-rate sensitivity of flow stress only over a small, finite variation of strain rate. It is in fact the relative value of strain rate at a local stress concentration as compared to other locations that will ultimately determine the materials response to plastic instability. The m is simply a convenient and meaningful parameter which can be used to indicate the degree of the strain-rate sensivity of flow stress.

37

Tensile specimens of this material were also pulled to failure in uniaxial tension at constant strain rates to determine total elongation and work hardening characteristics. For all uniaxial tests, specimens of the conventional dog-bone shape having a gage length of 2.54 cm and a cross section of approximately 9.5 mm x 2.0 mm, were tested in tension at a constant (true) strain rate. An Instron machine was modified such that the crosshead velocity could be automatically adjusted as the specimen elongates in order to maintain an approximately constant strain rate. This test procedure is described in Ref. 6.

3.3.2 Gas Pressure Forming

Superplastic forming was accomplished by applying gas pressure on one side of the aluminum sheet causing the aluminum to form down into the die by constant strain rate superplastic deformation. Sheet surfaces were coated with a layer of boron nitride to provide lubrication over the die entry radii and to prevent sticking. The rate at which pressure was applied was determined analytically and was dependent on the part geometry and the prescribed strain rate. The objective of time/ pressure schedules was to maintain a constant true strain rate.[7]

As a means to evaluate the influence of stress state on cavitation rate, a grid pattern was etched on the surface to provide a measure of subsequent strains. A number of different geometries resulting in different stress distribution were formed as illustrated in Figs. 2-4. The rectangular pan

38
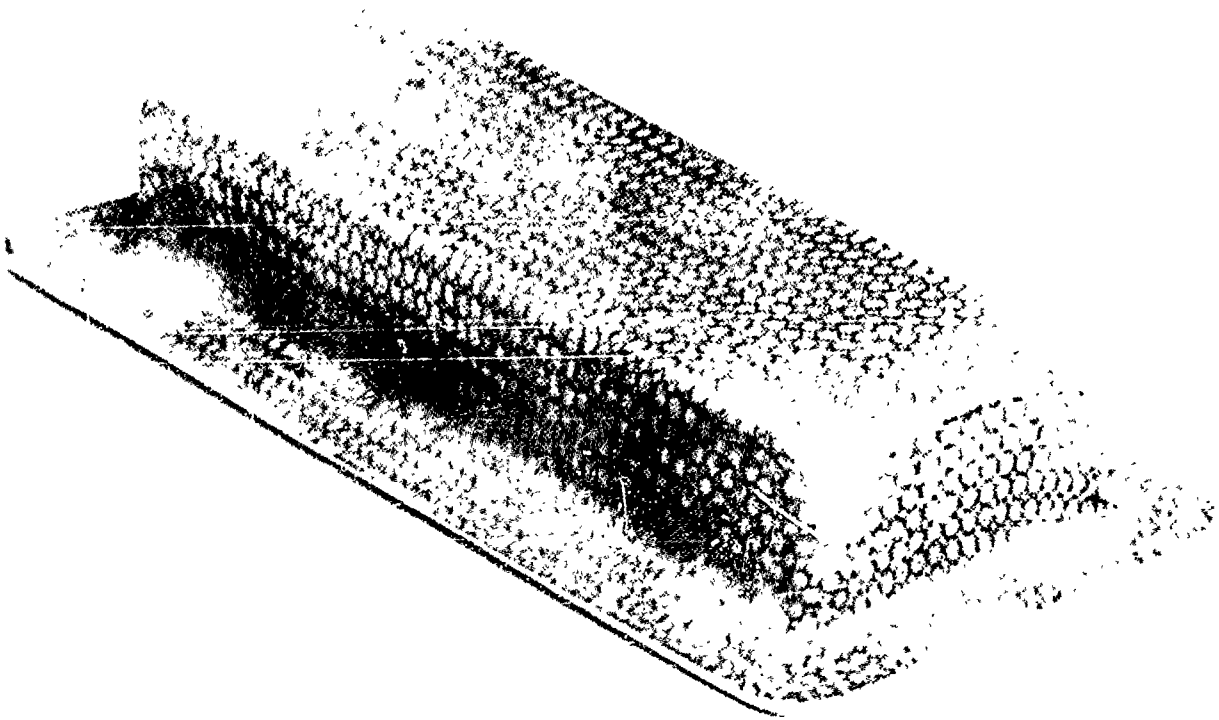
Fig. 2 Rectangular pan shape used as a test part for demonstrating
superplastic formability of sheet materials in a state of
plane stress.

Fig. 3   Cone test geometry made from 7475 Al to demonstrate superplastic
formability of sheet materials in an equibiaxial and mixed biaxial
state of stress.

Fig. 4 A spherical capped part formed in a cylindrical die to demonstrate equibiaxial formability of 7475 Al sheet.

shown in Fig. 2 provides superplastically formed specimens of both balanced biaxial strain at the corners and plane strain at the mid length. The cone and cylinder shown in Figs. 3 and 4 provide specimens of both balanced biaxial (apex of the cone and cylinder) and unequal biaxial. Unequal biaxial specimens were taken some distance from the apex but in regions not complicated by frictional effects caused by contact with the die wall. These three strain states can be compared with tensile data by comparing the void volume as a function of effective strain to determine the influence of stress state on cavitation rate. Effective strain is invariant and as such the influence of different stress states can be compared.

3.3.3   Cavitation Measurements

The extent of cavitation was quantitatively assessed through a high precision density measurement method using a suspended flotation technique. The density of individual specimens was measured by suspending cavitated specimens in a solution of neothane and di-iodomethane inside a specific gravity bottle. Neothane has a density less than that of aluminum whereas the density of di-iodomethane is greater than that of aluminum. The volume ratio of these two liquids is then adjusted such that a specimen of cavitated aluminum neither floats nor sinks but remains suspended in solution. When this occurs the density of the specimen equals the density of the solution and through simple calculations this density can be determined.

3.4 RESULTS

3.4.1 Effect of Temperature

During superplastic flow, it is generally accepted that grain boundary sliding makes a major contribution to the deformation process. It is the influence of superplastic forming (SPF) test parameters on this deformation mechanism that governs both the initiation and growth rate of internal cavities. That is, whenever the rate of grain boundary sliding exceeds the rate of accommodation at triple points, second phase particles and so forth, void nucleation occurs. For example, during superplastic flow, accommodation involving diffusion is necessary to maintain grain boundary cohesion. An increase in test temperature should increase the diffusivity and thus increase the diffusional accommodation. On the other hand, if accommodation is incomplete, cavities could initiate at grain boundaries where stress concentrations are present. Likely initiation sites would include triple points, grain boundary precipitates, inclusions and other boundary irregularities. Recent investigations have now shown that certain types of grain boundary inclusions do play an important role in cavity nucleation in the 7475 Al alloy.[8] The magnitude of this stress concentration would also be influenced by the test temperature; an increase in temperature resulting in a decrease in these built-up stresses due to lower flow stresses.

Flow stress behavior for the fine grain 7475 Al alloy is shown in Fig. 5 as a function of true strain at a strain rate of 2×10^{-4} s^{-1} for temperatures of 499, 516 and 527°C. As shown, flow stress increases with

43
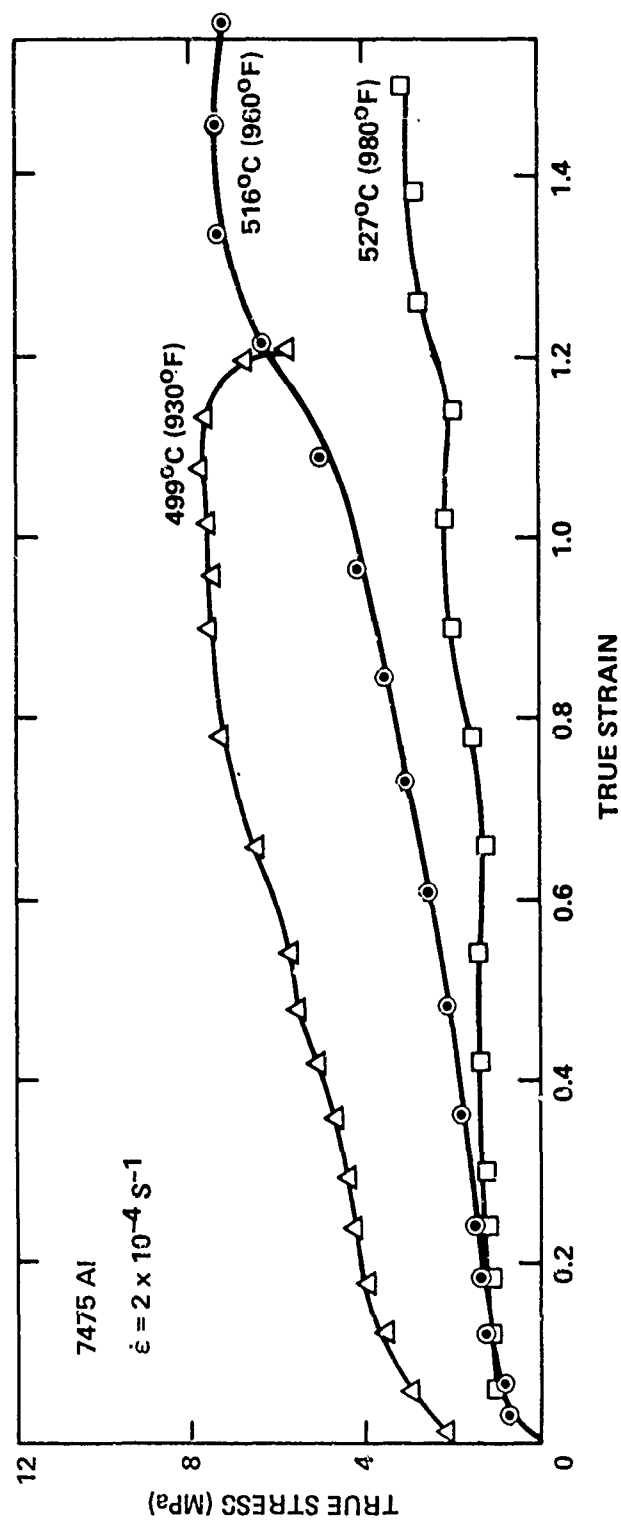
Fig. 5 Flow stress of 7475 Al as a function of temperature and true strain at a strain rate of 2×10^{-4} s^{-1}.

44

increasing strain at each temperature indicating strain hardening. This strain hardening has been reported to be associated with both dynamic grain growth and the development of a defect structure.[4,9] The contribution of each of these mechanisms to the increase in flow stress has not been separated. However, since hardening is less at the higher temperature where greater grain growth would occur it appears that the defect structure would be the major contributor to the increase in flow stress with strain. Furthermore, flow stress increases rapidly with decreasing temperature. For example, a decrease from 527°C to 499°C for strains > 0.6 causes a four fold increase in flow stress.

Figure 6 illustrates the influence of temperature on void volume for temperatures of 499, 516 and 527°C as a function of true tensile strain. These cavitation measurements were made from uniaxial tensile specimens of 7475 Al with no heat treatment subsequent to forming. A re-solution heat treatment followed by age hardening to the T-6 condition has been shown to reduce the initial density. As shown, cavity density decreases with increasing temperature up to 527°C. Since the melting range of this alloy is 538 to 635°C, temperatures higher than 527°C were not evaluated due to the possibility of incipient melting at grain boundaries. This decrease in cavitation density with increasing temperature corresponds to the large decrease in flow stress with temperature shown in Fig. 5 and thus the associated decrease in the tendency for cavity nucleation. In some materials an increase in temperature also leads to an increase in void growth rate,[10] however, this has not been observed here. Based on these mechanical property

45
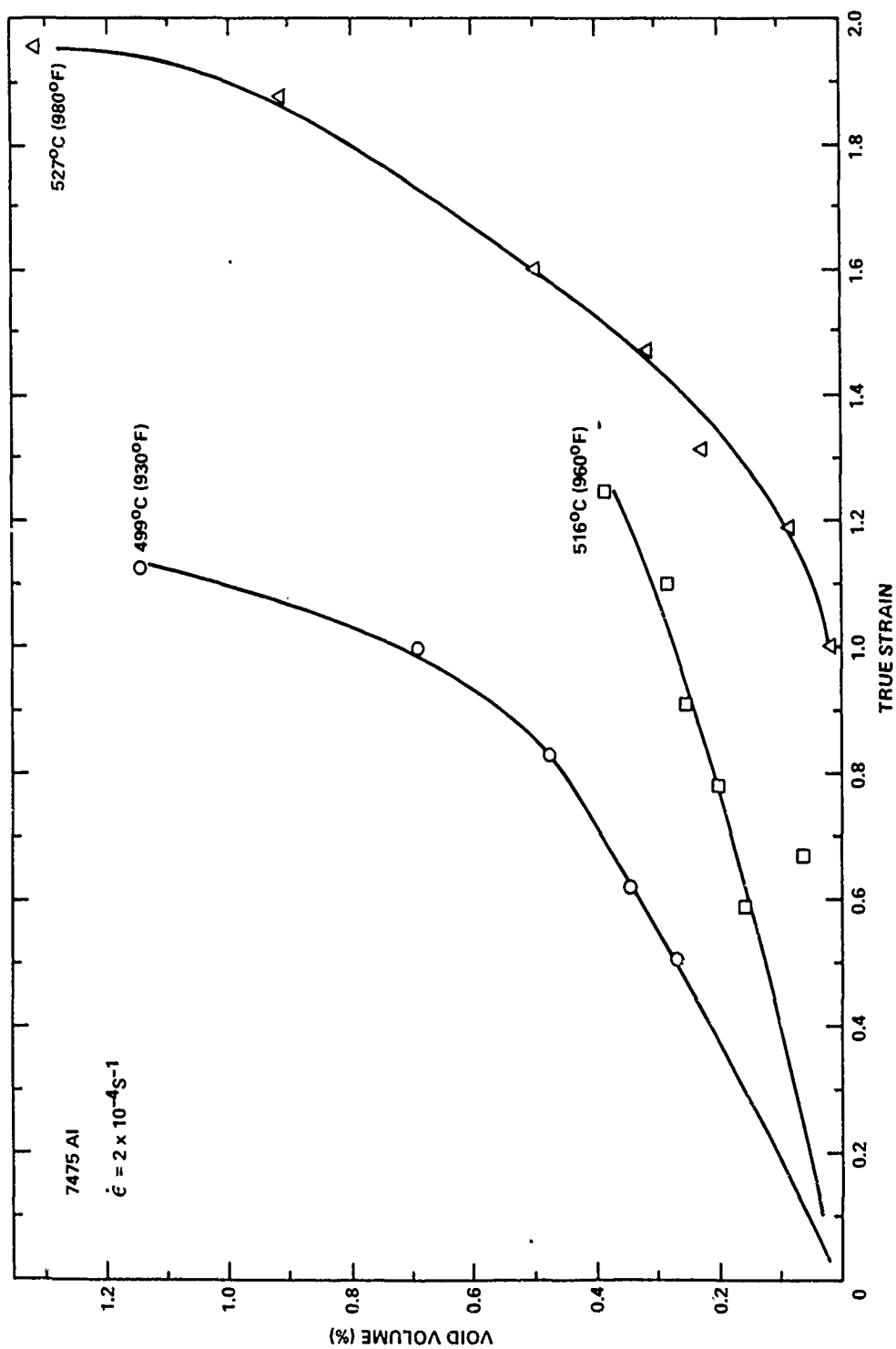
Fig. 6 Void volume in superplastically formed 7475 Al as a function of temperature and true strain at a strain rate of 2 x 10⁻4 s⁻1.

results it follows that an increase in the SPF temperature could result in a decrease in cavitation rate by contributing in two ways: (1) greater diffusional accommodation and (2) lower stress concentrations at microstructural irregularities due to lower flow stresses.

Clearly, the mechanism of cavity nucleation and growth is much more complicated than this simple correlation between flow stress and cavity density. However, it can be concluded that forming parameters and/or material processing parameters that result in lower flow stresses will also lead to a decrease in the volume fraction of cavities. If the lower flow stresses lead to a decrease in the magnitude of stress concentrations at potential nucleation sites then this would decrease the number of cavities nucleated, and lead to a decreased volume fraction of voids.

3.4.2 Effect of Strain Rate

Flow stress is shown in Figs. 7 and 8 as a function of true strain for strain rates from 8×10^{-5} s^{-1} to 5×10^{-3} s^{-1} and temperatures of 499 and 516°C. Strain hardening is again evident at all strain rates while the flow stress is shown to increase significantly both as the strain rate increases and as temperature decreases.

As discussed above, flow stress influences the stress concentration at grain boundary irregularities and thus the driving force for cavity nucleation.[11] If nucleation were the only consideration in the development of cavities then this observed large increase in flow stress with increasing

47
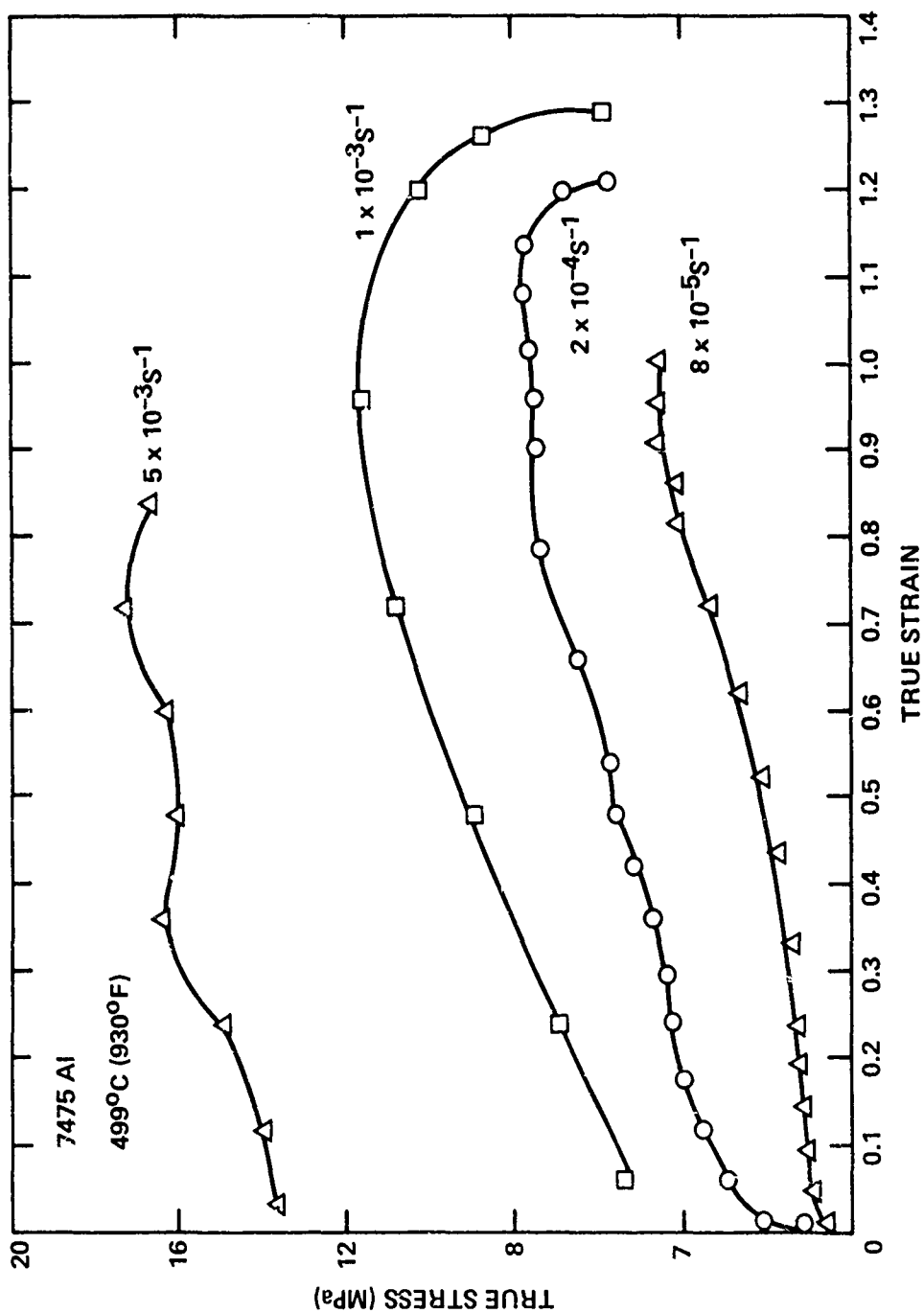
Fig. 7 Flow stress of 7475 Al as a function of strain rate and true strain at 499°C.
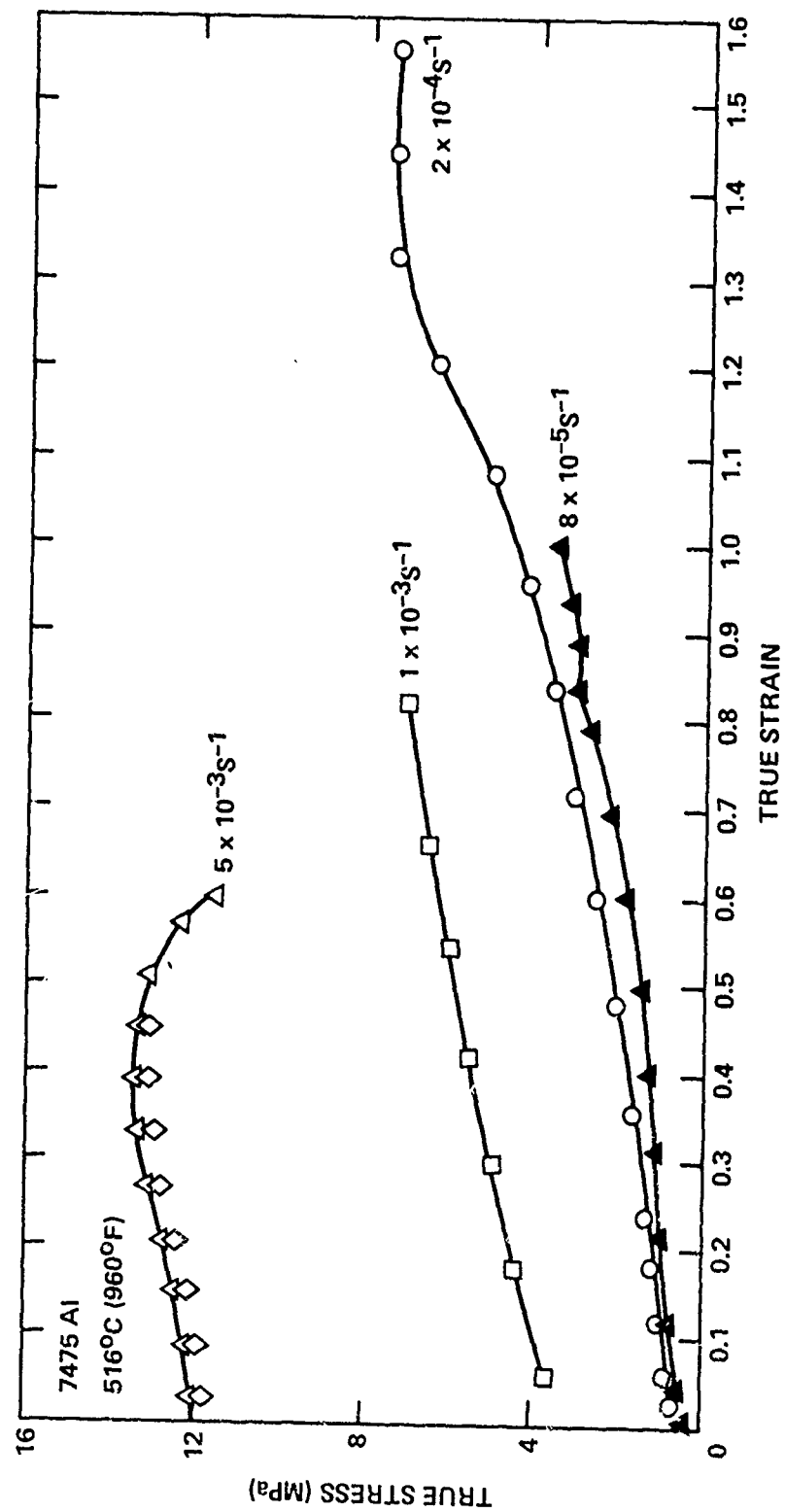
Fig. 8 Flow stress of 7475 Al as a function of strain rate and true strain at 516°C.

strain rate would result in a high cavitation density. However, Fig. 9 shows a maximum in cavitation density at intermediate strain rates of 1 to 3×10^{-4} s^{-1}. This maximum is more clearly shown in Fig. 10, where void volume is illustrated as a function of strain rate for constant levels of true strain. In this figure, void volume is shown as a function of strain rate for specimens superplastically strained for different periods of time. On each constant time curve, equal true strains can be selected as shown by the solid lines. Again, the peak in void volume occurs between strain rates of 1 to $3 \times 10^{-4} s^{-1}$ for all levels of true strain.

This maximum in cavitation density has been observed previously and has been attributed to the dependence of cavitation density on both the nucleation and growth characteristics of these voids.[4] For example, at low strain rates the growth rate of voids would be high due to the large contribution of grain boundary sliding to the deformation process and the long time available for vacancy diffusion to the voids. However, the number of nucleation sites would be expected to be low due to the low flow stresses associated with low strain rates and thus the low driving force for nucleation. At higher strain rates the reverse would be true. That is, the driving force for nucleation would be high due to the larger flow stresses but the growth rate of voids would be less due to the decreased contribution of grain boundary sliding to the deformation process and the shorter times available for vacancy diffusion. However, it appears that in the intermediate strain rate regime of 1 to $3 \times 10^{-4} s^{-1}$ the contribution of both the nucleation and growth rate mechanisms combine to result in a maximum cavitation density.

50
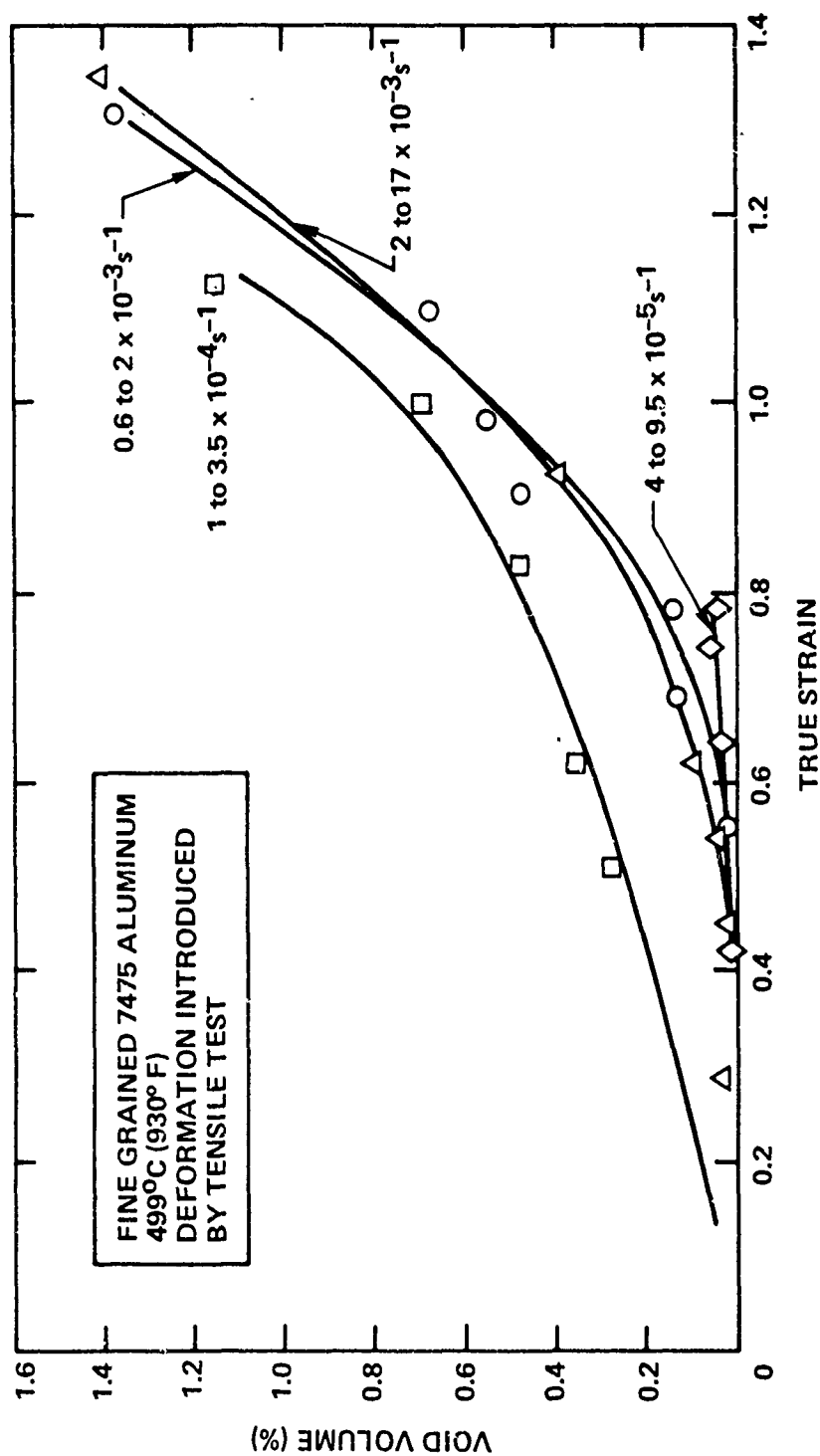
Fig. 9 Void volume in superplastically formed 7475 Al as a function of strain rate and true strain at a temperature of 499° C.
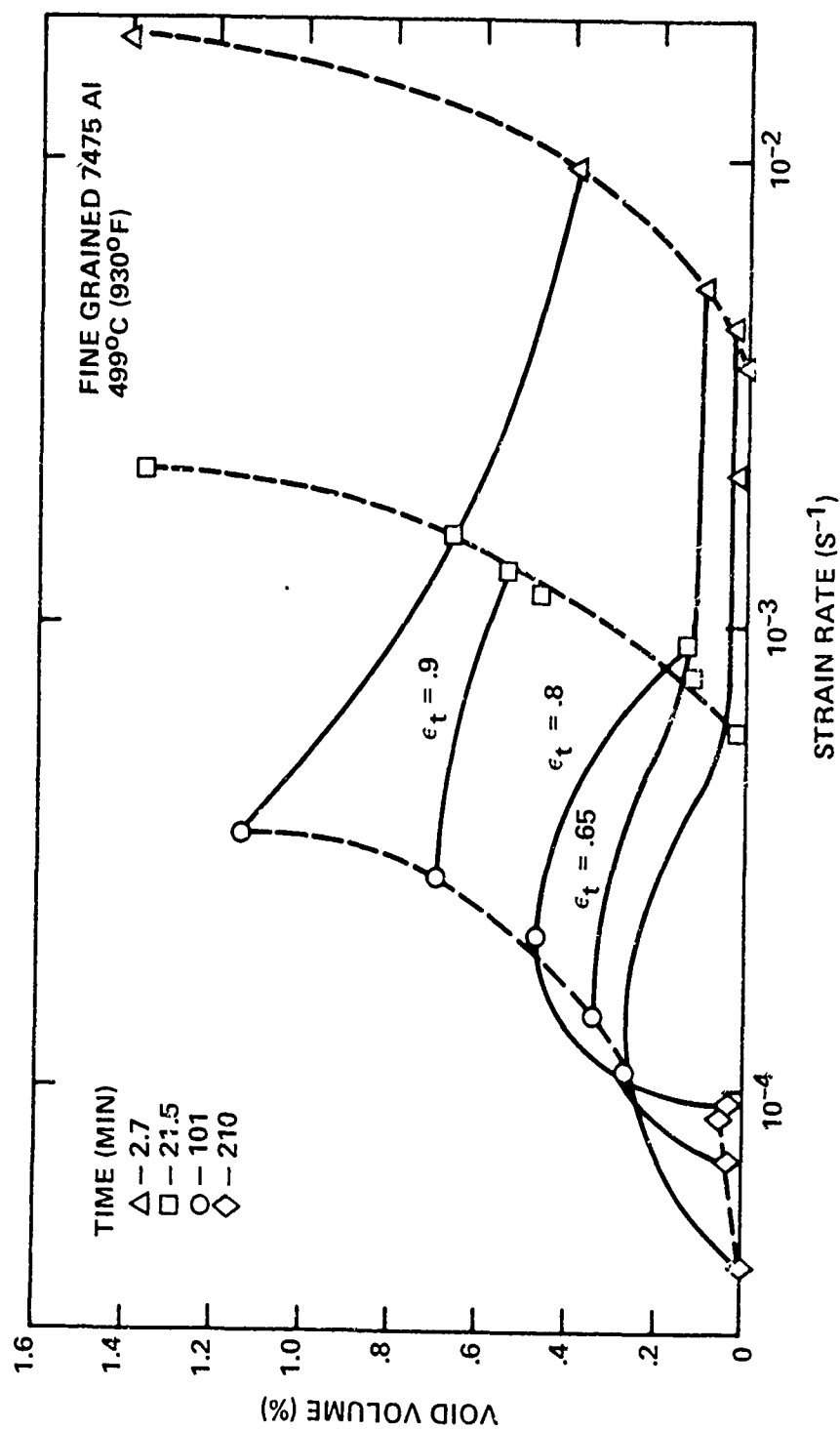
Fig. 10 Isostrain curves illustrating the maximum in void volume at a strain rate of 1 to 3 x 10⁻⁴ s⁻¹.

Figure 11 illustrates the effect of strain rate on both the number of cavity nucleation sites and cavity volume. Test conditons of temperature (499°C) and true strain (0.74) were the same for Figs. 11a and 11b, however, strain rates were 8×10^{-5} and 5×10^{-3} s^{-1} respectively. Clearly, the number of cavities nucleated at a strain rate of 5×10^{-3} s^{-1} is much greater than that at 8×10^{-5} s^{-1}. Also, considering that the volume of a cavity is approximately proportional to the radius cubed, the size of cavities developed at 8×10^{-5} s^{-1} is much greater than those generated at 5×10^{-3} s^{-1}.

In addition to this influence on cavitation, strain rate also influences the degree of formability achievable during superplastic forming. Figure 12 illustrates flow stress as a function of strain rate for temperatures of 499, 516 and 527°C. It is the instantaneous value of these flow stresses as they are determined by the local strain rate that determines the response of the 7475 Al to a local stress concentration. That is, the rate of change in stress with strain rate (slope of the curve shown in Fig. 12) determines each materials resistance to necking. This is commonly called the strain rate sensitivity index "m" and is shown in Fig. 13 for flow stress behavior at 499°C. Unfortunately, as Fig. 12 illustrates the strain rate sensitivity shows a maximum over the same strain rate range where maximum cavitation occurs. Unless precautions are taken to eliminate caviation, a compromise in the selection of strain rate would be necessary to select between maximum formability or a reduction in the magnitude of cavitation.

53
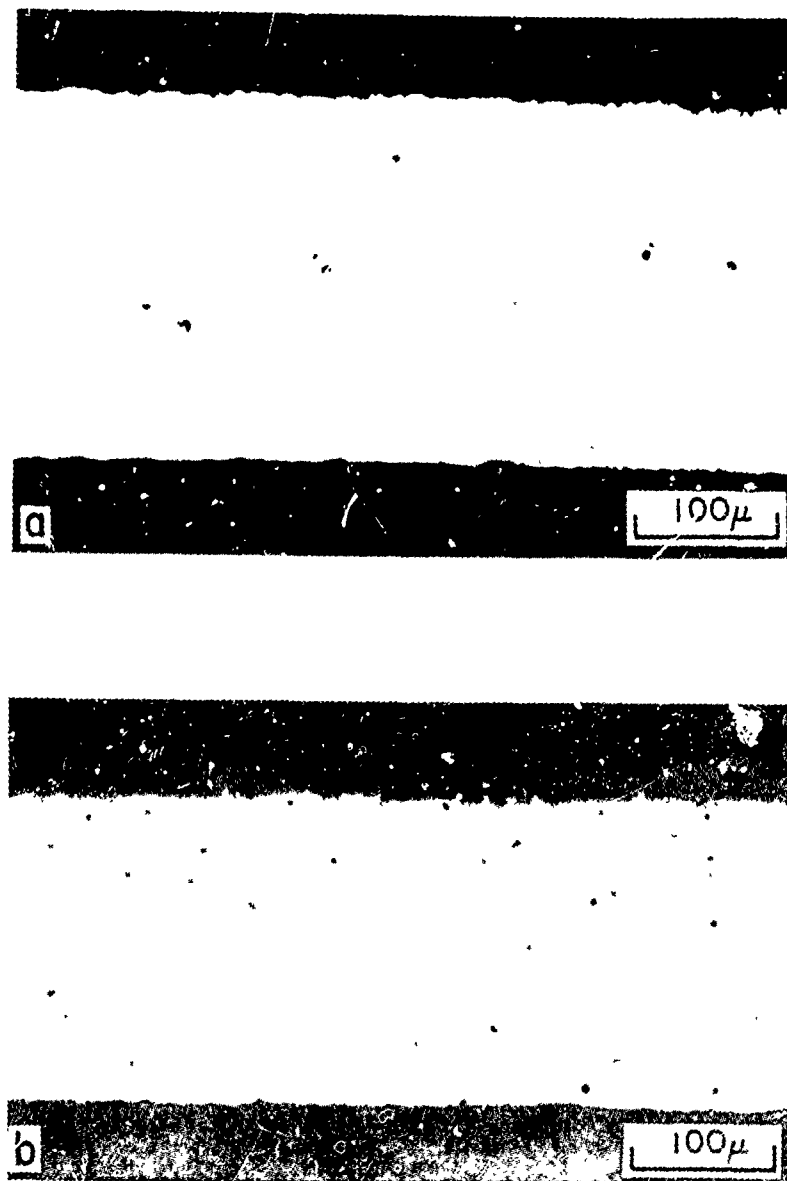
Fig. 11 Micrographs illustrating the effect of strain rate on the initiation and growth of cavities. (a) $\varepsilon_t = 0.74$, $\dot{\varepsilon} = 8 \times 10^{-5}$ s^{-1}, (b) $\varepsilon_t = 0.74$, $\dot{\varepsilon} = 5 \times 10^{-3}$ s^{-1}.
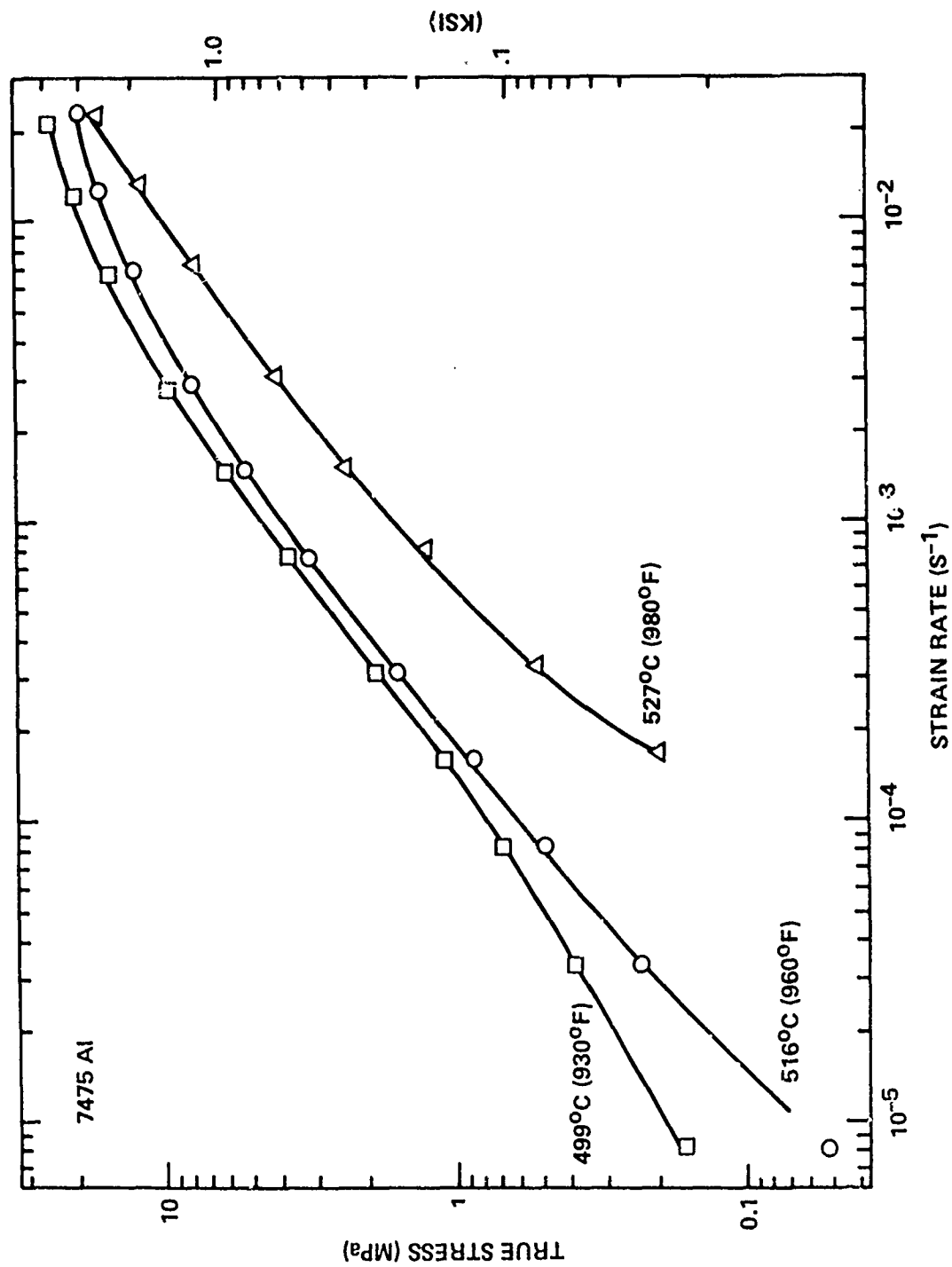
Fig. 12   Flow stress of 7475 Al as a function of temperature and strain rate.

55
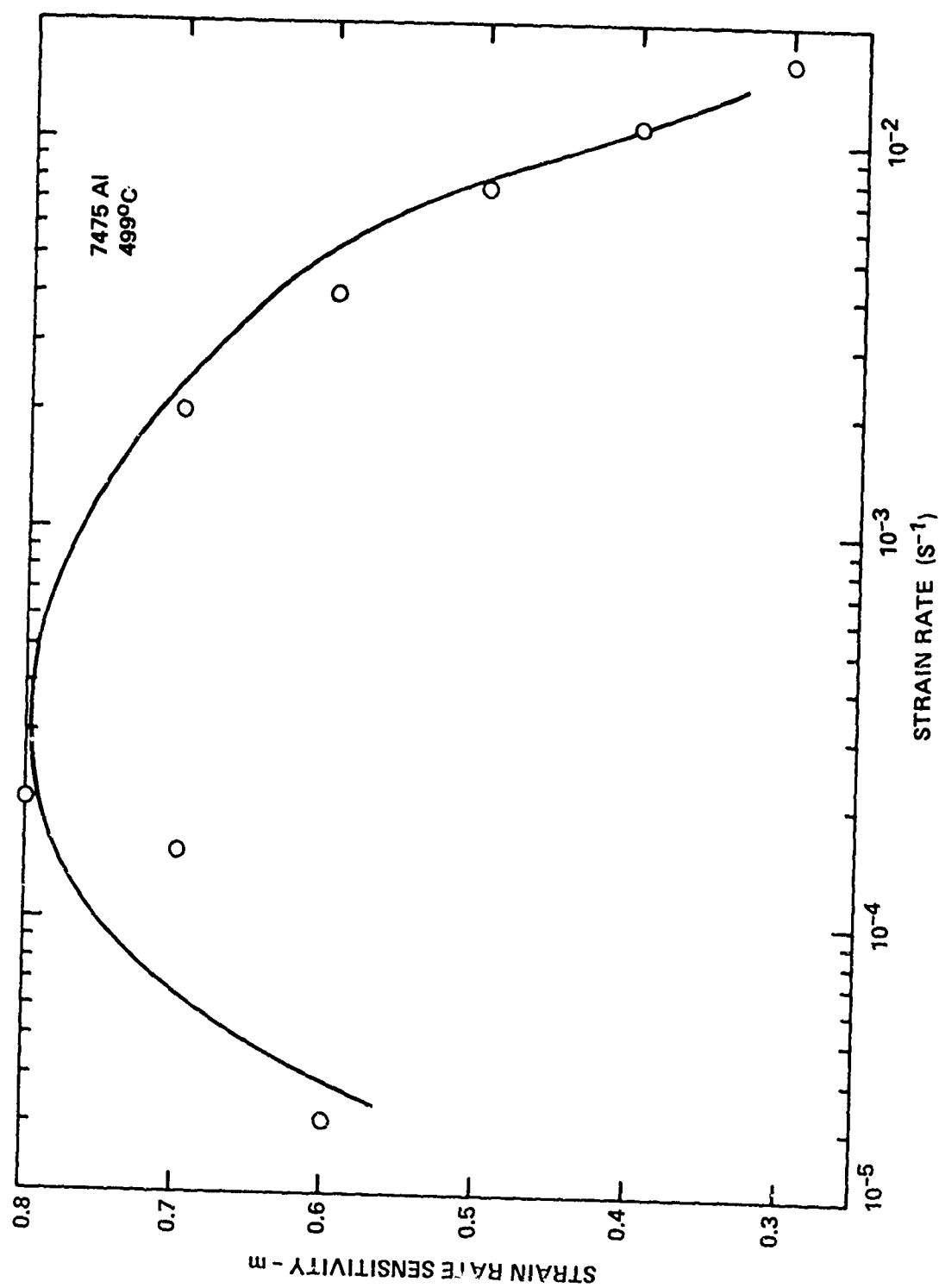
Fig. 13   Strain rate sensitivity of 7475 Al at 499 °C.

56

3.4.3 Effect of Strain State

In order to nondestructively determine the extent of cavitation in a superplastically formed component it would be necessary to predict the extent of cavitation not only as a function of test and material variables but also as a function of the different strain states developed during forming. A part exhibiting a complex geometry could include strain states of equibiaxial, unequal biaxial and plane strain. Additionally, it would be both economical and convenient to be able to predict cavitation in complex components based upon data acquired from uniaxial tensile tests. To this purpose, gas pressure forming tests were performed at 516°C and at a strain rate of 2×10^{-4} s^{-1} to determine the relationship between different strain states and cavitation density.

Superplastically formed test pieces shown in Figs. 2-4 and uniaxial tensile test specimens provided the necessary range of strain states as illustrated in Fig. 14. Directions of principal strain are noted for each component. In addition to the areas shown, specimens were also taken from regions experiencing an unequal biaxial state of strain.

Following gas pressure forming, cavitation density was measured without intermediate heat treatment. Void volume for the different strain states is shown in Fig. 15 for effective strains up to 1.5. There is some scatter in the data, perhaps due to sampling errors associated with the small specimens used for flotation measurements. However, it is clear that strain state has no measurable influence on cavitation rate during superplastic

57

(a) UNIAXIAL TENSION

(b) EQUI-BIAXIAL

(c) PLANE STRAIN
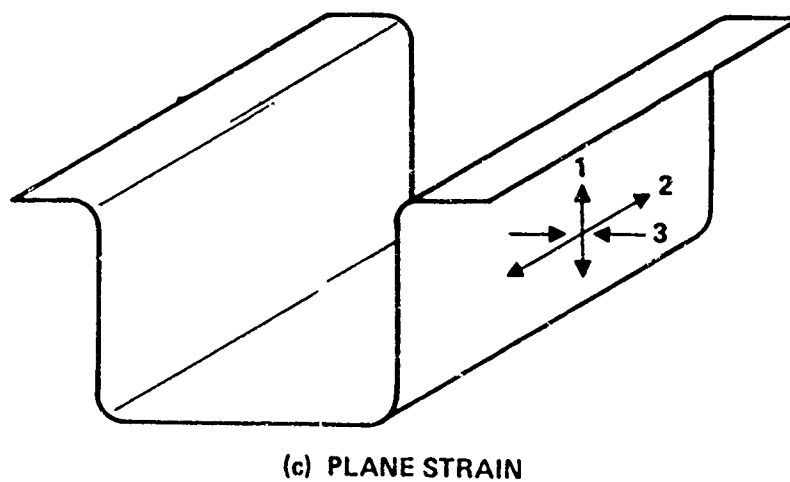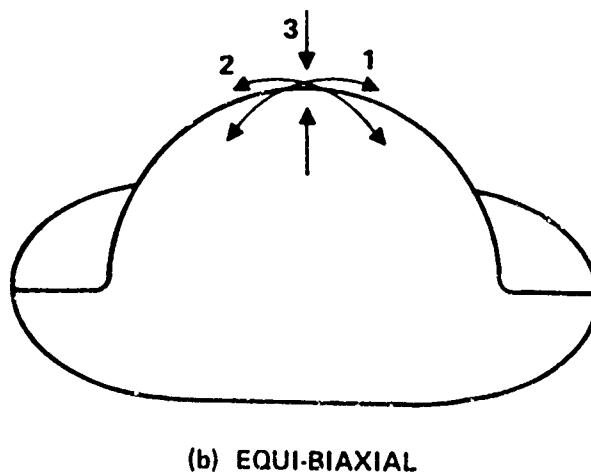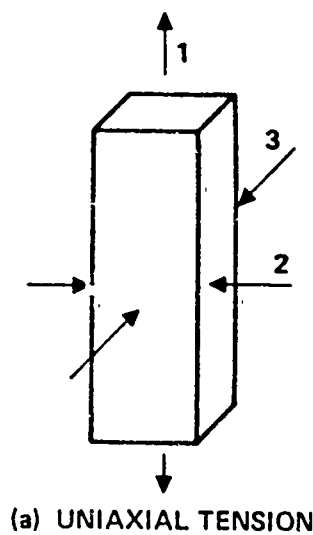
Fig. 14 Principal strain directions for the three strain-states.
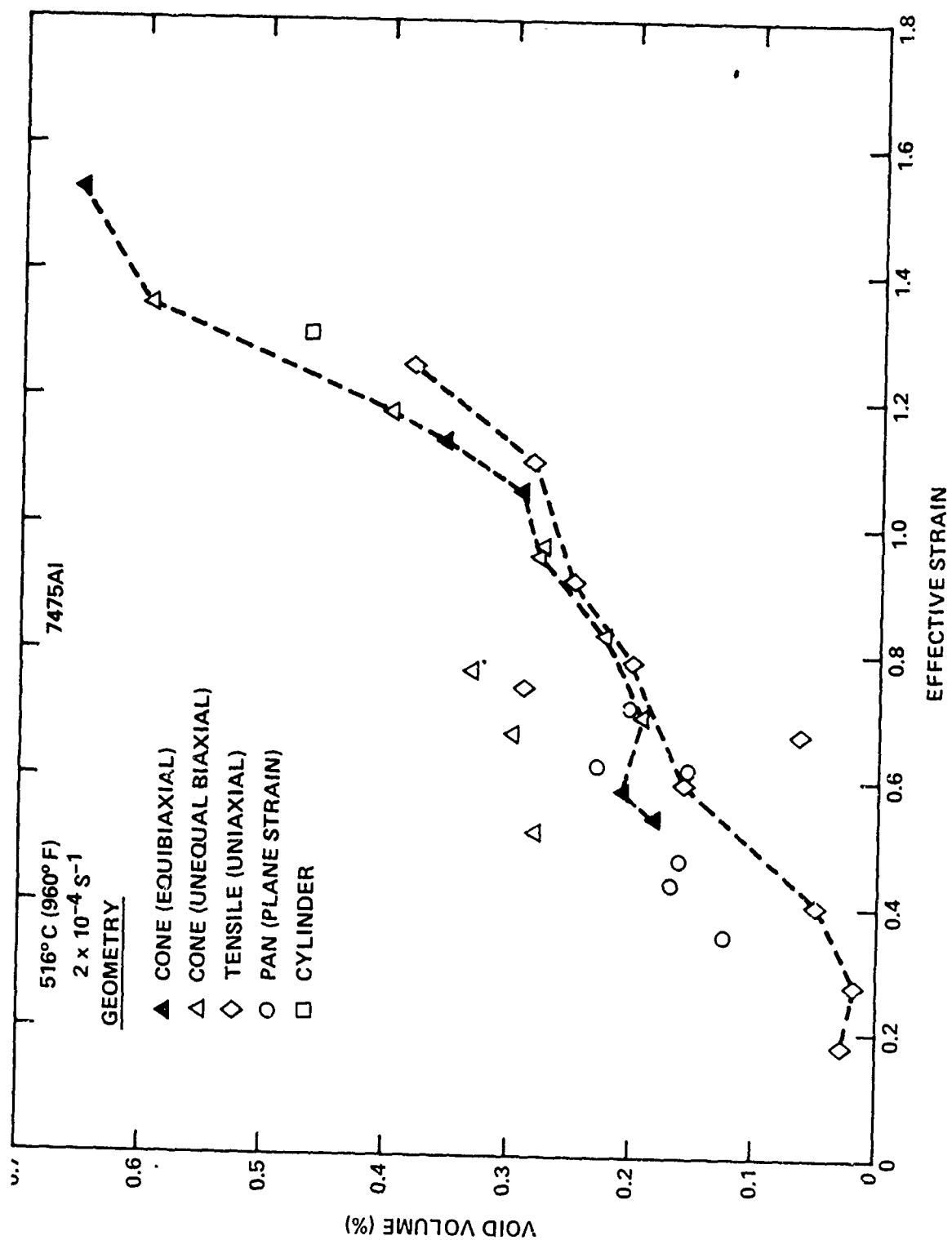
Fig. 15   Void volume of superplastically formed 7475 Al as a function of strain state and effective strain.

forming. Thus, for a given set of test conditions it should be possible to establish a unique relationship between void volume and effective strain regardless of the different strain states experienced by different locations of a complex component. For fixed effective stress, the change in mean stress within this range of strain states does not appear to influence the cavitation rate. It would, however, be difficult to infer the cavitation mechanism on the basis of this observation.

3.5 DISCUSSION

As in most alloy systems that are capable of superplastic deformation, the 7000 series aluminum alloys are inherently susceptible to cavitation during forming. Results presented above illustrate how test variables of strain, temperature, strain rate and component geometry can influence not only the extent of cavitation but also the size and distribution of voids.

The influence of these variables has been explained on the basis of their effect on high temperature material characteristics such as diffusional accommodation, grain boundary sliding, grain growth and void nucleation and growth. The principle concern, however, is the effect cavitation will have on both formability and resultant mechanical properties. This subject is addressed in detail in Ref. 12, but based upon the results presented herein some comments are in order.

Because of concurrent cavitation during forming, the useful levels of strain achievable in this material are not those at fracture, but at a certain level of cavitation beyond which tensile properties begin to become affected adversely. While the details of the influence of cavitation on mechanical properties is discussed in Ref. 12, Fig. 16 identifies equal levels of cavitation in a three-dimensional forming limit diagram. This diagram is similar to those used in the sheet metal forming literature[13,14] and represents the extent of cavitation (not fracture) along the third axis in
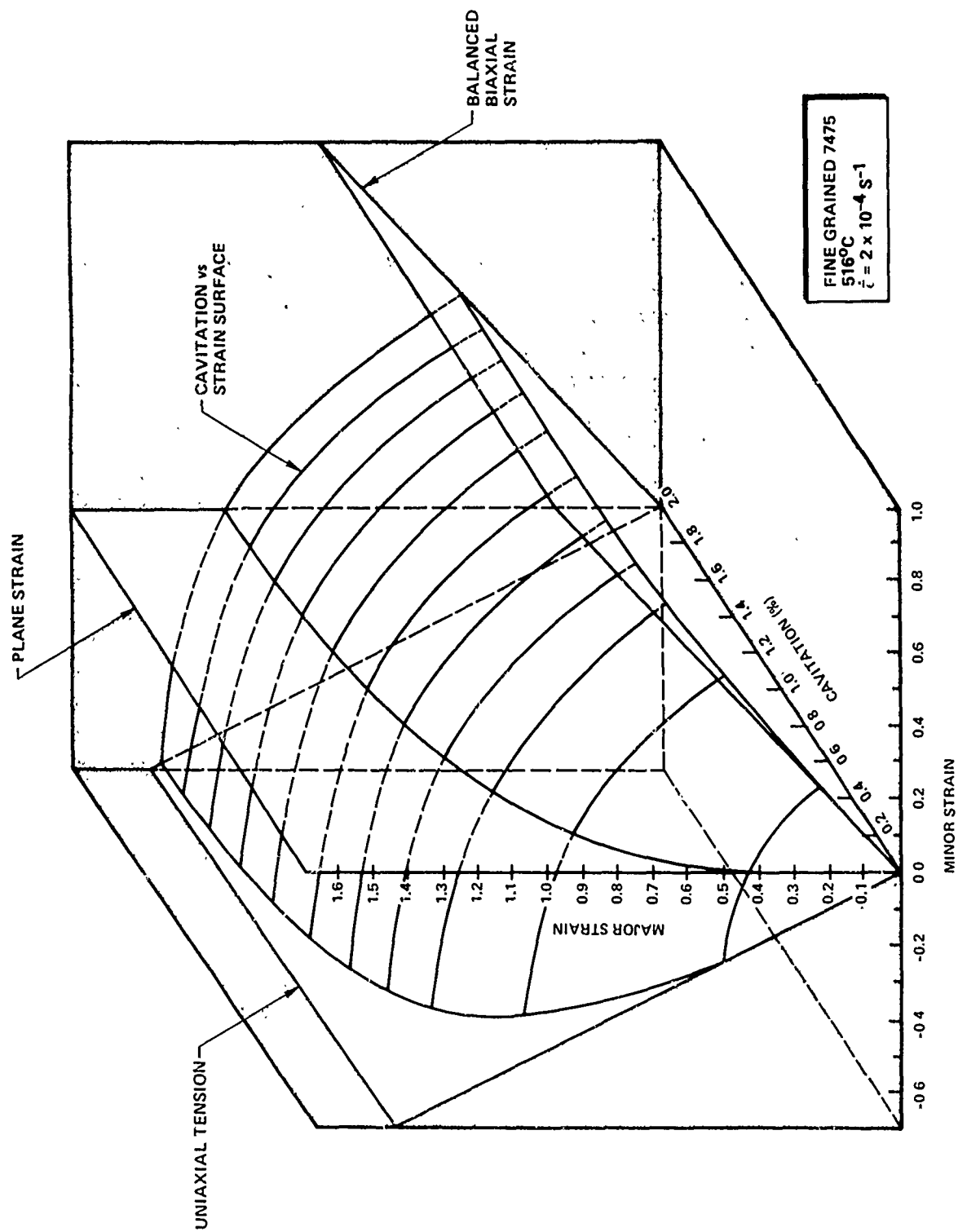
Fig. 16   Three dimensional illustration of a cavitation vs strain surface in relation to the strain state.

addition to the major and minor strain axes. The elliptical portions of these curves are reflections of a constant effective strain, (which is a quadratic function of ε_1 and ε_2) being related to isocavitation levels. Figure 16 is based on SPF results from fine grained 7475 Al at 516°C and a strain rate of 2×10^{-4} s^{-1}. From this plot isocavitation lines can be established for any level of cavitation by taking a plane perpendicular to the cavitation axis. Figure 17 illustrates this kind of result for cavitation levels of 0.3%, 0.6% and fracture. When coupled with the loss in tensile properties data as a function of cavitation levels, Fig. 17 provides a forming limit diagram. To complete this train of thought, mechanical properties data developed in Ref. 12 were used to establish design penalties. It can be predicted from this data that for cavitation levels of 0.3% and 0.6% the losses in mechanical properties would amount to only ~ 2% and ~ 6% respectively.

The elliptic isocavitation plots are also quite different in shape and level from the room temperature forming limit diagram of this material. The low plane strain limit at room temperature is believed to be a result of the onset of plastic instability, which is not a prevalent mode at the superplastic temperature.

Before addressing the subject of strain versus cavitation further, it should be pointed out that analytical models have been established that will predict (in advance of experimental SPF forming tests) the effective strain based on stress state and component dimensions.[7,15] An example of this is shown in Figs. 18 and 19 where the effective strain is predicted for both the corner and edge of a rectangular shape. In each figure, experimental data

63
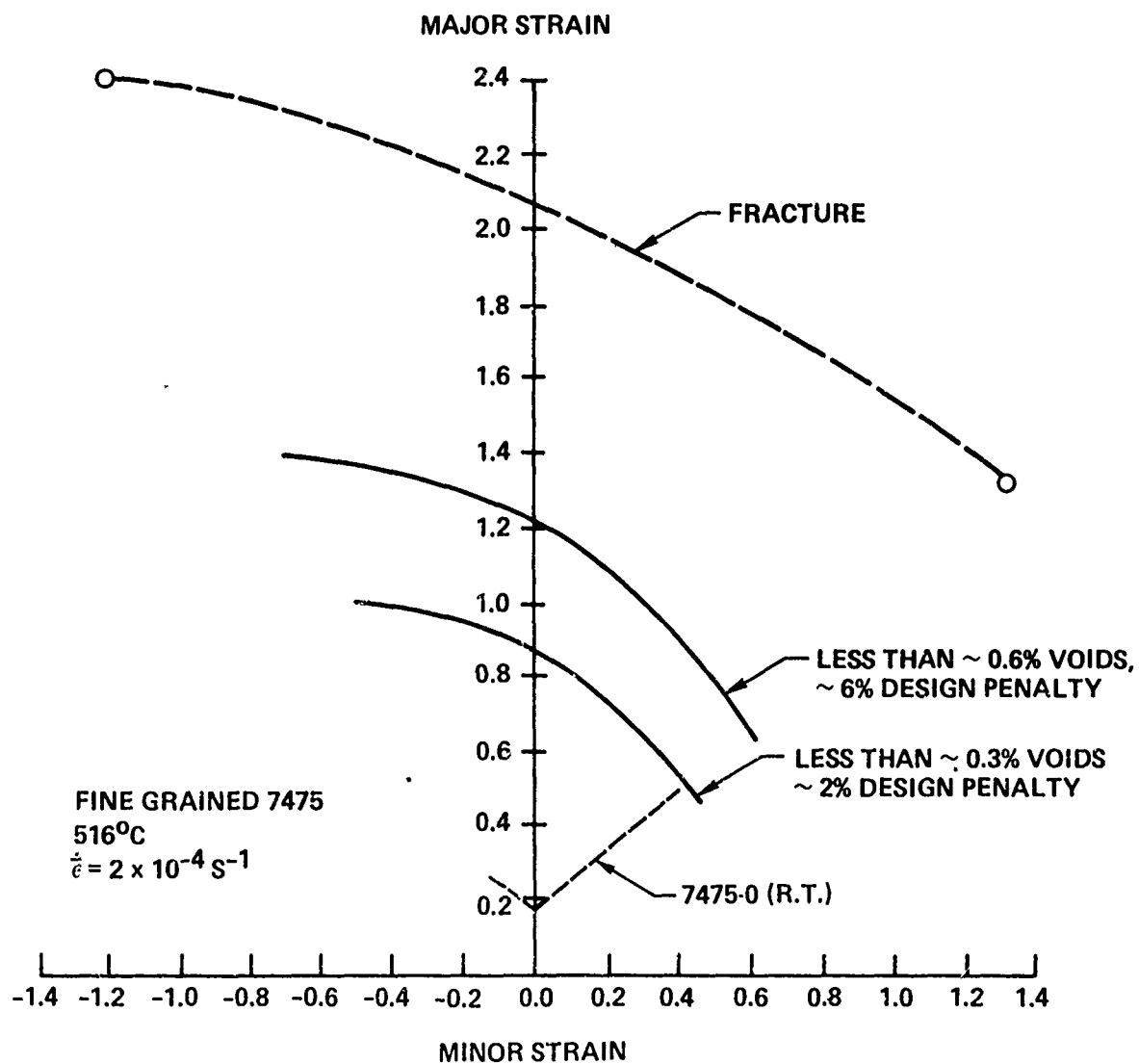
Fig. 17   Forming limit diagram representing the superplastic formability of 7475 Al at 516°C and 2 × 10^{-4} s^{-1}.

64
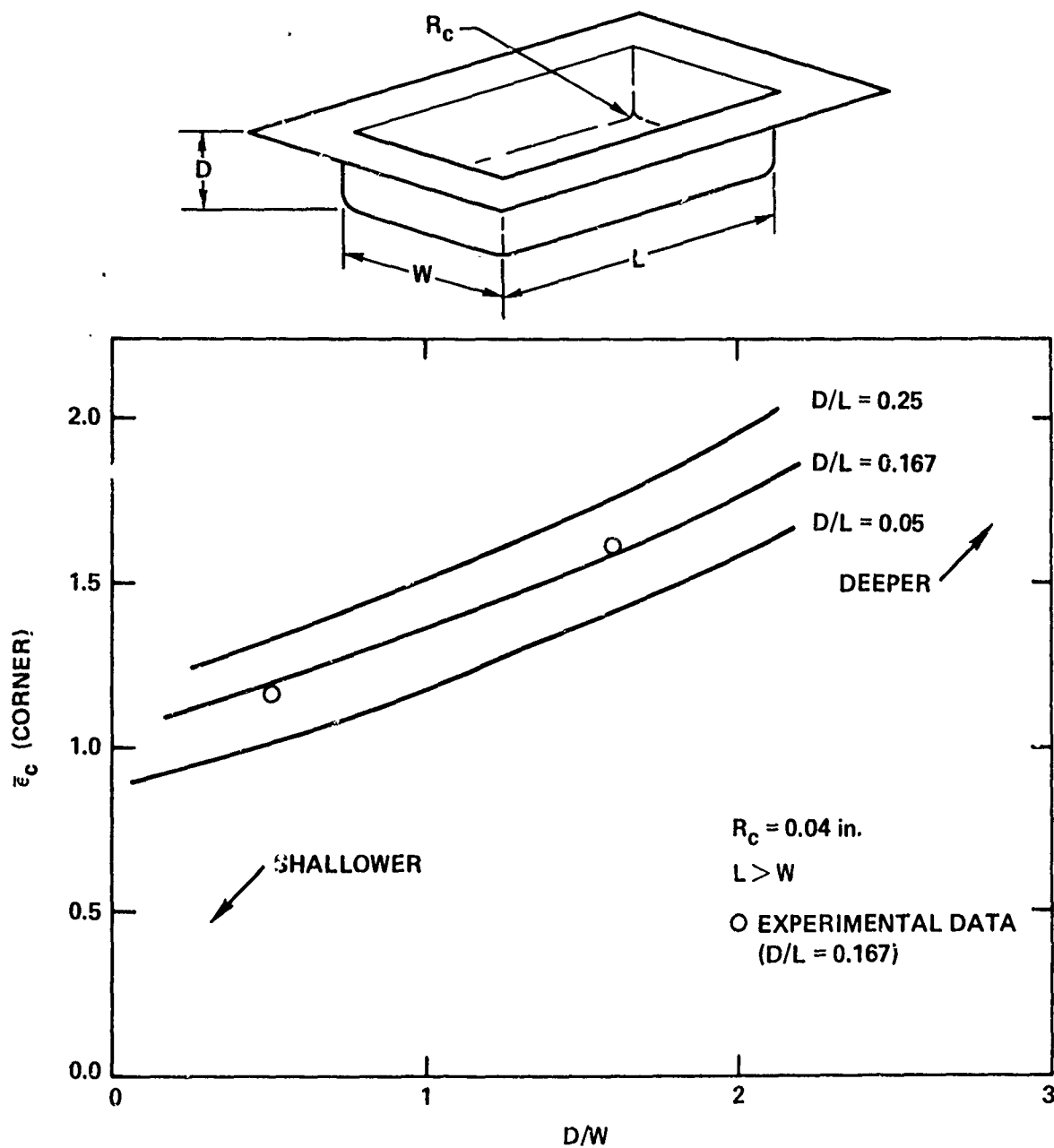
Fig. 18   Analytical prediction of strain in the corner of a rectangular shape
          as compared to experimental results.
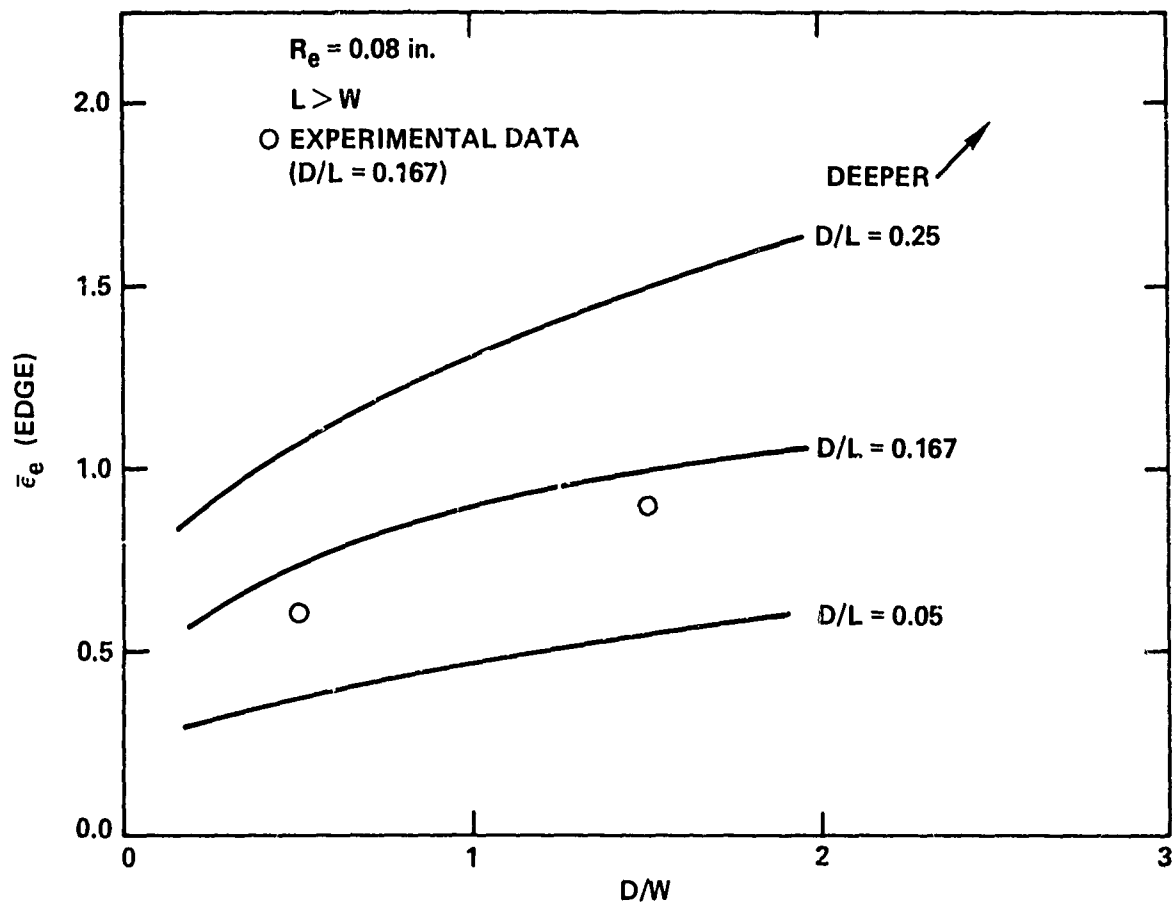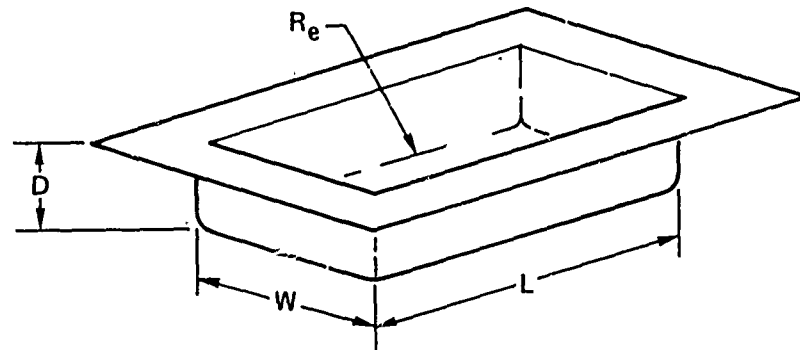
Fig. 19   Analytical prediction of strain at the edge of a rectangular shape
as compared to experimental results.

66

points compare favorably with the analytical curves established for the different rectangular geometries. From these results, cavitation limits can be established and finally the design penalty resulting from the SPF/cavitation interaction determined. In this manner, analytical information can be provided to facilitate the decision whether SPF is viable for a specific component prior to a large commitment of capital for forming dies.

Considering the magnitude of cavitation density, Figs. 6, 9, 10 and 15 all show void volume to increase with true effective strain. However, it is the magnitude of strain vs void volume level that is of practical interest for superplastic forming of structural components. In two other programs, two large aircraft components, an APU door and a T-39 Sabreliner frame, were superplastically formed using 7475 Al.[16,17] These parts are shown in Figs. 20 and 21 with effective strains noted on each figure. In spite of the large draw over a male die for the T-39 frame, (maximum depth/ width ratio equal to ~ 1.7), effective strains were less than 1 at all locations. For test parameters used in forming these two parts, 516°C and 2×10^{-4} s^{-1}, the results in Fig. 15 would predict cavitation levels to be less than ~ 0.3%. The design penalty for this level of cavitation, Fig. 17, would be an ~ 2% reduction in mechanical properties in only the most highly strained regions. It can be concluded from these results, that even without special precautions, the design penalty necessary to offset cavitation would be small for many components; even for components of relatively severe geometry.

This report has presented results that show how cavitation in 7475 AL is influenced by test variables associated with the SPF process. It has shown

67
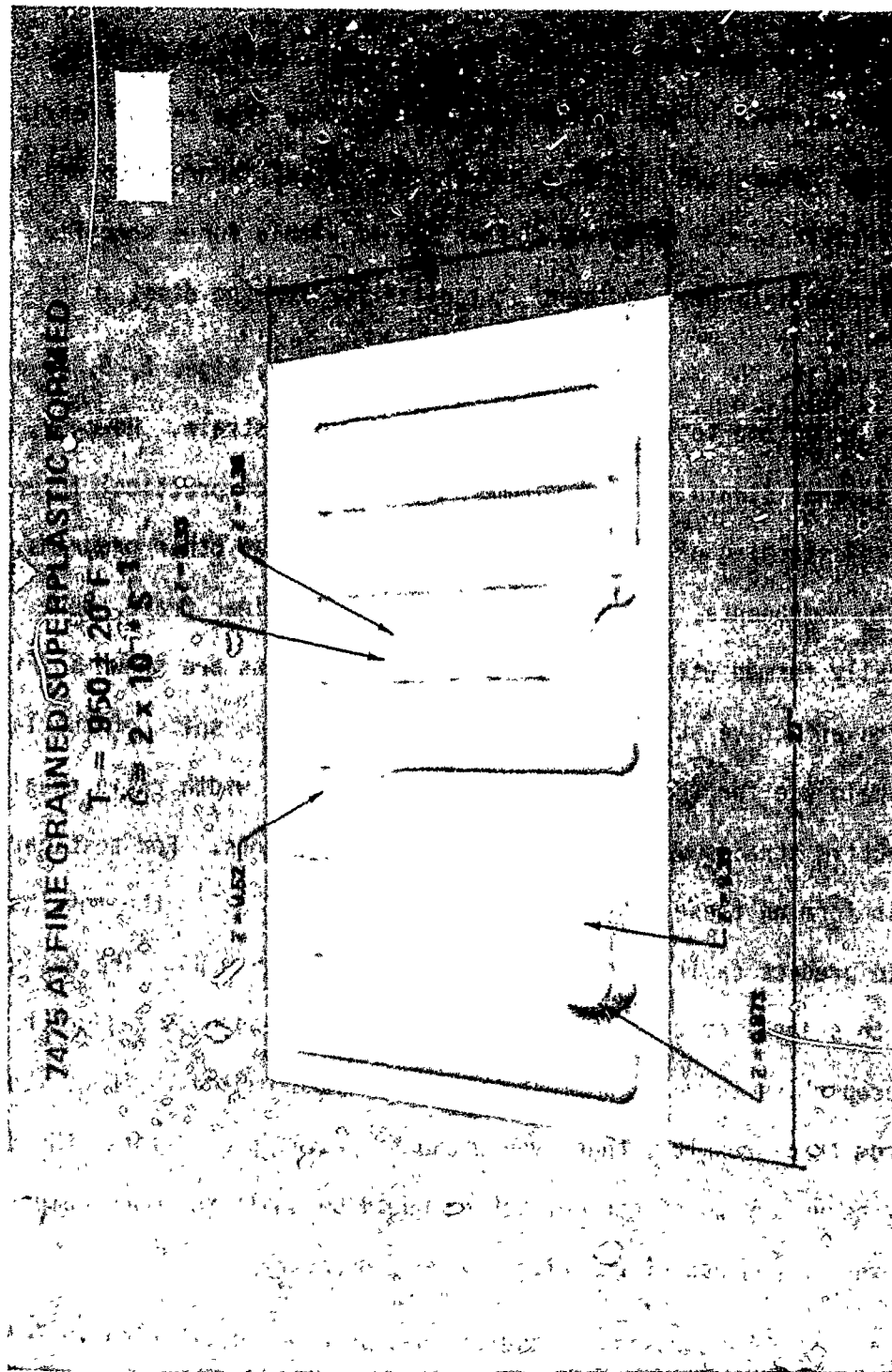
Fig. 20   Superplastic forming of an aircraft APU door with 7475 Al illustrating the resulting effective strains.
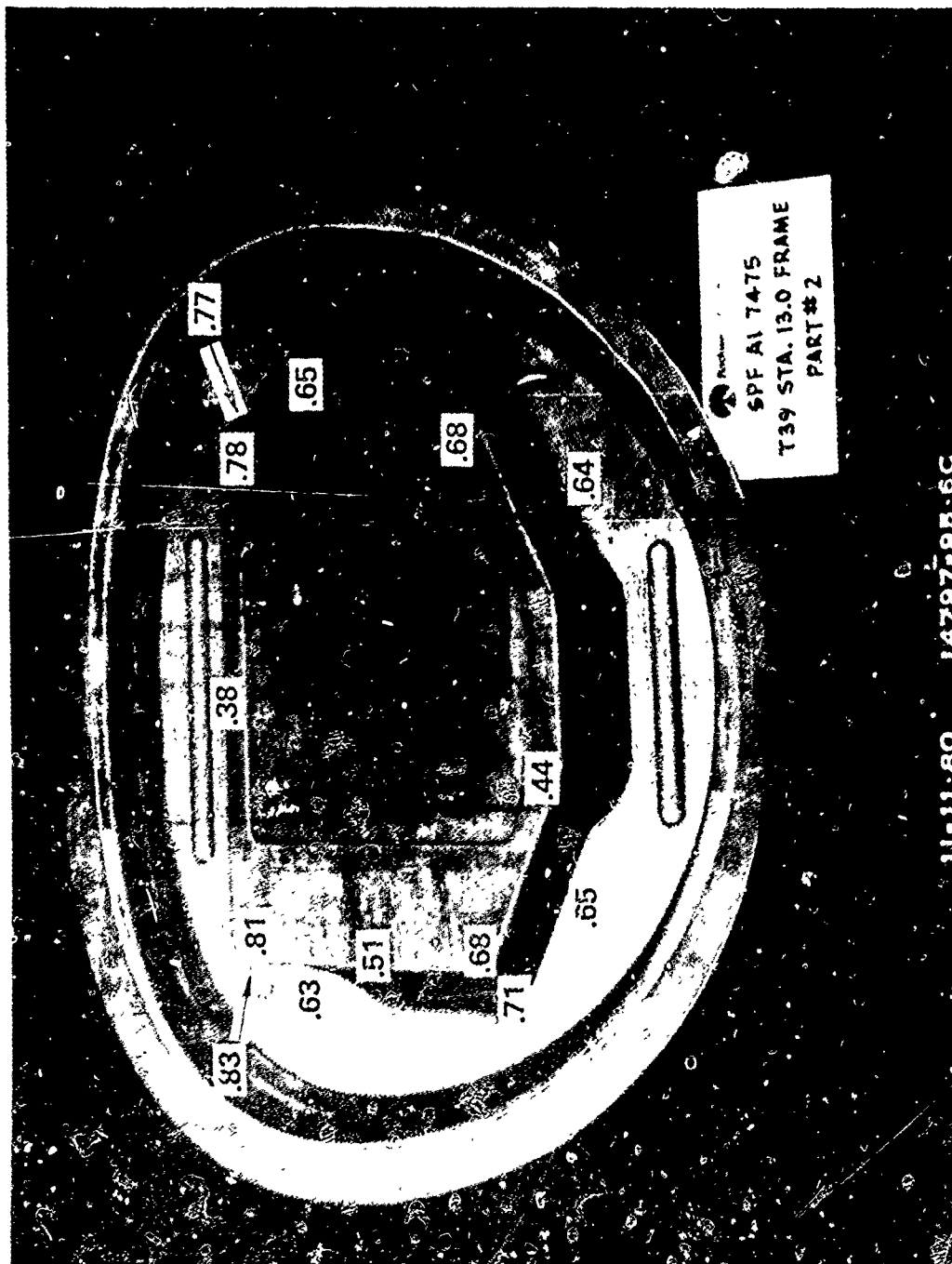
Fig. 21   Superplastic forming of the T-39 forward frame with 7475 Al
illustrating the resulting effective strains.

that with the appropriate selection of strain rate, temperature and extent of strain, cavitation can be held to levels below which mechanical properties are only slightly affected. This conclusion holds for even relatively complex, deep-draw aircraft components. Thus far there has been no mention of techniques to reduce or eliminate cavitation. However, a practical procedure has been developed where-by the level of cavitation can be controlled during superplastic forming by superimposing a hydrostatic state of stress during forming.[18] This procedure has been shown to eliminate cavitation entirely if the hydrostatic pressures are programmed to increase proportionately with the flow stress and concurrently mechanical properties are unchanged for subsequent superplastic forming and aging heat-treatments. Additionally, preliminary efforts have shown that appropriate heat-treatment procedures can result in a reduction in cavitation,[19] Thus, in conclusion it may be stated that not only can cavitation be maintained at low levels by the appropriate selection of forming variables but cavitation may also be reduced or eliminated by appropriate test and heat-treat procedures.

3.6 CONCLUSIONS

1. Within the temperature range of 499 to 527°C, cavitation density decreases with increasing temperature during superplastic forming.

2. Cavitation density as a function of true strain shows a maximum at a strain rate of 1 to 3×10^{-4} s^{-1}, whereas at faster and slower strain rates, cavitation density decreases. This maximum in cavitation rate with strain rate also corresponds to the maximum strain rate sensitivity index m.

3. Strain state conditions of uniaxial, plane strain, unequal biaxial and equibiaxial show no difference in their affect on cavitation rate as a function of effective strain. Therefore, it is possible to predict the cavitation density of complex shapes based upon uniaxial tensile behavior.

4. With increasing strain, cavitation density increases. However, cavitation may be maintained at low levels by the appropriate selection of superplastic forming variables. Accordingly, the resultant effect of cavitation on mechanical properties can be negligible.

71

5. Procedures have been developed to predict strains that are created in a component during superplastic forming. Using these models with appropriate forming limits data, the design penalty associated with cavitation can be predicted in advance of experimental forming trials. Data presented herein illustrate that even without special precautions, the design penalty necessary to offset cavitation would be small for many components.

3.7 ACKNOWLEDGMENTS

3.8 REFERENCES

1. J.A. Wert, N.E. Paton, C.H. Hamilton and M.W. Mahoney, Submitted to Met. Trans. July 7, 1980.

2. U.S. Patent 4,092,181, May 30, 1978, N.E. Paton and C.H. Hamilton, Method of Imparting a Fine Grain Structure to Aluminum Alloys Having Precipitating Constituents.

3. U.S. Patent 4,222,797, Sept. 16, 1980, C.H. Hamilton, M.W. Mahoney and N.E. Paton, Method of Imparting a Fine Grain Structure to Aluminum Alloys Having Precipitating Constituents.

4. A.K. Ghosh and C.H. Hamilton, 5th International Conference on the Strength of Metals and Alloys, Achen W. Germany, August 27-31, 1979.

5. W.A. Backofen, I.R. Turner and D.H. Avery, Trans. ASM 57, 980 (1964).

6. A.K. Ghosh and C.H. Hamilton, Met. Trans. 10A, p. 699, June 1979.

7. A.K. Ghosh and C.H. Hamilton, Proceedings of ASM Materials and processing Congress, Fall ASM Meeting, Chicago, November 1979.

8. C.C. Bampton and J.W. Edington, "Microstructural Study of Cavities Formed During Superplastic Deformation of Fine Grained 7475 Al," this document.

9. A.K. Ghosh, unpublished research.

10. D.W. Livesey and N. Ridley, Met. Trans. 9A, p. 519, April 1978.

11. N. Ridley, C.W. Humphries and D. Livesey, 4th International Conference on the Strength of Metals and Alloys, Nancy, France, p. 433, 1976.

12. C.C. Bampton and J.W. Edington, "Effect of Superplastic Deformation on Subsequent Mechanical Properties of Fine Grained Al," this document.

13. S.P. Keeler, Paper No. 680092, Presented at the SAE Automotive Engineering Congress, Detroit, January 1968.

14. G.M. Goodwin, Paper No. 680093, Presented at the SAE Automotive Engineering Congress, Detroit, January 1968.

15. A.K. Ghosh and C.H. Hamilton, Rockwell International, Internal Report to NAAD, IDWA L4222L, SC6184.14FR, February 1979.

16. Rockwell International Science Center Independent Research and Development, project No. 812, p. 331, 1980.

17. U.S. Air Force, Air Force Systems Command, Aeronautical Systems Division, Wright-Patterson AFB, Contract No. F33615-80-C-3240, "Superplastic Aluminum T-39 Frame."

18. C.C. Bampton, M.W. Mahoney, C.H. Hamilton, A.K. Ghosh and R. Raj, "Suppression of Cavitation by the Application of Confining Gas Pressure During Superplastic Deformation of Fine Grained 7475 Al."

19. Rockwell International Science Center Independent Research and Development, project 812, p. 339, 1980.

SECTION 4 A MICROSTRUCTURAL STUDY OF CAVITIES FORMED DURING SUPERPLASTIC DEFORMATION OF FINE GRAINED 7475 Al

C. C. Bampton and J. W. Edington

Rockwell International Science Center
Thousand Oaks, California 91360

ABSTRACT

The observations suggest that, with the optimum superplastic deformation conditions, cavity nucleation is generally the rate determining step in the overall development of cavitation with strain. Cavities do not generally form at even the largest of the common single phase inclusion particles unless forming conditions are such as to significantly increase the flow stress. It appears that, as well as local stress concentrations, additional effects are required, such as temperature induced particle decohesion and internal gas evolution, in order that cavities may grow to stable sizes. Such conditions may exist at certain two phase inclusion particles in the 7475 Al alloy. Suitable modifications to the standard alloy processing may therefore be devised which result in even lower rates of cavitation at the optimum superplastic forming conditions.

4.1 INTRODUCTION

Development of intergranular cavitation during superplastic deformation may be legitimately discussed under two headings: cavity nucleation and cavity growth.

4.1.1 Cavity Nucleation

From evidence in many superplastic alloy systems, it is generally held that cavities initiate at second phase particles in grain boundaries by a combination of sliding and diffusion. The second phase particles are thought to offer resistance to grain boundary sliding. Cavities have also been observed to form at triple junctions and at α/β interfaces in aluminum bronzes (1). Nucleation sites were identified as α/β interfaces, grain boundary particles and triple junctions in α/β brasses (2,3,4). Cavitation has been induced during superplastic deformation of the Pb-Sn eutectic, which does not normally cavitate, by incorporating a hard intermetallic phase (5). It has been noted (6), however, that nucleation of cavities at triple junctions alone is theoretically unlikely, unless other factors are introduced, such as segregation of trace impurities to grain boundaries. Several studies (7,8,9) have shown that cavitation is at a maximum when the strain rate sensitivity is at a maximun. Thus, it has been proposed (6) that grain boundary sliding is necessary to induce the initial breakdown of the particle/matrix interface. A model has been developed (10), based on decohesion of the particle, that predicts nucleation preferentially at large particles, which is generally

consistent with experimental observations in the literature. Furthermore, since thermodynamic considerations indicate that there is a minimum radius at which a cavity nucleus is stable against shrinkage, it may be expected that there is a minimum effective particle size.

4.1.2   Cavity Growth

Growth of stable sized void nuclei to large cavities may be controlled by diffusion or deformation during superplastic deformation. There has been considerable argument in the literature on the controlling mechanism of intergranular cavity growth (11,12,13,14) although it has been mainly concerned with creep deformation, or at best an extrapolation of creep data to the much higher strains encountered in superplastic deformation (15). Diffusion growth is controlled by grain boundary or bulk vacancy diffusion and deformation growth is controlled by power law creep of the surrounding matrix. Various studies have been carried out to determine the stress dependency of cavity growth during creep in order to distinguish the mechanism involved. It has been pointed out (16), however, that these analyses generally assume an already formed cavity structure in the grain boundary and do not take into account the stress dependency of cavity nucleation. The concensus of opinion in the literature (15,6) seems to be that deformation is the dominant factor in superplastic cavity growth.

Interactions between growing intergranular cavities and cavity interleakage, necking of ligaments between cavities and macroscopic failure

82

generally, are not considered in this section, but are discussed elsewhere in this document. (17).

The present microstructural study of cavitation in fine grained 7475 aluminum has concentrated on the nucleation stage since there is a greater chance of successfully reducing the rate of cavitation by control of the nucleation stage than of the growth stage.

4.2 MATERIALS

This work involved only 7475 Al. The compositional limits are shown in Table 1. The material was processed to hot rolled plate, 20 mm thick, by ALCOA Laboratories, followed by fine grain processing (18) at the Science Center. Final grain sizes were ~14 μm diameter in the rolling plane and ~8 μm in the short transverse direction.

Table 1. Composition Limits for 7475 Aluminum (wt. %)

Si	Fe	Cu	Mn	Mg	Cr
0.10 max	0.12 max	1.2-1.9	0.6 max	1.9-2.6	0.18-0.25

Zn	Ti	Others, Each	Others, Total	Al
5.2-6.2	0.06 max	0.05 max	0.15 max	Remainder

4.3 EXPERIMENTAL

Standard optical, scanning electron and transmission electron microscopy techniques were used to examine samples of fine grained 7475 Al that had undergone various amounts of superplastic deformation and thermal cycling treatments. Optical microspecimens examined for intergranular cavitation were cold epoxy resin mounted and were prepared by mechanical polishing and ultrasonic cleaning. The last stages of mechanical polishing usually involved kerosene lubricated diamond wheels. Electro polishing and etching were generally avoided so that cavities could be easily identified and were not excessively affected in size or shape by the sample preparation. An ion-beam etching technique (19) was used in some instances to examine cross sections of very small cavities.

In order to identify specific areas on microspecimens, microhardness indentations were used as markers. To determine depths of surface removal during final stage diamond re-polishing, the depths of microhardness indentations were measured by means of a high magnification optical microscope with small depth of field and vernier calibrated fine focus adjustment.

The fine grain processing and constant strain rate superplastic uniaxial tensile testing techniques have been described elsewhere (18,20).

This study has concentrated on the nucleation and growth of intergranular cavities during deformation at 516°C and a strain rate of 2×10^{-4} s^{-1}. These conditions have been established (20) as giving the

87

optimum formability as measured by both uniformity of sheet thinning and rupture strain.

4.4 RESULTS AND DISCUSSION

4.4.1 Distribution of Cavities

There are two significant and distinctive features of cavitation in the fine grained 7475 Al when strained at the optimum superplastic forming conditions (T = 516°C, ε = 2 × 10^{-4} s^{-1}). Firstly, cavity growth with strain to sizes detectable by density or optical metallography is very slow initially but increases to a relatively rapid rate over a small, critical strain range. This is shown in Fig. 1 where the volume fraction of cavities has been measured by density. Secondly, the cavitation tends to take the form of isolated, irregularly distributed cavities, which may grow to large diameters, rather than the more usual uniformly distributed and relatively closely spaced cavities found in other cavitating superplastic alloys. This is shown in Fig. 2. Groups of cavities are often found strung out in the longitudinal rolling direction. The progressive development of cavities with superplastic strain, shown in Fig. 2 suggests that the nucleation rate of new cavities is slow and the subsequent growth of stable sized cavities is relatively rapid. Figure 2c clearly shows the tendency for uneven distribution of cavities, especially at low strains. Cavities may be concentrated in regions near one, or both, surfaces, or in the sheet's center. Specimens showing high superplastic ductilities tend to show a continuous increase in the number of cavities as well as progressive growth of the existing cavities, with increasing strain up to the fracture strain. The inconsistent nature of cavity nucleation makes meaningful quantitative measurements of nucleation rate

89
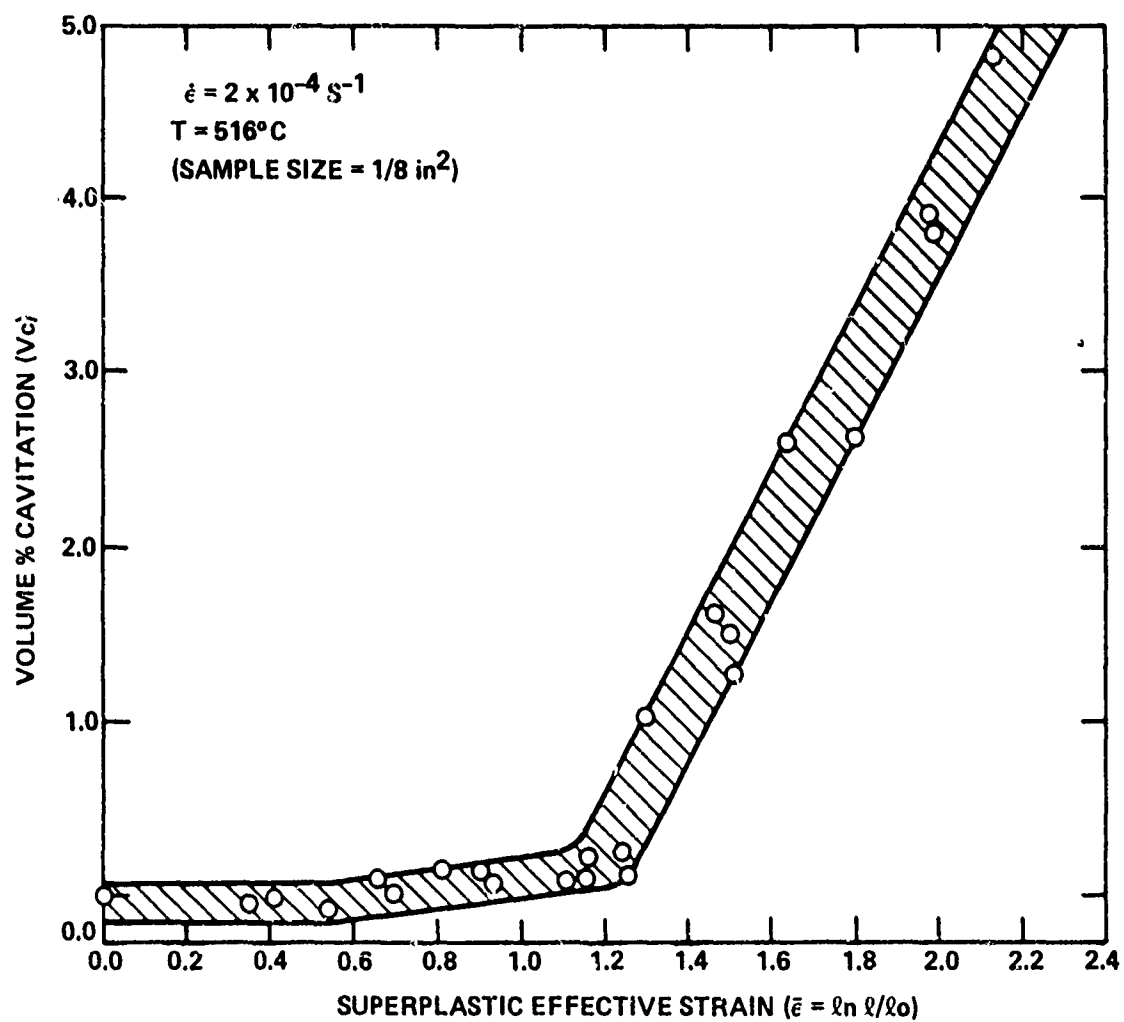
Fig. 1 Development of cavitation with superplastic uniaxial tensile
strain measured by density.

90

(a)
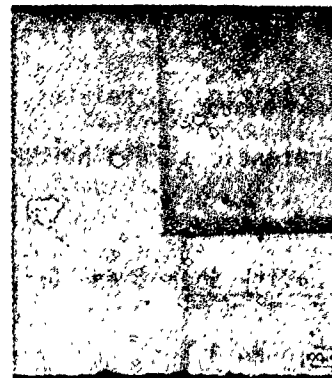
(b)

(c)
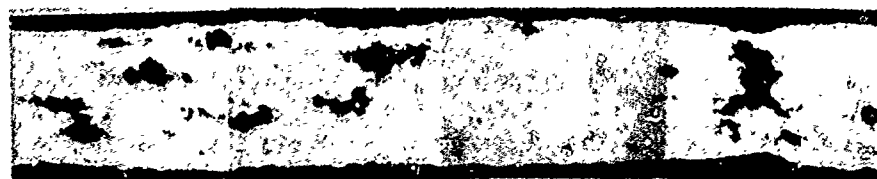
(d)

Fig. 2   Cross sections (L-ST) showing cavitation development
with superplastic uniaxial tensile strain (T = 516°C,
$\dot{\epsilon} = 2 \times 10^{-4}$ s^{-1}) (a) ϵ = 0 48, (b) ϵ = 0.54, (c) ϵ = 0.66,
(d) ϵ = 2.05. Mechanically polished to 1/4 μm diamond.

91

difficult. However, to a first approximation, it appears that the increase in number of cavities correlates with the increase in flow stress, which results from superplastic strain hardening in this material (20).

4.4.2   Cavity Shapes and Growth Directions

Figure 3 shows two series of optical micrographs obtained by mechanically polishing through small, deep cavities. Such cavities can be found in longitudinal-short transverse (L-ST) microsections after any superplastic strain between about 0.5 and fracture and are generally triangular shaped. A series of photographs of each cavity was taken after repolishing to remove 3-4 μm from the specimen surface between photographs. Series 3a and b show similar characteristic features. An initially single triangular shape becomes two neighboring triangular shapes which join to form a dog-bone shape and finally changes back to two separate shapes followed by a single triangular shape. The triangular and dog-bone shapes strongly suggest that these types of cavities grow by "unzipping" of grain boundaries from triple points, as shown in Fig. 4. The maximum cavity dimensions are generally found to follow the proportions shown by the two cavities in Fig. 3, i.e., $D_L \simeq 40$ μm, $D_{LT} \simeq 50$ μm, $D_{ST} \simeq 25$ μm. Thus these characteristically shaped cavities have their longest dimension in the LT direction and the shortest in the ST direction. Figures 5 and 2d, which show cavities formed after relatively high superplastic strains in the rolling plane of the sheet (L-LT) and thickness section (L-ST), respectively, confirm the generality of these cavity shapes. The proportions of the maximum cavity dimensions conform qualitatively to the
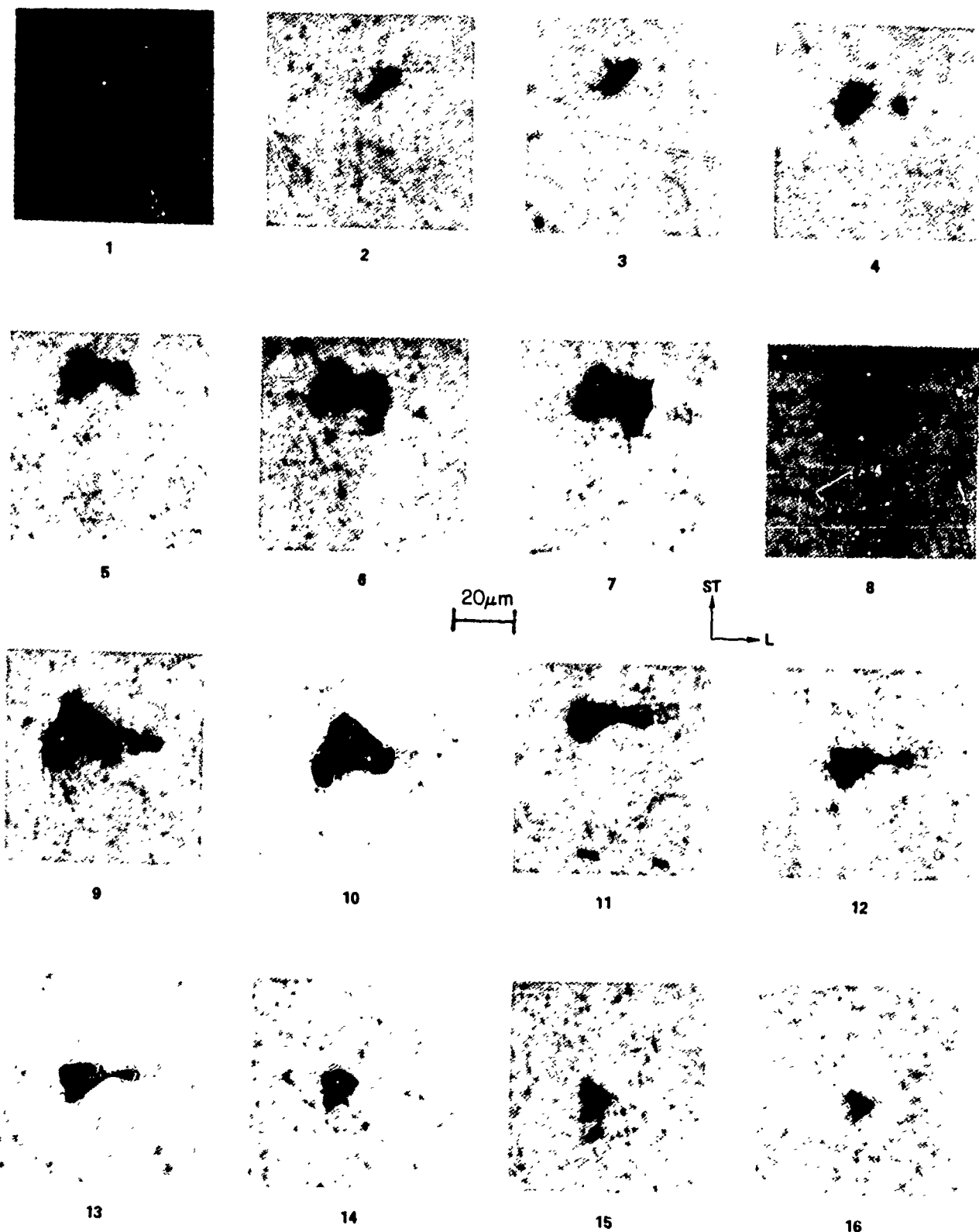
Fig. 3 (a) Cross sections through a single cavity in fine grained
7475 Al after superplastic uniaxial tensile strain,
($\varepsilon = 0.66$, $T = 516°C$, $\dot{\varepsilon} = 2 \times 10^{-4}s^{-1}$). Approximately 4 μm
of surface removed between each photograph (in LT direction).
Mechanically polished to 0.05 μm Al_2O_3.
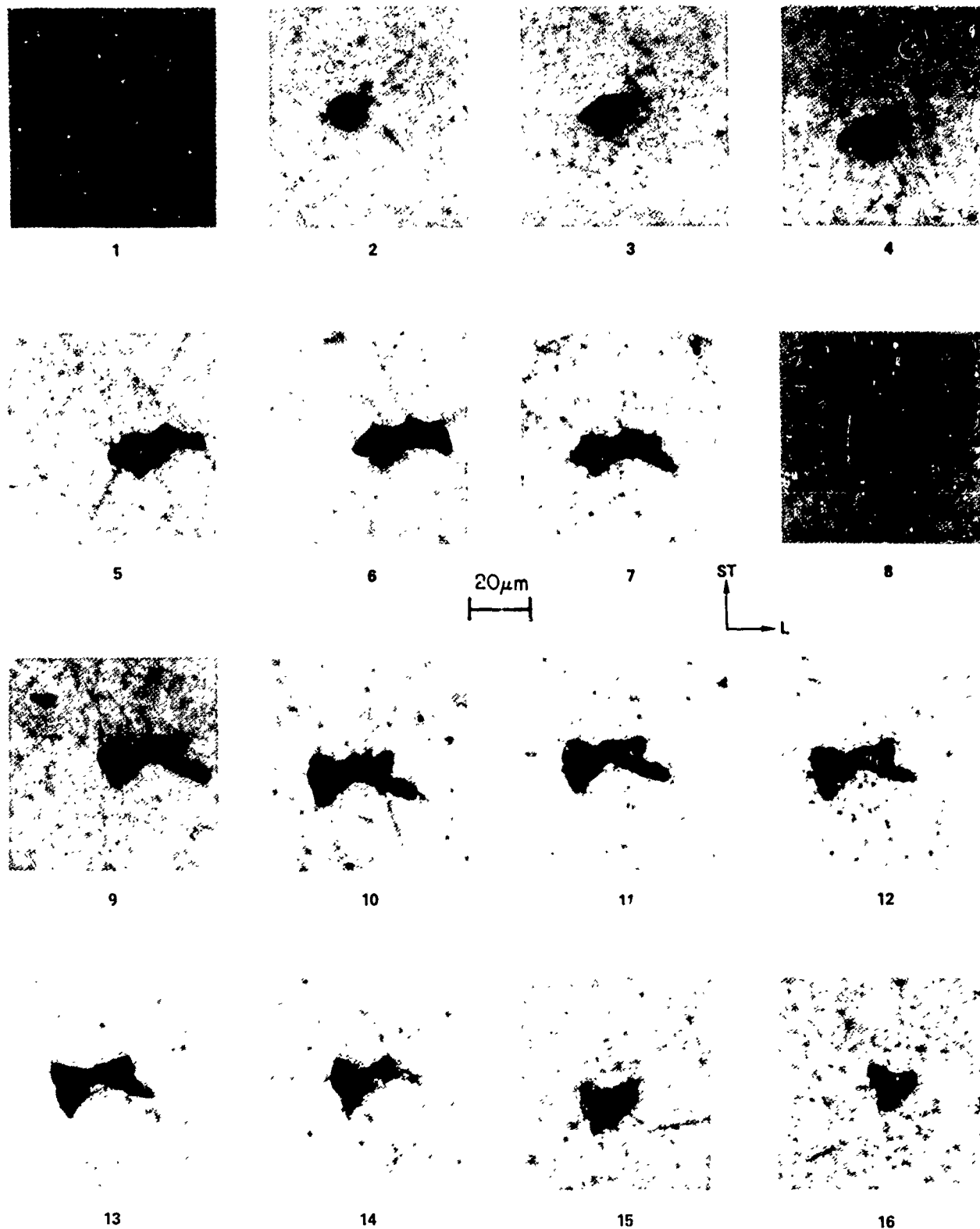
Fig. 3   (b) Similar series to 3a with a different cavity.
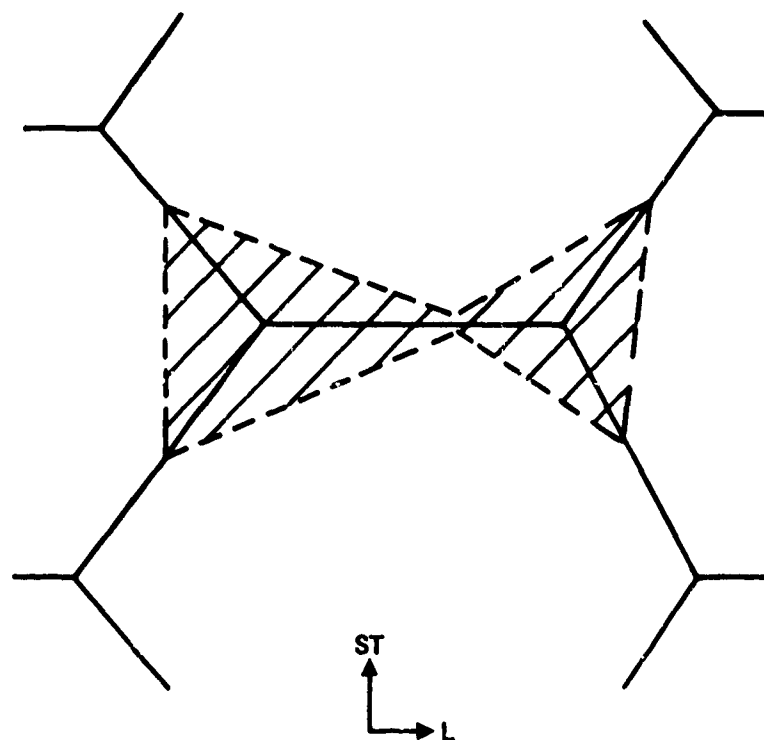
Fig. 4   Schematic drawing showing the formation of a "dog bone" shaped cavity by interlinking of two triple point cavities.
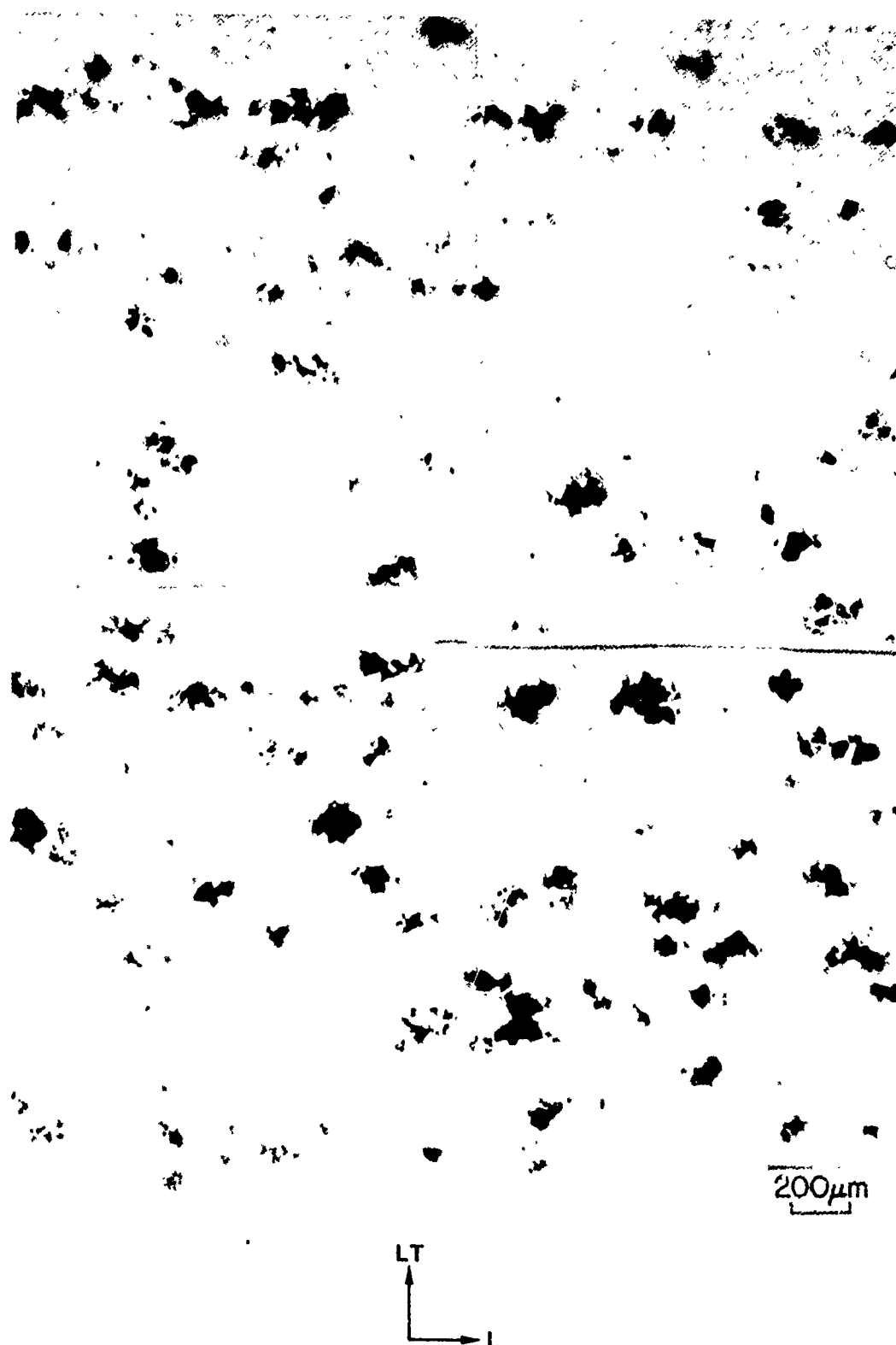
Fig. 5   Rolling plane cross section of fine grained 7475 Al after
          superplastic uniaxial tensile strain, (ε_e = 1.45, T = 516°C,
          $\dot{\varepsilon}$ = 2 × 10^{-4} s^{-1}). Volume % cavitation ≅ 1.64%. Mechanically
          polished to 1/4 um diamond.

general grain shapes after superplastic straining in uniaxial tension. It is not felt that there is sufficient exaggerated growth in the LT direction to prefer a diffusional cavity growth mechanism, rather than a plasticity controlled growth mechanism. The classical stress driven diffusion growth arguments would predict cavity growth predominantly in a direction transverse to the tensile axis whereas plasticity controlled growth predicts cavity growth predominantly parallel to the tensile axis. It seems likely that cavity growth occurs by both plasticity and diffusion. The large amount of grain boundary sliding causes plastic decohesion along grain boundaries, particularly triple boundary lines and this is followed by swelling of the grain boundary crack by some further plastic deformation and vacancy diffusion. The obviously irregular shapes shown by all cavities (e.g., Fig. 5) suggests a very strong influence of grain boundary sliding and decohesion on cavity growth.

4.4.3 Inclusions and Cavitation

The first observation to be made concerning the relation between inclusion particles and superplastic cavitation is that, in the fine grained 7475 Al superplastically strained at optimum forming conditions, cavities do not appear to form at all of the large inclusions. As an example, an L-ST microsection may show a fairly uniform distribution of inclusion particles with measured densities of 390 particles ($\geq$ 3 μm diameter) per mm^2 and 40 particles ($\geq$ 10 μm diameter) per mm^2. After superplastic deformation in uniaxial tension ($\dot{\varepsilon} = 2 \times 10^{-4}$ s^{-1}, T = 516°C) to a strain of 0.7, one area

97

may show 5 cavities per mm^2 and another 50 cavities/mm^2. Even at very high strains, as shown in Fig. 2d, relatively large areas may be seen which do not contain any cavities. Numerous examples may be found in polished microsections of superplastic cavities which are apparently associated with large inclusions, such as that shown in Fig. 6. Generally, however, it may be seen that the cavities are merely impinging on the large inclusions and do not extend along the inclusion/matrix interfaces. The cavities extend preferentially along the matrix grain boundaries. Figures 3a and 6 show examples of this. Figure 3b is an example of a cavity that has apparently no inclusion associated with it. In this case it is possible that inclusion particles did exist loosely inside the cavity and were lost during mechanical polishing.

Inclusion particles may be cracked by the rolling deformation, as shown in Figs. 7a and b. These cracks would seem to be obvious pre-existing nuclei for subsequent superplastic cavities. No evidence has been found, however, to suggest that such crack opening during the early stages of superplastic deformation does occur. In fact, it is generally difficult to find any cracked particles after small superplastic strains. There are instances, however, where the cracks have been partially, or wholly, filled in with matrix material, as shown in Fig. 7c and d. It is not clear at which stage of processing or forming this may have occurred.

Figures 8 and 9 indicate the complex range of inclusion phases and shapes present in the 7475 Al alloy. These phases have not yet been identified. The different etching responses, as indicated in Figs. 8 and 9, are not

(a)

ST

$\uparrow$

$\longrightarrow$ L
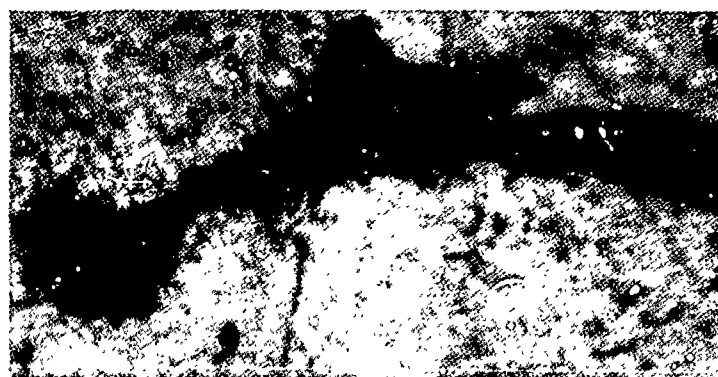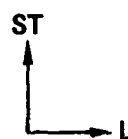
$\vdash$ 10μm $\dashv$
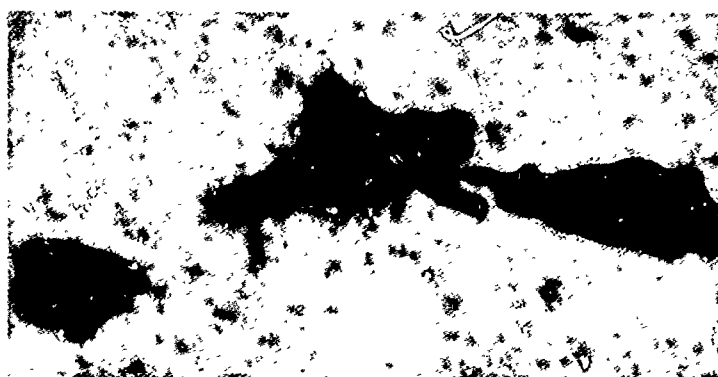
(b)

Fig. 6   Cross section showing a cavity in fine grained 7475 Al after
superplastic uniaxial tensile strain (ε_e = 0.66, T = 516°C,
$\dot{\varepsilon}$ = 2 × 10^{-4} s^{-1}). Mechanically polished to 0.05 μm
Al$_2$O$_3$. 4 μm surface removed between (a) and (b).

99
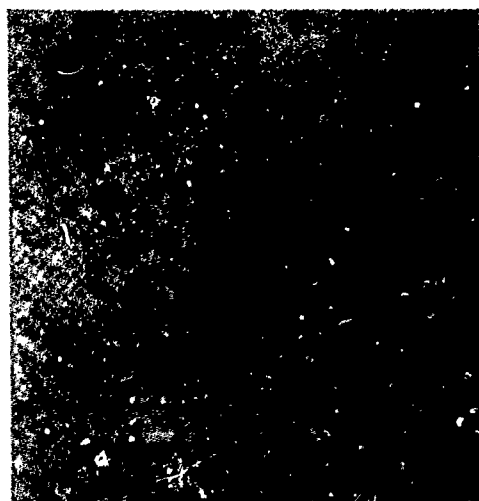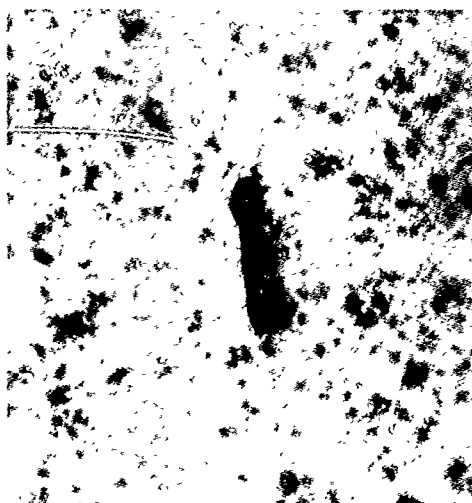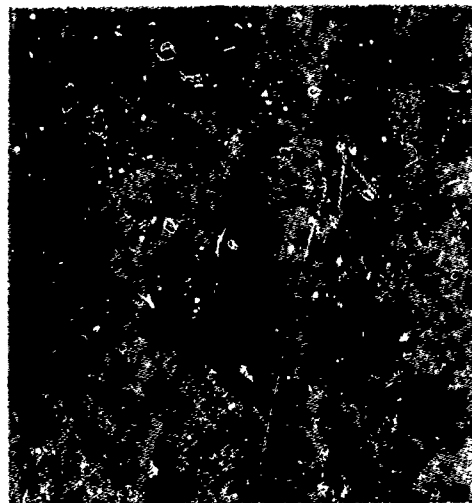
Fig. 7   Cross sections showing large cracked inclusion particles in
fine grained 7475 Al. (a) and (b) as warm rolled, (c) and (d)
after superplastic uniaxial tensile strain, (ε = 0.35,
T = 516°C, $\dot{\varepsilon}$ = 2 × 10^{-4} s^{-1}). Mechanically polished to
0.05 µm Al_2O_3.

100
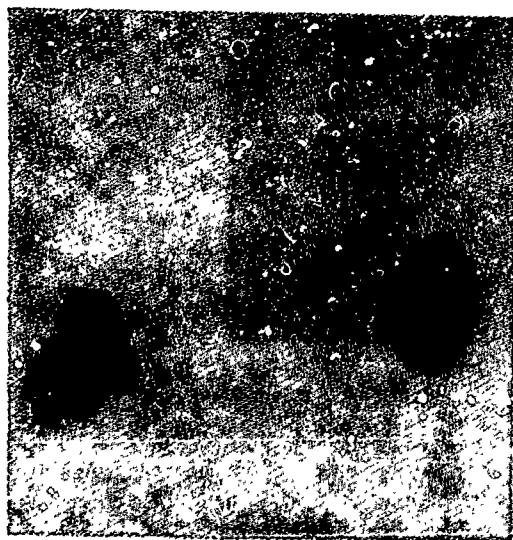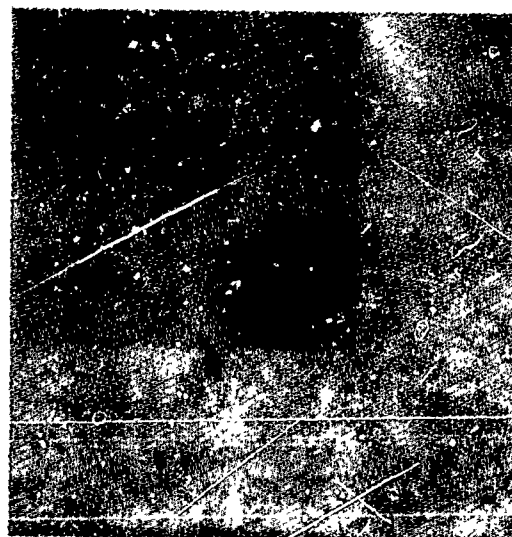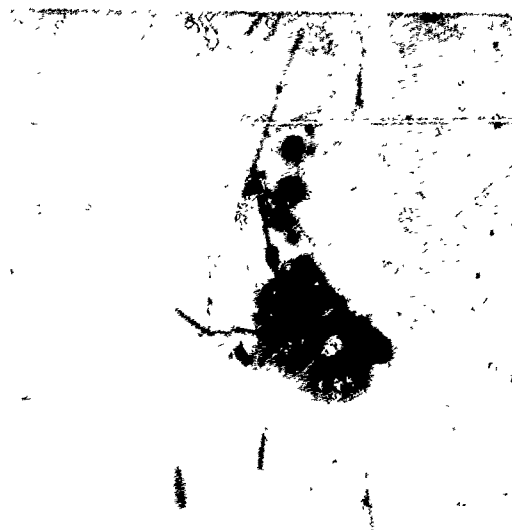
10μm

Fig. 8   Cross section (L-ST) of fine grained 7475 (T6) showing
different types of inclusion particles. As electropolished.

101
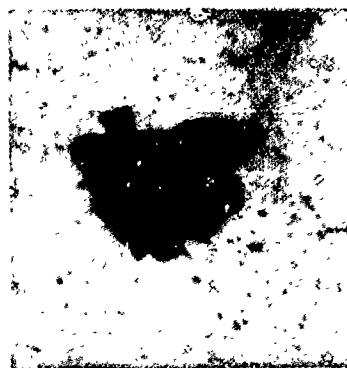
Fig. 9 Cross section (L-ST) of fine grained 7475 Al (T6) showing
different types of inclusion particles. NaOH/HF etch.

sufficient to unambiguously identify any of the phases. The most common inclusion phase, which generally includes the largest particles, is that shown in Figs. 8a and 9a.

Examination of material superplastically deformed to low strains has revealed very little cavitation, but Fig. 10 shows some cavities in material strained to 0.48. Figures 10a and b show cavities associated with two-phase inclusions, apparently the same as shown in Figs. 8b and 9b. Figure 10c shows a cavity associated with a bunch of small particles which again appear to be of two phases. The significance of the two-phase inclusions will be discussed further in Section 3.4.5.

4.4.4   Hydrogen Out-gassing at Elevated Temperatures

Figure 11 shows the progressive development of pores in the fine grained 7475 Al when soaked for increasing times (in molten salt) at the superplastic forming temperature (516°C) with no superplastic strain. The pores start to become optically visible between 30 and 60 minutes and increase in number and size up to 2 to 3 hours. Longer soaking times then tend to reduce the number of pores, although some of the largest may continue to grow for some time longer than 3 hours. Very few pores exist after soaking at 516°C for 24 hours or longer. Severe blistering of the sheet, as shown in Fig. 12, may occur concurrently with the internal pore growth and shrinkage, although this depends sensitively on the surface condition of the sheet and may, in some cases, be due to surface rolling defects. As shown in Fig. 13, the distribution of pores tends to be quite uneven and the maximum density

103

(a)

(b)

10μm

(c)

Fig. 10   Cross sections (LT-ST) of fine grained 7475 Al (T6) after
          superplastic tensile strain (ε_e = 0.48, T = 516°C,
          $\dot{\varepsilon}$ = 2 × 10^{-4} s^{-1}) showing small cavities associated with
          two-phase inclusions. NaOH/HF etch.

104
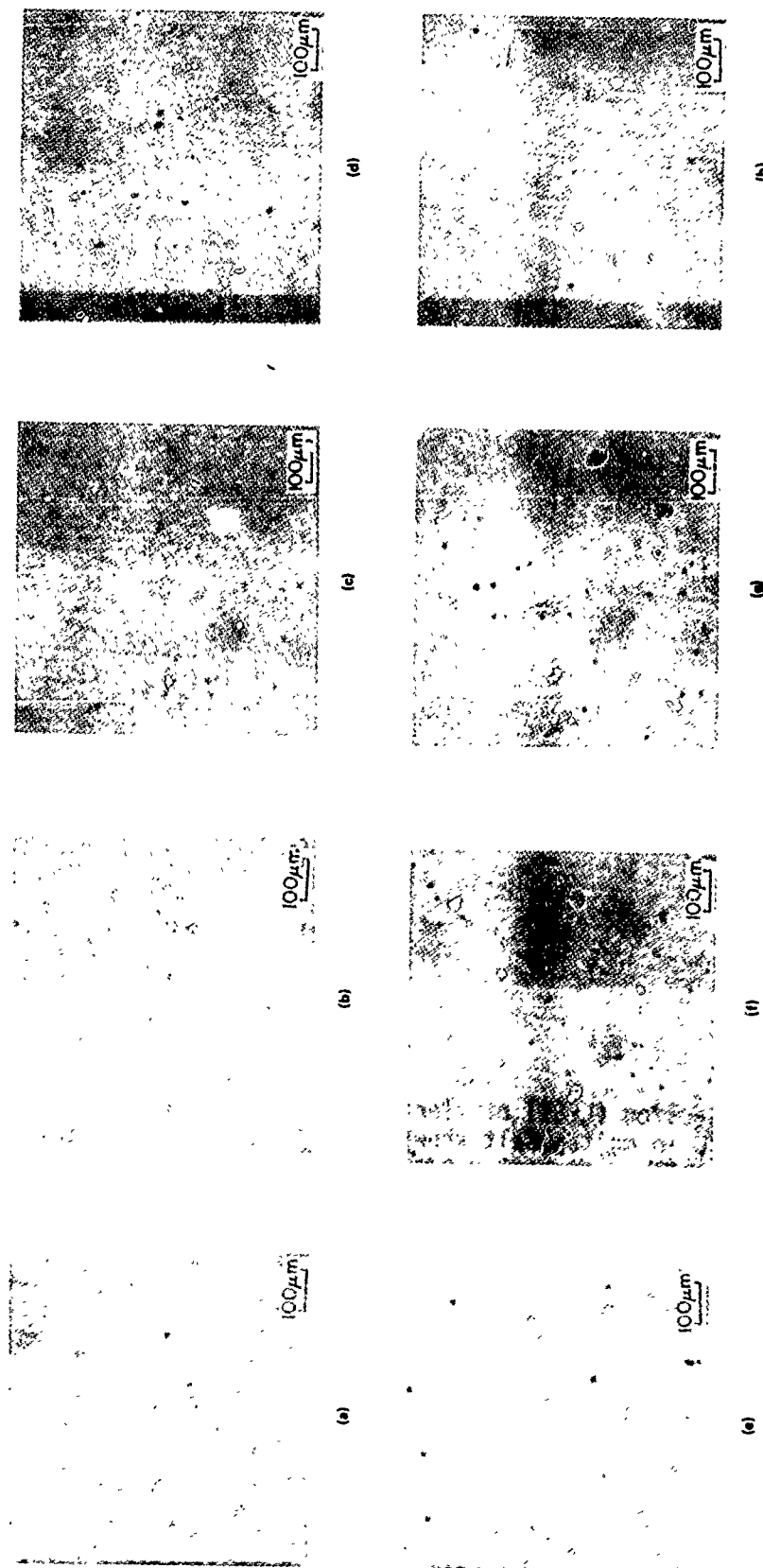
Fig. 11 Cross sections (L-ST) of fine grained 7475 Al after various times at 516°C in molten salt showing growth and shrinkage of pores: (a) As rolled, (b) 3 min, (c) 30 min, (d) 1 hour, (e) 2 hours, (f) 3 hours, (g) 9 hours, (h) 24 hours. Mechanically polished to 1/4 μm diamond.
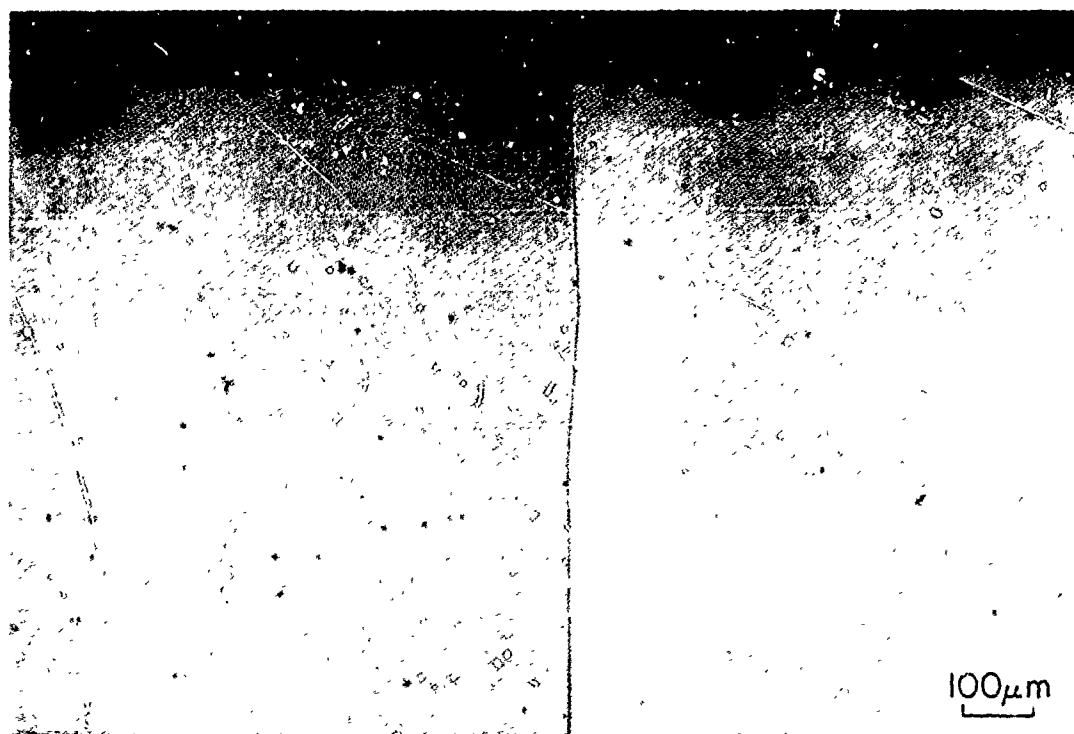
Fig. 12 Cross section (L-ST) of fine grained 7475 Al after 8 hours at 516°C in molten salt showing large surface "blisters". Mechanically polished to 1/4 μm diamond.
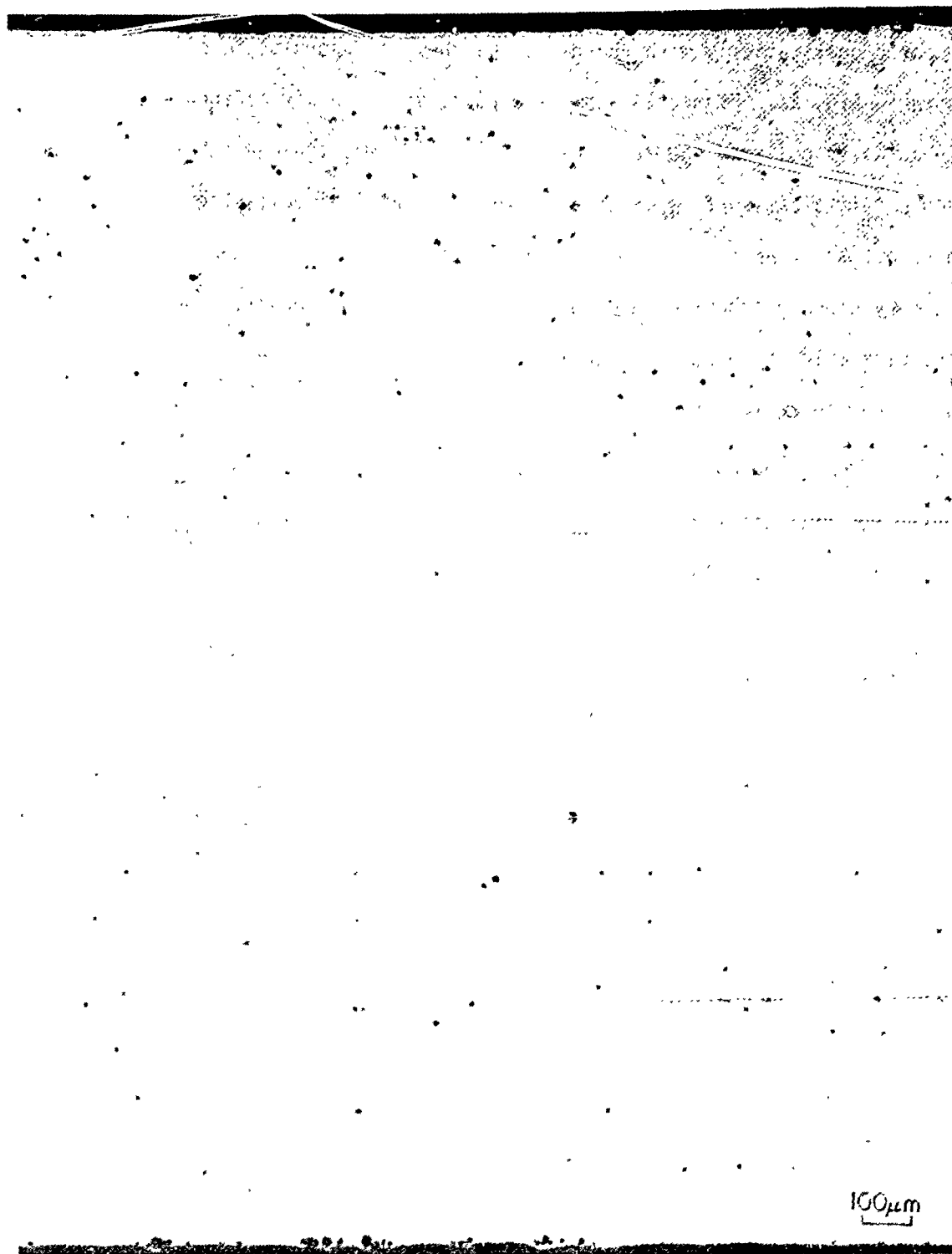
Fig. 13   Cross section (L-ST) of fine grained 7475 Al after 200 min
          at 516°C in molten salt. Mechanically polished to 1/4 μm
          diamond.

107

compares qualitatively with the denser patches of superplastic cavities, as shown in Fig. 2c. Figure 14 shows the pores more clearly defined. The mechanically polished sample, shown in Fig. 11e, was ion-beam etched so as to remove sufficient surface material to avoid mechanical polishing artifacts and to reveal the true features of the small pores. It can be seen that the pores are very closely spherical and in some cases contain centrally located particles which have become totally separated from the material. The internal pores grow to maximum sizes of about 16 μm diameter.

The evidence suggests that the high temperature annealing porosity is due to out-gassing of hydrogen. It has long been established (21) that aluminum and its alloys, in both the cast and the wrought form, almost invariably contain large numbers of microscopic spherical pores, which may be revealed by mechanical or electropolishing when care is taken. These pores are present in aluminum even at low hydrogen contents (e.g., <0.2 ml/100 g N.T.P. in semi-continuously cast 99% metal) when the metal is ostensibly sound, as shown by density measurements (22). Hydrogen has a relatively high solubility in liquid aluminum and, in the absence of elaborate protection or outgassing techniques, aluminum alloy melts will generally be saturated in hydrogen just prior to casting. This is because liquid aluminum reacts very readily with atmospheric water vapor to form aluminum oxide and hydrogen. The hydrogen (already in monoatomic form) is very rapidly dissolved by the liquid aluminum. Furthermore, the great majority of commercial aluminum alloys, including the 7075 Al type, are semi-continuously cast, which involves direct water quenching of the partly solidified block. Thus the local environment of the casting has, inevitably, a very high water vapor content. The rapid

108
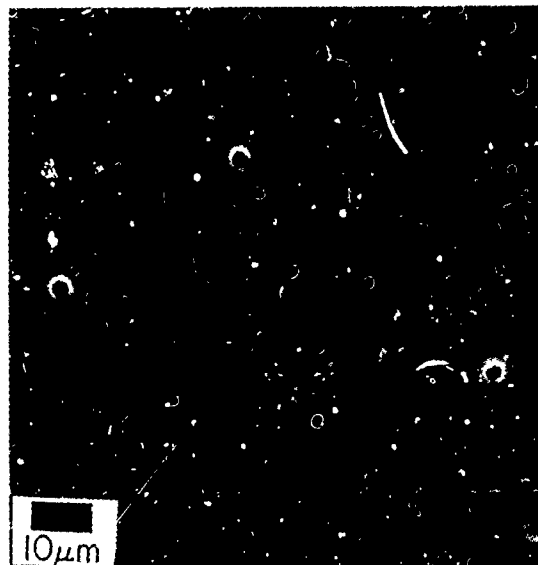
(b)

Fig. 14   Scanning electron micrographs of a cross section (L-ST) of
fine grained 7475 Al after 2 hours at 516°C in molten salt.
Final specimen surface preparation by ion beam etching:
(8 hours at 5 kV, Ar gas, 50 mA, 17° tilt to beam).

109

solidification rates, characteristic of semi-continuous casting of aluminum

alloys, together with the low diffusion rate of hydrogen in solid aluminum

(23), cause much of the hydrogen dissolved in the liquid metal to be trapped

in the solid. Since the gas is considerably less soluble in the solid than

the liquid (24) there will generally be excess hydrogen trapped in the cast

metal. Coarse, interdendritic porosity is generally avoided by conventional

degassing techniques prior to casting. The hydrogen retained in cast aluminum

is partitioned between solid solution and "secondary pores", ~25 mm diameter

(25). These pores are probably nucleated immediately after solidification on

imperfections or minute inclusions and they expand on reheating. The secon-

dary pores may be collapsed by hot or cold working, but it has been shown (25)

that the pores recover and expand on reheating. Such recovery is apparently

an easier process than the initial expansion of secondary pores. It has also

been shown (25) that loss of dissolved hydrogen by diffusion to the free sur-

face at an elevated temperature causes shrinkage and eventual "dissolution" of

the pores due to the surface tension forces. Such hydrogen loss may be great-

ly reduced by the presence of a thick, dense oxide surface layer or by rapid

expansion of internal gas pores. Expansion of the pores increases the propor-

tion of hydrogen in pores and decreases the proportion in solution and thus

lowers the driving force for hydrogen diffusion and escape from the free

surfaces.

4.4.5   Inclusions Associated With Annealing Pores and Superplastic Cavities

Figure 15 shows SEM micrographs of the same specimen shown in Fig. 13

(i.e., 200 minute static anneal at 516°C in molten salt). It can be seen in

ST ↑ → L
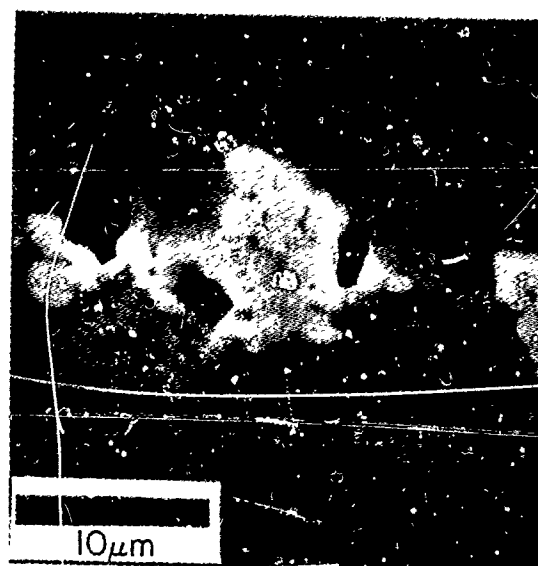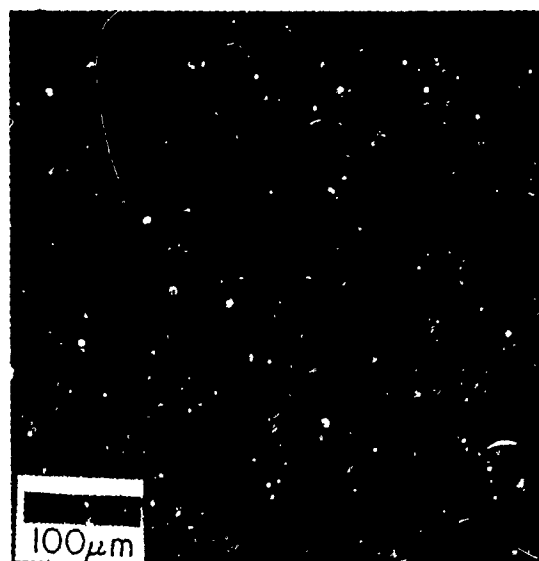
(b)

Fig. 15   Scanning electron micrographs of a cross section of fine
grained 7475 Al after 200 min at 516°C in molten salt.
Mechanically polished to 1/4 μm diamond.   Gold coated.
45° tilt to electron beam.

111

Fig. 15b that gas pores have formed at one of the large, common type of inclu-sion particles. Closer examination shows that these pores generally contain smaller, angular particles that have a darker appearance in the SEM than the large rounded particles. The small angular particles are generally well separated from the matrix. Figure 16 shows a mechanically polished cross section through a small cavity in material superplastically deformed to a strain of 0.66. Loose particles of similar appearance to those in the gas pores may be seen inside this superplastic cavity. This was found to be a fairly general feature. Figure 17 shows EDAX spectra from the small angular particles inside the superplastic cavity in Fig. 16, from a nearby large, common type inclusion particle and from the matrix. Essentially, identical spectra were obtained from the loose, dark particles, the lighter, rounded inclusion phase and the matrix shown in Fig. 15. Thus it appears that both the static annealing gas porosity and the early stages of superplastic cavita-tion may be associated with a particular type of inclusion phase. This inclusion phase is not the most common phase present but tends to be closely associated with the most common phase. The preliminary EDAX analyses suggest that the common phase is Cu_2FeAl_7 (β_2, containing little or no Si) and the phase which becomes detached from the matrix inside the pores and superplastic cavities is $(Fe,Cr)_3SiAl_{12}$ (β_1 containing little or no Cu) (26). The obser-vation of two phase particles (Figs. 8b, 9b and 10) further suggests that such particles may be formed by the incomplete peritectic reaction of Cu_2FeAl_7 + liquid $\rightarrow$ $(Fe,Cr)_3SiAl_{12}$. The invariant temperature for this peritectic reac-tion is 534°C (27). Further work is necessary to clarify these preliminary

Fig. 16   Scanning electron micrograph of a cross section through
a cavity in fine grained 7475 Al after superplastic uniaxial
tensile strain, (ε_e = 0.66, T = 516°C $\dot{\varepsilon}$ = 2 × 10^{-4} s^{-1}).
Mechanically polished to 1/4 μm diamond. Gold coated.
45° tilt to electron beam.

113
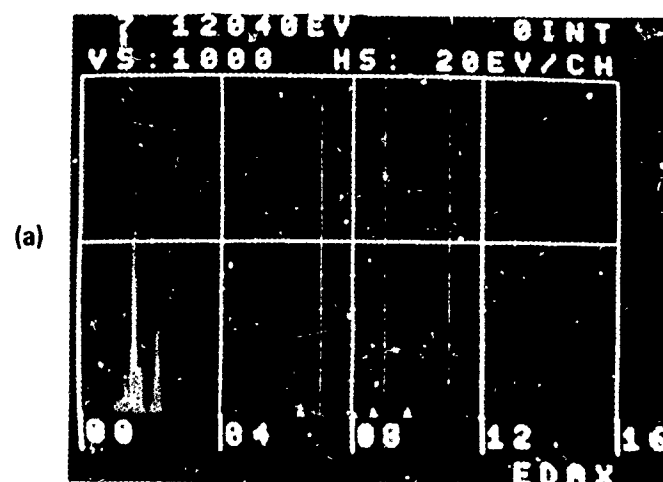
PEAK ENERGIES	ELEMENT
1.28	Mg
1.50	Al
1.76	Si
2.20	Au
5.96	Cr or Mn
6.42	Fe
8.08	Cu
8.64	Zn
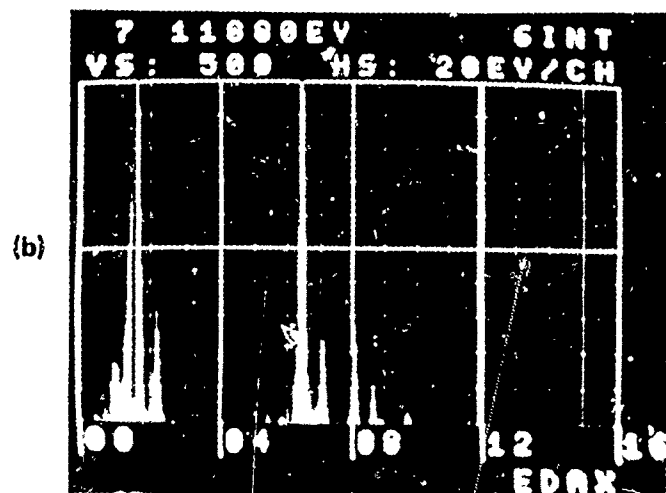
0.96	Cu
1.52	Al
2.20	Au
6.42	Fe
7.06	Fe
8.06	Cu
8.64	Zn
8.94	Cu
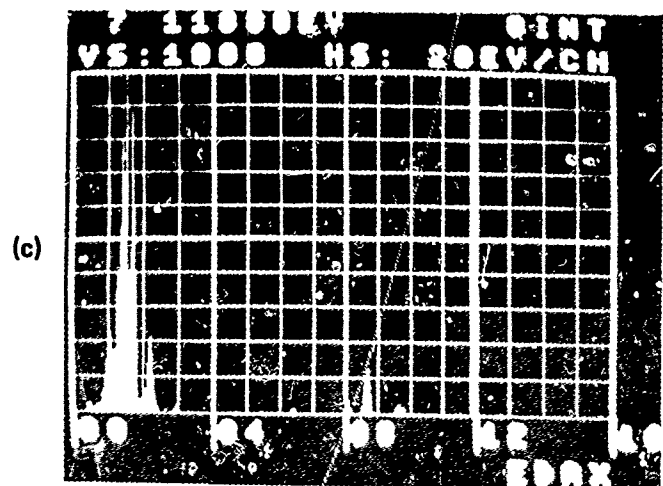
0.48	Ti
1.04	Zn
1.30	Mg
1.52	Al
2.16	Au
2.94	Au
6.36	Fe
8.06	Cu
8.66	Zn

Fig. 17   Typical EDAX spectra from (a) dark, angular, loose particles $((Fe,Cr)_3SiAl_{12})$, (b) light, rounded, large particles (Cu_2FeAl_7), (c) matrix.

114

observations. A purely speculative theory may, however, be proposed which fits with the current information.

The critical stage of cavity formation is growth of the cavity to the minimum size which is stable against dissolution due to surface tension forces. Applied tensile forces will tend to promote cavity formation whenever stress concentrations build up across grain boundaries. Under the super-plastic deformation conditions considered here, however, the flow stresses are very low, and the capacity for relaxation of stress concentrations (by diffu-sion and plastic flow) is high. It appears, therefore, that grain boundary sliding and stress concentrations caused by large inclusion particles are not sufficient, on their own, to form stable cavities. Additional conditions, which may lead to successful nucleation of cavities, are weak, or decohesed matrix/particle interfaces and positive gas pressures inside the cavities. Both of these additional conditions may be present in the superplastic deformation of fine grained 7475 Al. The weak or decohesed interfaces may be provided by the β_1 component of two phase β_1/β_2 intermetallic inclusions. The peritectic transformation of β_2 + liquid $\rightarrow$ β_1 during solidification of the alloy is not likely to be either complete or to be at equilibrium since peritectic reactions are inherently slow (involving diffusion of the reacting phases through the newly formed solid phase) and the solidification rate of commercial aluminum alloy casting is rapid. Thus the last of the β_1 phase to form may have a composition which has a liquidus temperature considerably below the invariant peritectic temperature (534°C) (27). In this case, some localized incipient melting may occur in the two-phase β_1/β_2 inclusions at or

115

around the usual superplastic forming temperature (516°C). Such melting would only be temporary since solid state diffusion would eventually complete the peritectic reaction and remove all of the liquid. If, however, this temporary melting occurred during superplastic deformation, the essentially decohesed particle would provide a very favorable site for nucleation of a strain-induced cavity. In addition, if a high supersaturation of hydrogen exists in the alloy, a region of incipient melting would again provide a highly favorable site for nucleation and growth of a gas pore.

It may be noted here that cavitation during superplastic deformation of 7075 Al is both more general, in terms of cavity distribution, and more rapid than is found with the 7475 Al of similar grain size. This may now be rationalized by (i) the higher flow stress of 7075 due to the lower optimum forming temperature (~480°C) (28) which produces more stress concentrations of sufficient magnitude to form stable sized cavities, (ii) the higher Fe and Si contents which may introduce higher concentrations of the damaging duplex β_1/β_2 inclusion particles and (iii) the 7075 may possibly contain higher hydrogen content, since the 7075 is a lower purity alloy than 7475 and is thus likely to contain considerably higher proportions of recycled scrap metal. It is known (29) that hydrogen contents of commercial aluminum alloys are strongly dependent on the amount of scrap used in making the alloys and on the nature of the scrap surface (i.e., cleanliness).

116

4.5 CONCLUSIONS

1. Nucleation of cavities during superplastic deformation of fine grained 7475 Al at optimum forming conditions is relatively slow and occurs continuously with increasing strain. The continuous formation of new cavities may be due to the strain hardening and continuous increase in flow stress.

2. It appears that the flow stress is generally too low to form stable sized cavities by stress concentrations alone (such as at large inclusion particles) at optimum forming conditions.

3. Nucleation of cavitation appears to be associated with internal hydrogen out-gassing and de-cohesion of one component in two-phase inclusion particles. The hydrogen supersaturation may persist from the casting stage of alloy production; and the two-phase inclusion particles may result from an incomplete peritectic reaction, during alloy solidification, of complex iron, silicon, copper, chromium, aluminum intermetallic compounds.

4. Hydrogen assistance to superplastic cavity formation and stabilization may be reduced or eliminated, by suitable modification of the thermomechanical processing (30).

5. The minority inclusion particles apparently associated with superplastic cavity formation may be removed or modified to less damaging forms by suitable changes to alloy processing.

6. Subsequent growth of stable sized superplastic cavities with increasing strain is relatively rapid. Cavity growth appears to procede by plastic decohesion, induced by grain boundary sliding, along grain boundaries (particularly triple junction lines) and is followed by swelling of these grain boundary cracks, possibly by a combination of vacancy diffusion and plastic deformation. The combination of plasticity and diffusion leads to essentially equiaxed cavity growth, although there are indications that transverse growth, and thus diffusional mechanisms, may predominate.

4.6 ACKNOWLEDGEMENTS

119

4.7 REFERENCES

1. G. L. Dunlop, E. Shapiro, J. Crane, and D.M.R, Taplin, Met. Trans, $\underline{4}$, 2039 (1973).

2. S. Sagat, P. Blenkinsop and D.M.R. Taplin, J. Inst. Metals, $\underline{100}$, 268 (1972).

3. S. Sagat and D.M.E. Taplin, Acta Met, $\underline{24}$, 307 (1976).

4. N. Ridley, C.W. Humphries and D.W. Livesey, Proc. 4th Int. Conf. on the "Strength of Metals and Alloys," ENSMIM, Nancy, 433 (1976).

5. N. Ridley and D.W. Livesey, "Fracture 1977," Vol. 2, editor D. M. R. Taplin,Univ. of Waterloo Press, 1977.

6. D.M.R. Taplin and R.F. Smith, ibid.

7. C.I, Smith and N. Ridley, Metals Techn., $\underline{1}$, 191, (1974).

8. R.G. Fleck, C.J. Beevers and D.M.R. Taplin, J. Mat. Sci., $\underline{9}$, 1737, (1974).

9. S. Sagat, PhD. Thesis, Univ. of Waterloo, 1974.

10. R.G. Fleck, C.J. Beevers and D.M.R. Taplin, Acta Met., $\underline{23}$, 415 (1975).

11. A.J. Perry, J. Mat. Sci., $\underline{9}$, 1016 (1974).

12. D. Hull and D.E. Rimmer, Phil. Mag., $\underline{4}$, 673 (1959).

13. W. Beere and M.V. Speight, J. Met. Sci, $\underline{12}$, 172 (1978).

14. R. Raj and M.F. Ashby, Acta Met., $\underline{23}$, 653 (1975).

15. M.J. Stowell, Met. Sci, July (1980) 267.

16. D.A. Miller, Scripta Met., $\underline{13}$, 7, 595 (1979).

17. C. C. Bampton, M. W. Mahoney, C. H. Hamilton, A. K. Ghosh and R. Raj, "Suppression of Cavitation by the Application of Confining Gas Pressure During Superplastic Deformation of Fine Grained 7475 Al," this document.

18. J. A. Wert, N. E. Paton, C. H. Hamilton, M. W. Mahoney, submitted to Met. Trans. A, 1980

19. B. Lehtinen and A. Melander Metallography, $\underline{13}$, 283 (1980).

20. C.H. Hamilton, Rockwell Int. Science Center, Report for U.S. Army Armament Research and Developmnt Command, ARSCD-CR-8001, February 1980.

21. C. Renon and Calvet, Mem. Sci. Rev. Met., 58, 835 (1961).

22. C.E. Ransley, and D.E.J. Talbot, Z. Metallkunde, 48, 73 (1957).

23. W. Eichenauer and A. Pebler, Z. Metallkunde, 48, 373 (1957).

24. C.E. Ransley and H. Neufeld, J. Inst. Metals, 74, 599 (1948).

25. D.E.J. Talbot and D.A. Granger, J. Inst. Metals, 92, 290 (1963).

26. P.R. Sperry and M.H. Bankard, ASM Metals Handbook, Vol. 8, 8th Edition, pp. 120-129.

27. "Equilibrium Diagrams of Aluminum Alloy Systems," Information Bulletin No. 25, The Aluminum Development Association, London, 1961, pp. 125-127.

28. A. K. Ghosh and C. H. Hamilton, Proc. 5th Int. Conf. Strength of Metals and Alloys, Aachen, W. Germany, 1979, p. 905.

29. C.C. Bampton, unpublished work.

30. Science Center IR&D Report, 812 (1980) pp. 339-342.

SECTION 5   SUPPRESSION OF CAVITATION BY THE APPLICATION OF CONFINING GAS PRESSURE DURING SUPERPLASTIC DEFORMATION OF FINE GRAINED 7475 Al

C. C. Bampton, M. W. Mahoney, C. H. Hamilton, A. K. Ghosh and R. Raj

Rockwell International Science Center
Thousand Oaks, CA 91360

ABSTRACT

It has been shown that the application of hydrostatic gas pressures during superplastic deformation of fine grained 7475 Al, can entirely prevent the intergranular cavitation normally encountered at atmospheric pressure. A critical ratio of confining pressure to flow stress may be defined for each superplastic forming condition above which virtually no cavitation occurs. In low strain rate superplastic deformation conditions, where intergranular cavitation plays a significant part in final tensile rupture, the superplastic ductility may be improved by the application of confining pressures. Similarly, the detrimental effects of large superplastic strains on service properties may be reduced or eliminated by the application of suitable confining pressures during the superplastic forming. In this case the superplastically formed material may have the same design allowables as conventional 7475 Al sheet.

5.1 INTRODUCTION

An undesirable characteristic of many superplastic alloys is their tendency to cavitate (form small intergranular voids) during superplastic stretch-forming. The cavitation may limit the superplastic ductility of the material, as well as reduce its subsequent mechanical properties, as discussed elsewhere in this document (1). The possible degradation of service properties may be particularly serious in the case of the 7475 Al type alloys since these alloys are often used in structural aerospace components.

A method has been proposed, and demonstrated (2), that controls superplastic cavitation by the simultaneous imposition of a confining (compressive hydrostatic) pressure during the superplastic deformation.

This work was carried out in order to determine the effects of confining pressures on superplastic cavitation, superplastic ductility and subsequent service properties.

127

5.2 MATERIALS

The 7475 Al alloy, processed to fine grain size (3), was used for all of this work. The metal was all from a lot which was processed to 2.5 mm thick warm rolled sheet by ALCOA Laboratories with the fine grain processing completed at the Science Center. The compositional limits are shown in Table 1. Final grain sizes were ~ 14 µm diameter in the rolling plane and ~ 8 µm in the short transverse direction.

Table 1
Compositional Limits for 7475 Aluminum (wt%)

Si	Fe	Cu		Mn	Mg	Cr
0.10max	0.12max	1.2-1.9		0.06max	1.9-2.6	0.18-0.25
Zn	Ti	Others, each		Others, Total		Al
5.2-6.2	0.06max	0.05max		0.15max		Remainder

5.3 EXPERIMENTAL

Two methods of superplastic deformation were used with the application of various confining gas pressures. The first involved uniaxial tensile testing, at constant true strain rate, inside a pressurized retort. The second involved blow forming, at constant true strain rate, against a positive back gas pressure. These methods will now be more fully described.

5.3.1 Uniaxial Tensile Testing

The superplastic tensile testing was carried out in an Instron testing machine modified to allow constant true strain rate tests. The equipment designed to provide a controlled temperature and pressure environment is shown in Fig. 1. The set-up is sketched schematically in Fig. 2. The load cell was placed inside the retort in order to measure flow stresses accurately and avoid corrections for friction forces from sliding pressure seals. Pressures up to 7 MPa could be obtained by using compressed argon. The temperature control was more difficult at high pressures because of convection currents and because of the elongations of up to 1200% which were being obtained, however the variation was kept below ±5°C along the specimen length.

The specimen shape and dimensions are shown in Fig. 3. These specimens were economical to make and the grips were designed so that up to ten specimens could be "gang tested" simultaneously if desired. The lack of shoulder radii is not important for materials with high strain rate

131
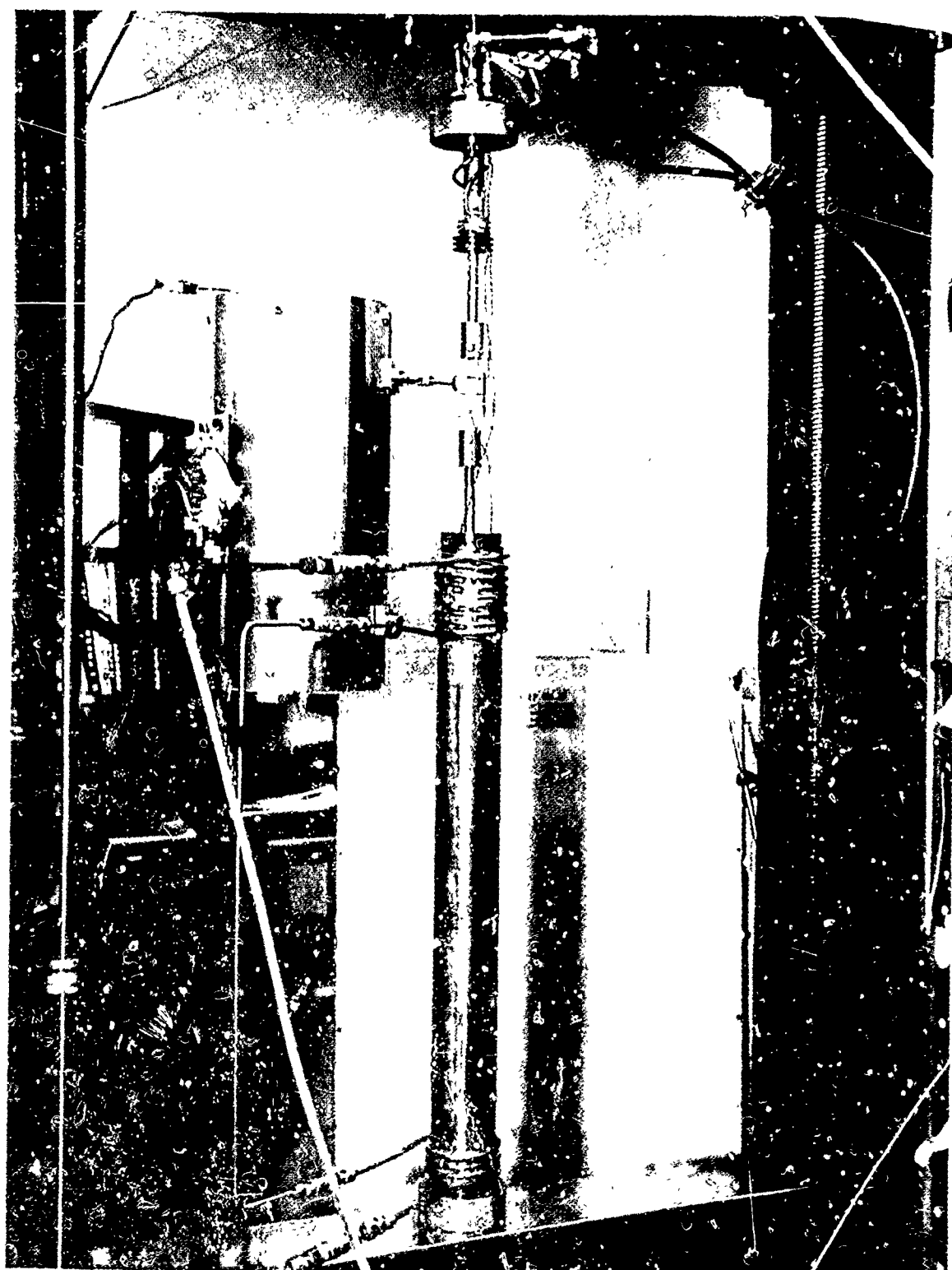
Fig. 1 The set-up used for the superplastic uniaxial tensile testing with confining gas pressures, shown with the furnace and pressure tube withdrawn from the specimens.
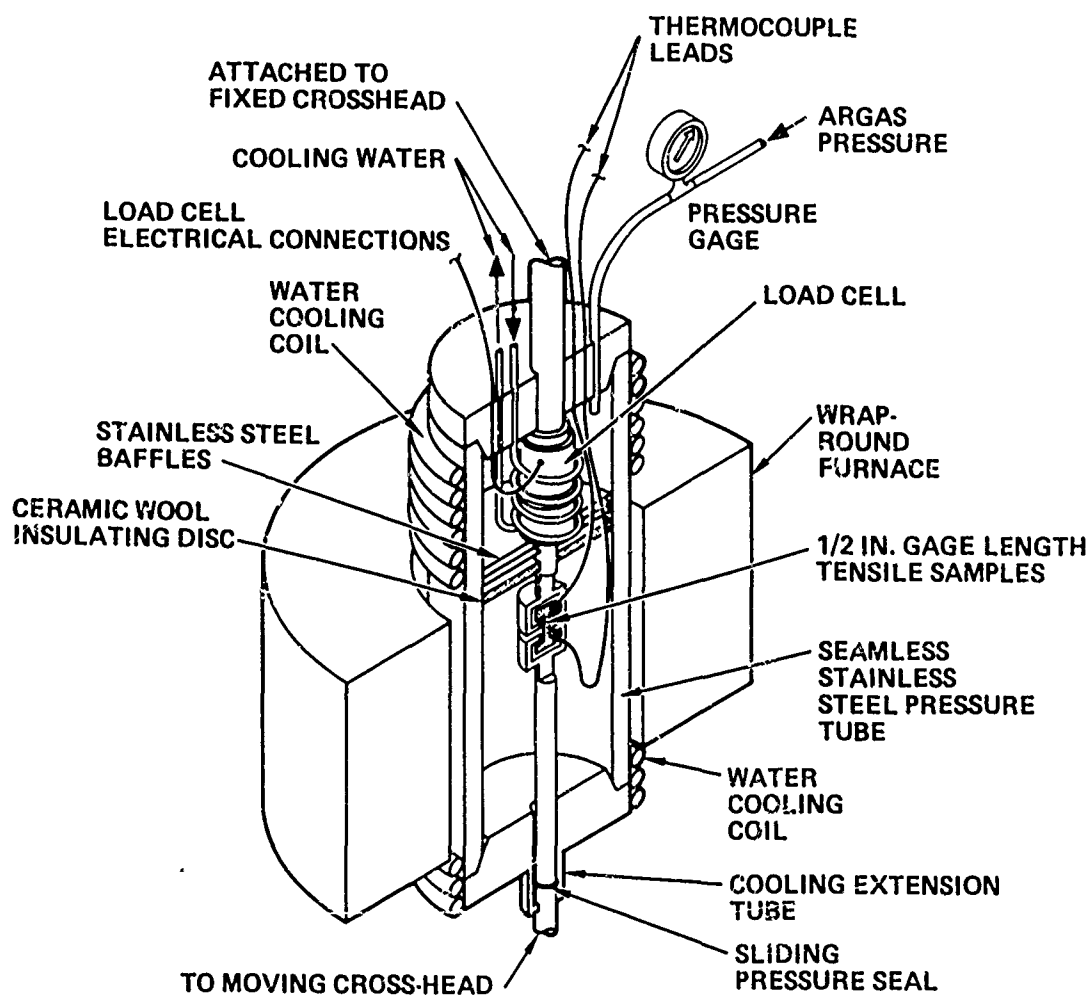
Fig. 2 Schematic drawing of the set-up for the superplastic uniaxial tensile testing with confining pressures.

133
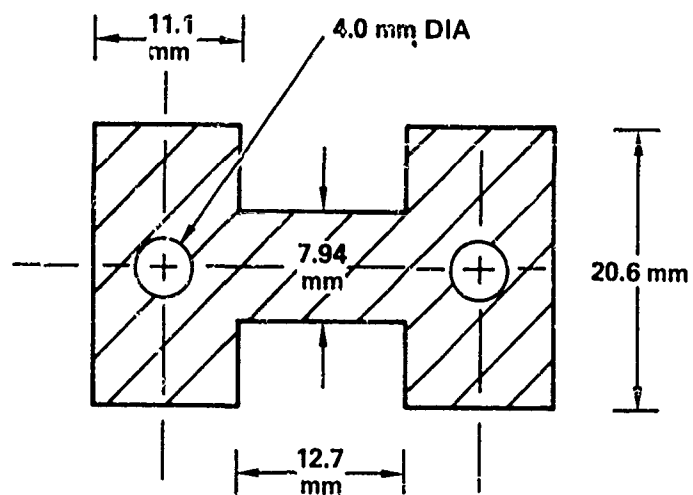
Fig. 3 Superplastic uniaxial tensile specimen dimensions.

sensitivity. Despite the short gage lengths (12.7 mm), the testing set up did not allow sufficient cross-head travel to obtain elongations greater than about 1200%.

5.3.2 Blow Forming

The techniques and equipment used for constant strain rate blow forming have been described elsewhere (4). The only modifications necessary for this work were to provide for the application of a constant positive back pressure between the forming sheet sample and the female die. In practice, confining pressures were obtained by pressurizing (with compressed argon) the die chamber on both sides of the sheet sample before applying an excess pressure to one side of the sheet to drive the deformation. The differential pressure was kept the same as in the calculated pressure time profiles used in ambient pressure forming, regardless of the back (confining) pressure.

Two main die configurations were used; a deep cylindrical die and a shallow rectangular die. The depth to width ratios in both configurations could be increased by means of inserts. Examples of parts formed in these dies are shown in Fig. 4. The cylindrical die provided balanced biaxial forming conditions whereas the rectangular die provided essentially plane strain forming conditions.

Superplastic strains were measured from grid circles etched on the sheet (as shown in Fig. 4) or by using a pointed micrometer to measure thicknesses. Cavitation volume percent was measured by cutting out small

135
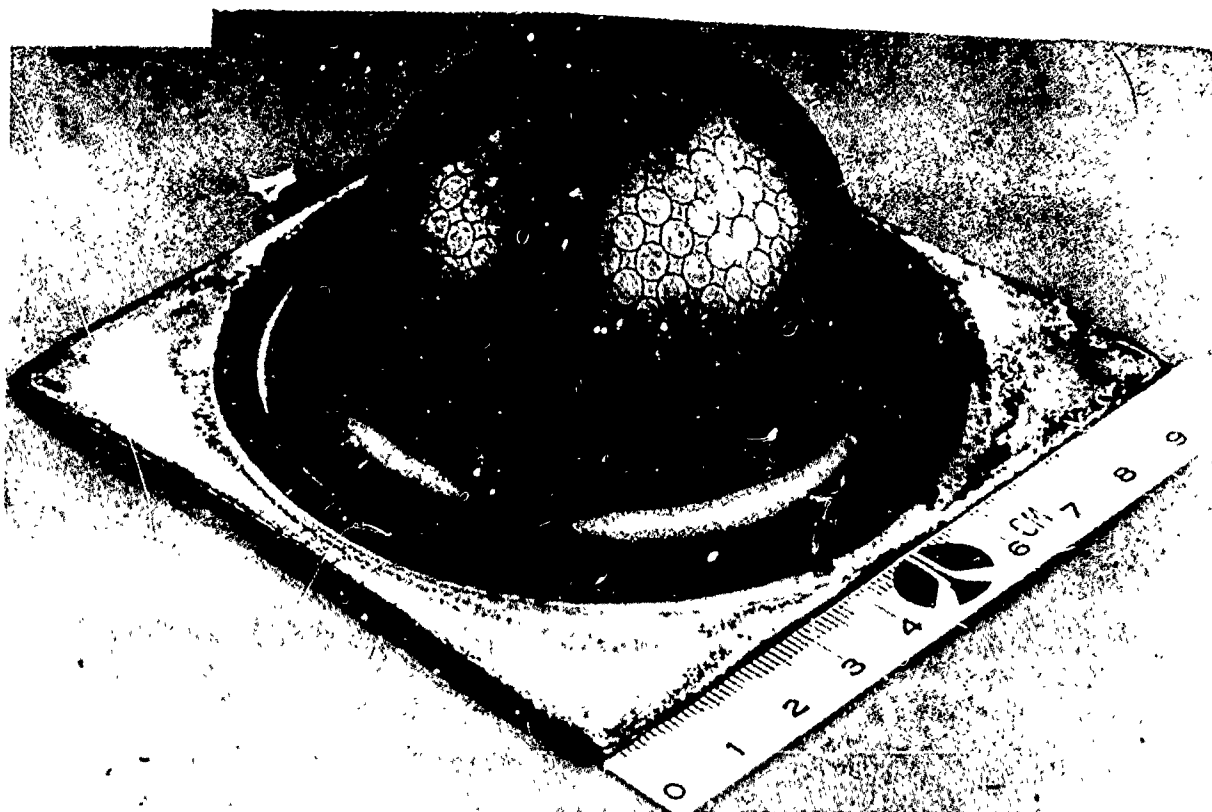
(a)
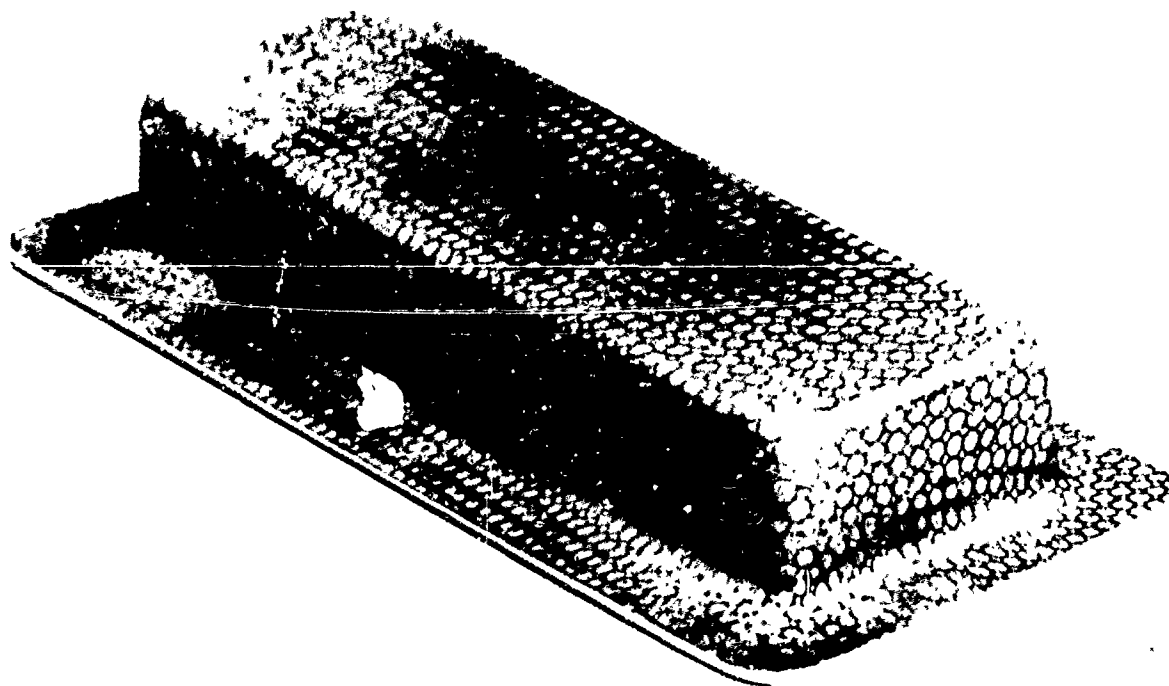
(b)

Fig. 4   Examples of parts formed with (a) the deep cylindrical die (b) the
shallow rectangular die.

136

regions of strained material and using the variable-density liquid flotation technique, described elsewhere in this report (5).

Optical and scanning electron microscopy were used to examine superplastic cavity formation more qualitatively.

The flat areas of parts formed with the rectangular die and a range of confining pressures were used to provide specimens for ambient temperature tensile and fatigue tests in the T6 condition as described elsewhere in this document (1).

5.4 RESULTS AND DISCUSSION

5.4.1   Effects on Cavitation at Optimum Superplastic Forming Conditions

Figures 5, 6 and 7 show the volume percent cavitation developed in
fine grained 7475 Al with increasing superplastic strain when deformed in
uniaxial, equibiaxial and plane strain tension respectively; all at the
optimum forming conditions of temperature and strain rate ($T = 516°C$
$\dot{\varepsilon} = 2 \times 10^{-4} S^{-1}$) (6). Firstly, it appears that the strain state has no
significant influence on the cavitation. A simple definition of superplastic
strain in terms of effective strain is sufficient to predict the cavitation
level whatever the strain state used. The maximum cavitation levels in the
blow forming cases are generally low and the forming conditions inherently
less well controlled than in the uniaxial straining case, so a certain amount
of experimental scatter is expected. This may be exacerbated in the blow
formed cases by anisotropy of cavitation rate with respect to the rolling
direction, which has been observed. (7). Secondly, the imposition of
confining pressure significantly reduces the rate of cavitation with
superplastic strain if the presssure is sufficiently high. For the optimum
forming conditions, constant confining pressures up to about 1.0 MPa do not
significantly affect cavitation. Progressively higher confining pressures
progressively reduce the rate of cavitation. Confining pressures greater than
about 3.5 MPa effectively prohibit almost all cavitation.

Figure 8 shows the effect of confining pressure on cavitation in
uniaxial deformation at a constant strain of 2.0. Since the flow stress (σ_e)

139
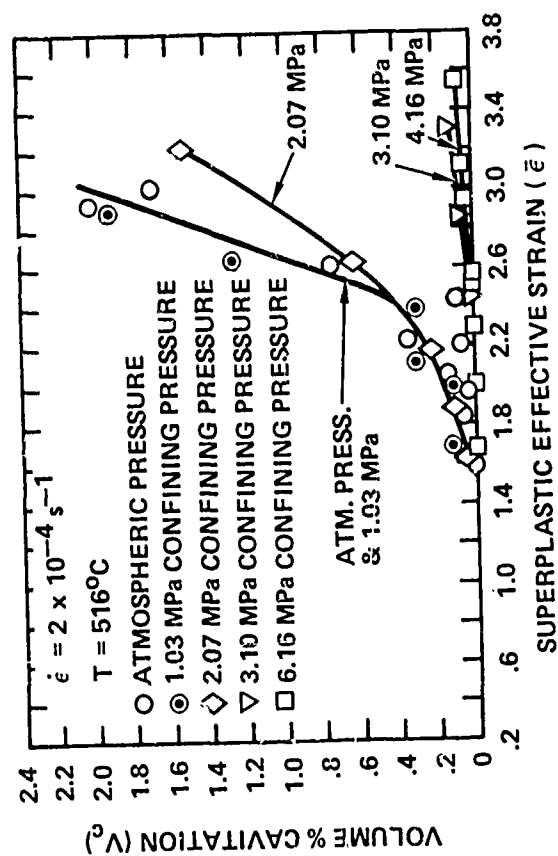
Fig. 5 Effect of confining pressure on cavitation in super-plastic uniaxial tensile deformation at maximum m conditions (T = 516° C, $\dot{\varepsilon}$ = 2 x 10-4 s -1).
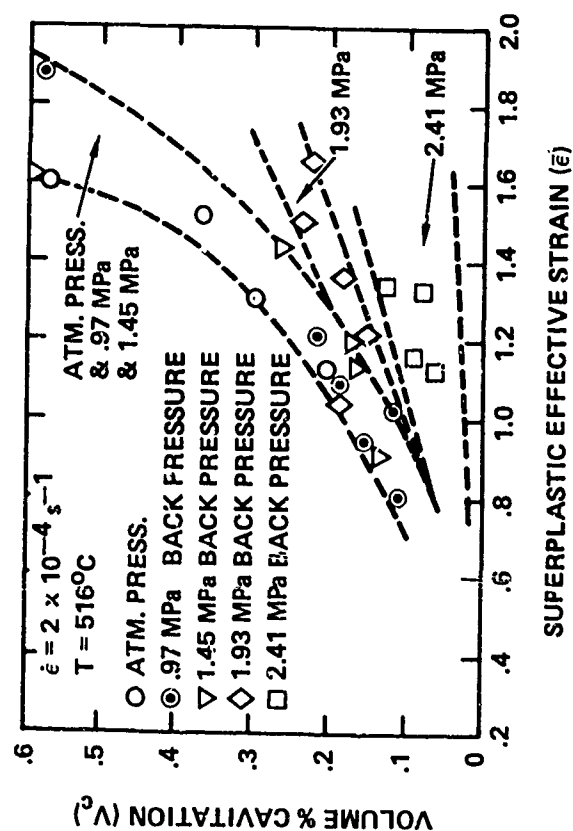
Fig. 6 Effect of confining pressures on cavitation with superplastic equibiaxial blow forming ($T = 516°C$, $\dot{\varepsilon} = 2 \times 10^{-4}$ s^{-1}).

141
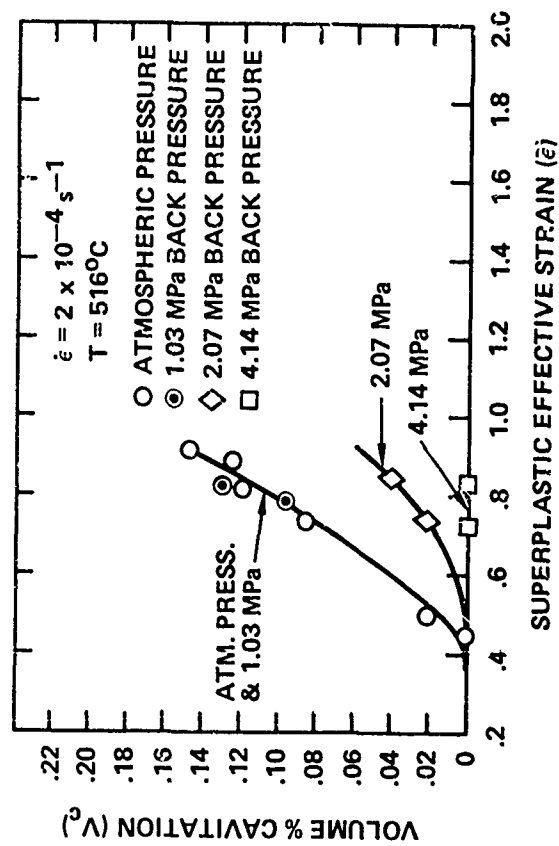
Fig. 7   Effect of confining pressures on cavitation with superplastic plane strain blow forming ($T = 516°C$, $\dot{\varepsilon} = 2 \times 10^{-4}$ s^{-1}).
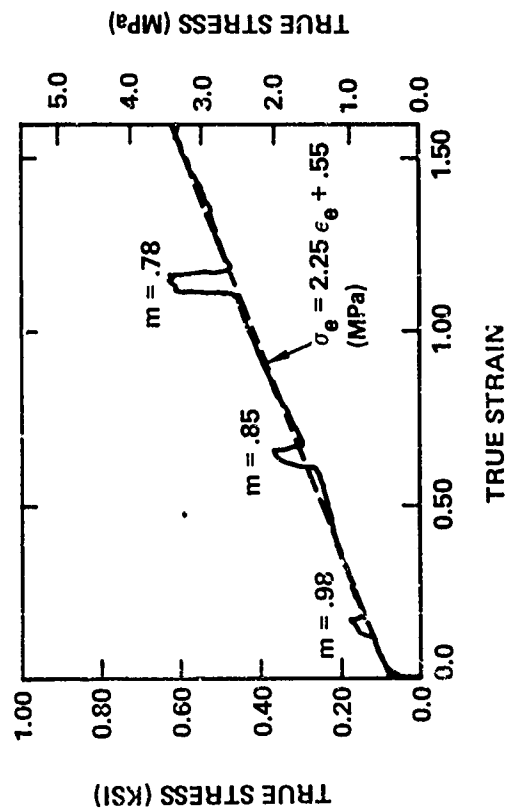
Fig. 9   Superplastic true stress-true strain curve (uniaxial tension) for fine grained 7475 Al (T = 516°C, $\dot{\epsilon}$ = 2 × 10⁻⁴ s⁻¹) at ambient pressure. Short 40% jumps in $\dot{\epsilon}$ to give m values.

144
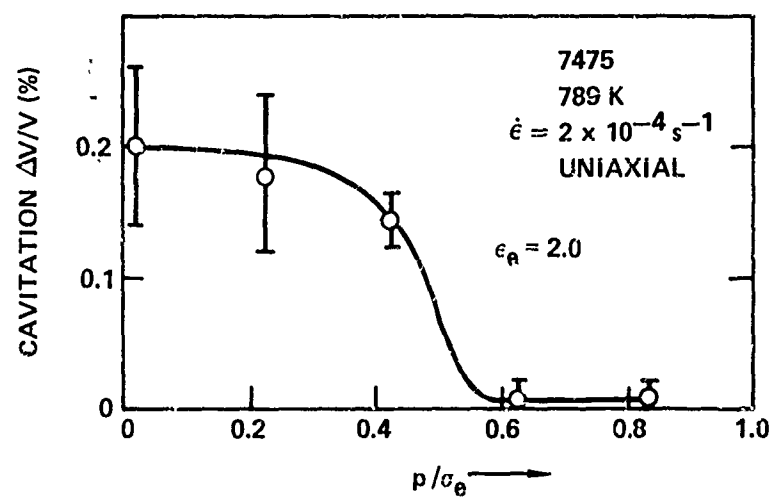
Fig. 8   Effect of confining pressure, p, normalized with respect
to superplastic flow stress, σ_e, on cavitation in super-
plastic uniaxial tensile deformation at a constant strain,
$\varepsilon = 2.0$, ($T = 516°C$, $\dot{\varepsilon} = 2 \times 10^{-4}$ s^{-1}).

increases with strain, as shown in Fig. 9, the confining pressure (p) has been normalized with respect to flow stress. It was found that confining pressures, at least up to 4 MPa, have no effect on the superplastic flow characteristics (flow stress and m value). The uniaxial results show that there is little change in cavitation until $p/\sigma_e > 0.4$. The plane strain and equibiaxial results are similar, although it was not possible to obtain sufficiently high superplastic strain in these cases to show the effects as clearly. The results suggest that confining pressures greater than about 0.6 of the flow stress prevent nucleation and growth of stable sized cavities. Since, as shown in Fig. 9, the flow stress increases with strain occording to a relation of the form

$$\sigma_e = 2.25 \ \varepsilon_e + 0.55 \ (MPa) \tag{1}$$

it would seem that, in order to avoid virtually all nucleation of cavities, the confining pressure, p depends on the maximum strain attained (ε_e) according to the relation:

$$p > 1.35 \ \varepsilon_e + 0.33 \ (MPa) \tag{2}$$

5.4.2   Effects on Cavitation at Higher Flow Stress Superplastic Forming Conditions

Figures 10 and 11 show the effects of confining pressures on cavitation during superplastic deformation at a lower temperature and a faster

145
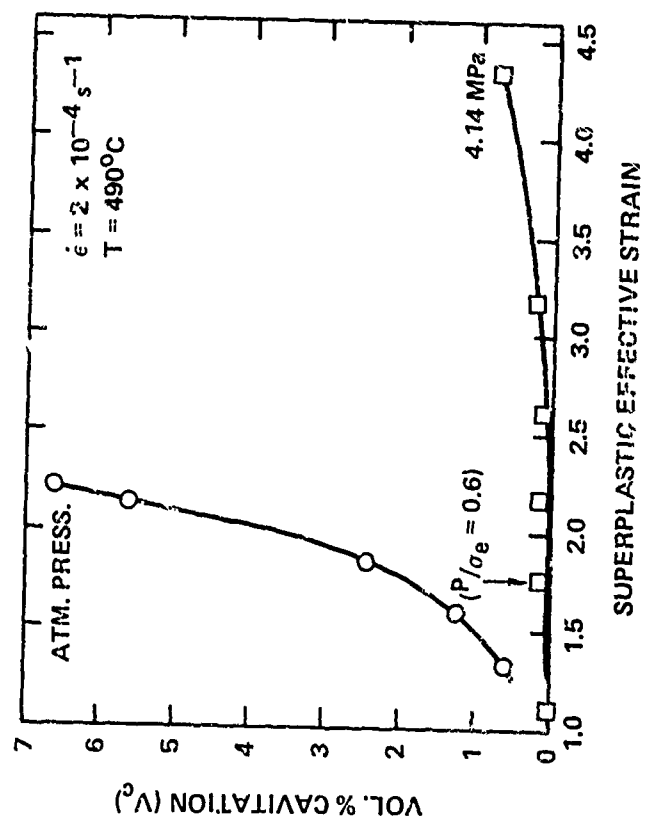
Fig. 10 Effect of confining pressure on cavitation in superplastic uniaxial tensile deformation at a lower temperature $(T = 490°C, \dot{\epsilon} = 2 \times 10^{-4} \, s^{-1})$.
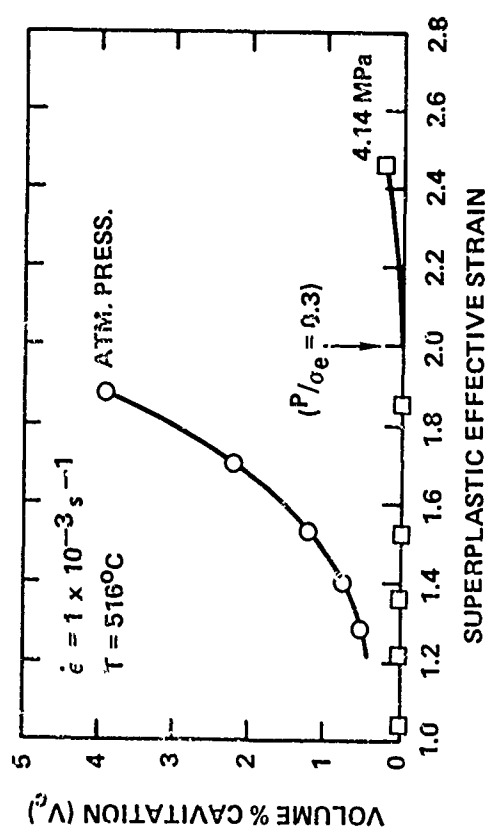
Fig. 11. Effect of confining pressure on cavitation in superplastic uniaxial tensile deformation at a higher strain rate (T = 516°C, $\dot{\epsilon} = 1 \times 10^{-3}$ s^{-1}).

147

strain rate respectively, than the optimum forming conditions. In both of these cases, the cavitation rate at ambient pressure is considerably greater than that at maximum m superplastic straining conditions. This corresponds qualitatively with higher flow stresses in both cases. The flow stresses are found to depend on effective superplastic strain, ε_e according to:

$$\text{At } 490\,°C, \ \dot{\varepsilon} = 2 \times 10^{-4} \ s^{-1}, \quad \sigma_e = [3.48 \ \varepsilon_e + 0.79] \text{ MPa} \tag{3}$$

$$\text{At } 516\,°C, \ \dot{\varepsilon} = 1 \times 10^{-3} \ s^{-1}, \quad \sigma_e = [5.76 \ \varepsilon_e + 1.83] \text{ MPa} \tag{4}$$

The application of 4.14 MPa confining pressure dramatically reduces the cavitation rates, but does not eliminate cavitation completely. In the case of the lower temperature test, shown in Fig. 10, the condition that $p/\sigma_e > 0.6$ is necessary to prevent cavitation, appears to apply once again. In the case of the faster strain rate, however, as shown in Fig. 11, it appears that it is only necessary to satisfy the condition $p/\sigma_e > 0.3$ in order to prevent cavitation. The difference in the critical p/σ_e ratios reflects the higher flow stresses in the fast strain rate case. Cavitation rates with superplastic strain are actually very similar in both cases. This suggests that the extent of grain boundary sliding is at least as important as the flow stress in determining the volume fraction of cavitation developed. It seems likely that flow stress is the dominant factor in determining the rate of nucleation of stable sized cavities but that subsequent cavity growth has a more complex dependence on such factors as flow stress, vacancy diffusion, test time, grain boundary sliding and plastic flow.

148

The observation, discussed above, that cavitation rate is greater with forming conditions of $\bar{T} = 516°C$, $\dot{\varepsilon} = 1 \times 10^{-3}$ s^{-1}, than with $T = 516°C$, $\dot{\varepsilon} = 2 \times 10^{-4}$ s^{-1}, at ambient pressure is apparently inconsistent with the results discussed elsewhere in this document (5), section 5.2. In that work it was shown that, at 516°C, the cavitation was maximum at $\dot{\varepsilon} = 2 \times 10^{-4}$ s^{-1}. A tentative explanation may be offered that is based on inherent material variability.

Firstly, with reference to the tensile tests at optimum forming conditions ($\dot{\varepsilon} = 2 \times 10^{-4}$ s^{-1}, $T = 516°C$) in this work, it was noted that very high elongations and relatively low rates of cavitation were obtained, even at ambient pressure, compared with tests on earlier lots of fine grained 7475 Al. It is felt that the bulk of the apparent improvement in ductility of the lot used in this work was due to improvements in the testing technique which provided a more uniform temperature distribution along the specimen gage lengths throughout the tests. Thus, total elongations achieved on earlier lots were "improved" from about 500% to 850%. There was, however, also a significant improvement in the inherent material ductility of the lot used in this work, compared to an earlier lot. Thus the lot used in this work has elongations of 1200% or greater, compared to identically tested early lot material of about 950%. The lower rate of cavitation in the lot used for this work is also apparently due to inherent material variability. The material used for the tests discussed elsewhere in this document (5) was from the early lot which, it may be assumed, had a greater inherent tendency to nucleate cavities, during superplastic deformation, than material from the lot used in

149

this work. Increasing superplastic flow stress has a dominant effect on cavity nucleation and a less dominant effect on subsequent cavity growth (temperature having a more significant effect on cavity growth due to thermally activated processes). It might therefore be expected that the material with the lowest inherent cavity nucleation potential will be relatively more affected, in terms of cavity formation, by increasing strain rate and thus increasing flow stress, than the material which has a higher inherent cavitation rate. At higher flow stresses, the materials may have substantially the same cavity nucleation rates but at lower flow stresses the cavitation rates are different, perhaps because of a different concentration of the most highly favored nucleation sites (probably the two-phase inclusions discussed elsewhere in this document (8) Section 3.4.5. The overall effect is therefore to shift the peak in cavitation rate to higher strain rates as the inherent cavity nucleation potential of the material decreases.

5.4.3   Effects on Superplastic Ductility and Final Failure

Figure 12 shows the total elongations to failure of the uniaxial tension tests and Fig. 13 shows the fracture strains for the same tests measured from reduction in cross-sectional area of the test samples close to the fracture surfaces. These figures may be discussed by reference to the corresponding micrographs in Fig. 14, which show cross sections through typical examples of fractured tensile specimens.

The practical problems of achieving uniform temperatures over long, thin gage lengths and the limitations on the testing machine cross head travel

150
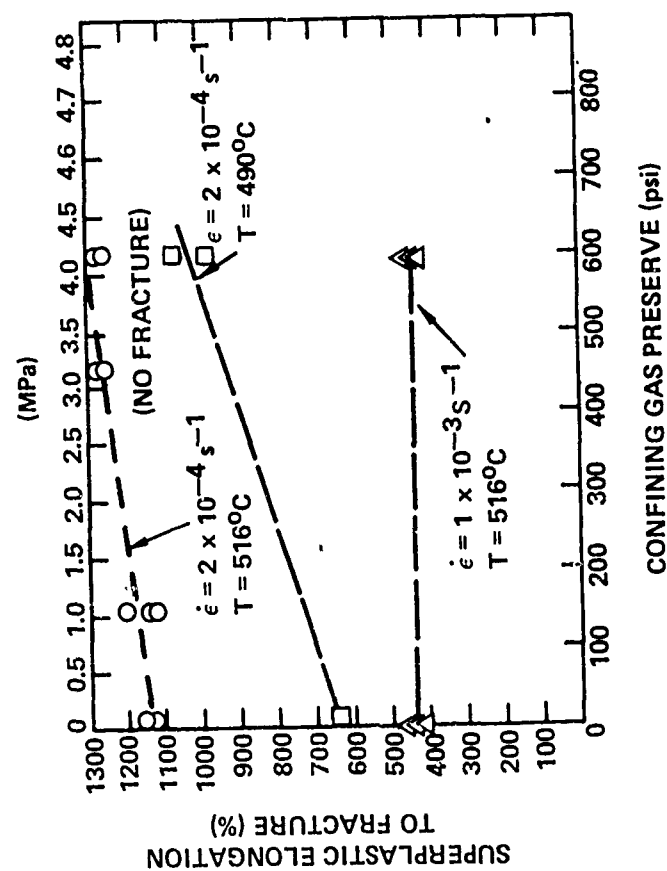
Fig. 12 Effect of confining pressure on superplastic uniaxial tensile ductilities.

151
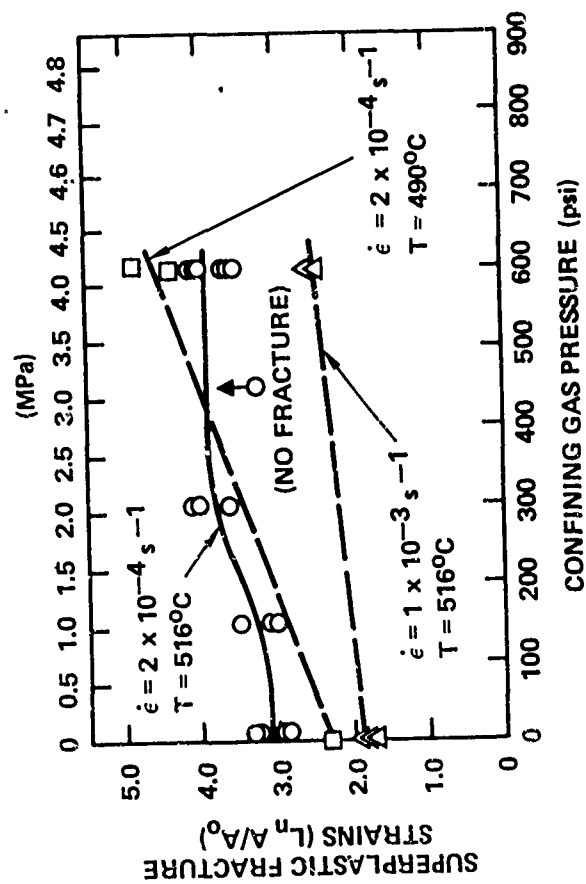
Fig. 13   Effect of confining pressure on superplastic uniaxial tensile fracture strains.
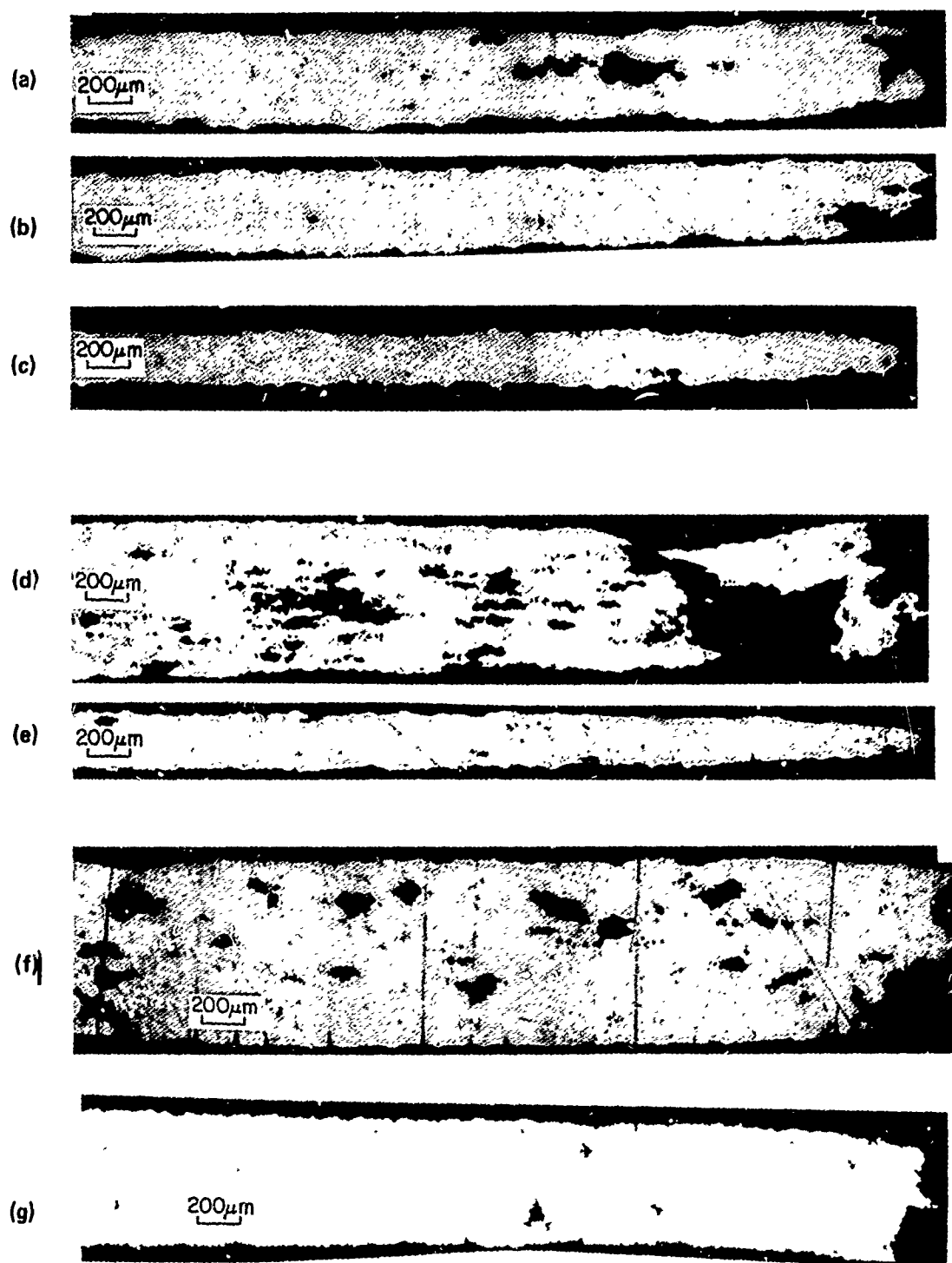
Fig. 14 Cross sections (L-ST) of typical superplastic uniaxial tensile specimens after failure. (a) $T = 516°C$, $\dot{\epsilon} = 2 \times 10^{-4}$ s^{-1}, p = At.Press., (b) $T = 516°C$, $\dot{\epsilon} = 2 \times 10^{-4}$ s^{-1}, p = 2.07 MPa, (c) $T = 516°C$, $\dot{\epsilon} = 2 \times 10^{-4}$ s^{-1}, p = 4.14 MPa, (d) $T = 490°C$, $\dot{\epsilon} = 2 \times 10^{-4}$ s^{-1}, p = At.Pres., (e) $T = 490°C$, $\dot{\epsilon} = 2 \times 10^{-4}$ s^{-1}, p = 4.14 MPa, (f) $T = 516°C$, $\dot{\epsilon} = 1 \times 10^{-3}$ s^{-1}, p = At.Press., (g) $T = 516°C$, $\dot{\epsilon} = 1 \times 10^{-3}$ s^{-1}, p = 4.14 MPa.

153

discussed earlier, reduce the significance of the total elongation results achieved at the optimum forming conditions. A small improvement in superplastic ductility, as a result of applying confining pressures, may be suggested, however, by Fig. 12. Similarly, an improvement in fracture strain, as shown in Fig. 13, is suggested over the confining pressure range 1.0 to 2.75 MPa. This corresponds qualitatively with the effect of confining pressure on cavitation as shown in Fig. 5. The micrographs in Fig. 15 a, b and c illustrate these points by showing increasing uniform strains and fracture strains and decreasing cavitation with increasing confining pressure. It appears that, even in the case of ambient pressure testing, the rate of cavitation is not sufficient to cause catastrophic failure by interlinkage of coarse cavities. The presence of cavities does, however, reduce the bulk fracture stress due to effective reduction in cross sectional area and stress concentrations around large cavities. The fracture surfaces in Figs. 14a, b and c indicate the increasing contribution of coarse cavitation to final failure as p/σ_e is decreased.

Tensile tesing at a lower temperature (490°C) shows more clearly (Figs. 12 and 13) the improvement in both elongation and fracture strain as p/σ_e is increased. Figure 14d shows the extensive cavity nucleation and growth at ambient pressure and the significant contribution that that coarse cavitation has on final failure. Figure 14e shows the dramatic reduction in cavitation by the increased p/σ_e and the corresponding improvement in uniform and fracture strains. It may be noted that the fracture surface in Fig. 14e
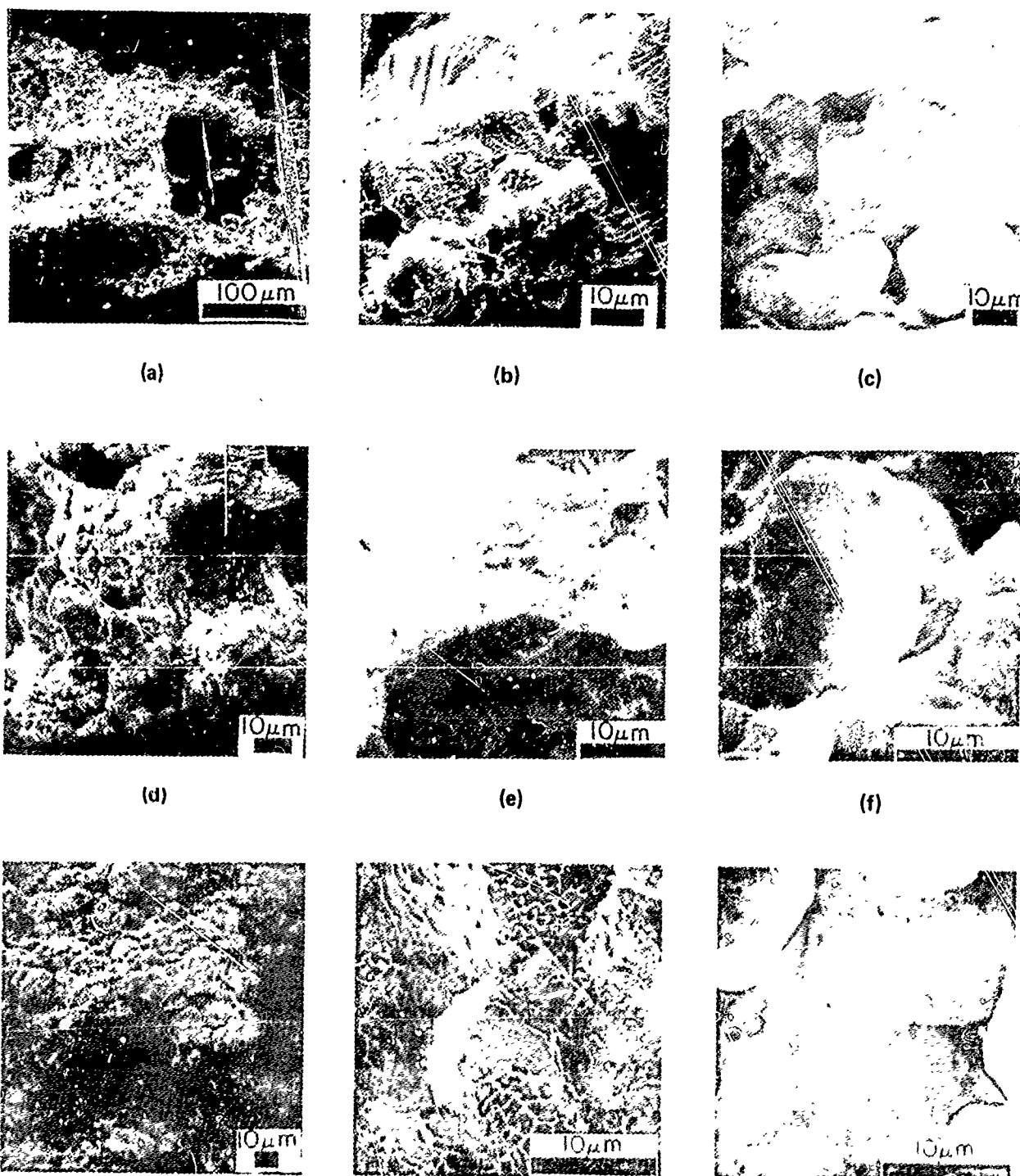
154

Fig. 15 Scanning electron micrographs of superplastic uniaxial tensile fracture surfaces at ambient pressure.
(a), (b) and (c), $T = 516°C, \dot\varepsilon = 2 \times 10^{-4}$ s^{-1}
(d), (e) and (f), $T = 490°C, \dot\varepsilon = 2 \times 10^{-4}$ s^{-1},
(g), (h) and (i), $T = 516°C, \dot\varepsilon = 1 \times 10^{-3}$ s^{-1}.

155

has the form of a near-perfect chisel edge indicating a totally ductile failure mode.

Tensile testing at the faster strain rate (1×10^{-3} s^{-1}) shows no improvement in superplastic elongation (Fig. 12) and only a small increase in fracture strain (Fig. 13) with increasing p/σ_e. Figures 14f and g show these effects but also show that cavitation is dramatically reduced by the increase in p/σ_e. It therefore appears that, unlike the low temperature case, catastrophic failure is induced in the faster strain rate samples by some fundamental mechanism other than interlinkage of coarse cavities or ductile necking. It may be significant that the principal stress at fracture (calculated from equations 3 and 4) are essentially tne same in both cases ($\sim$ 12.5 MPa) of high flow stress.

Figure 15 shows SEM fractographs from typical failed tensile specimens all tested at ambient pressure. Figure 16 shows the corresponding fractographs when tested with 4.14 MPa confining pressure. The first general observation is that all of the superplastic fracture surfaces show marked intergranular failure characteristics. The ambient pressure cases all show coarse cavities exposed in the fracture surfaces as seen in Figs. 15a and g. These cavities have similar surface features, as shown in Figs. 15c, f and i, whether deformed at the optimum forming conditions, lower temperature or higher strain rate. The cavity surfaces consist of exposed grain surfaces which tend to be smooth, except where dispersoid particles (Al-Mn/Cr intermetallics) are located, and at boundaries with adjacent grains, where ridges show evidence of plastic tearing as the grains separate during superplastic
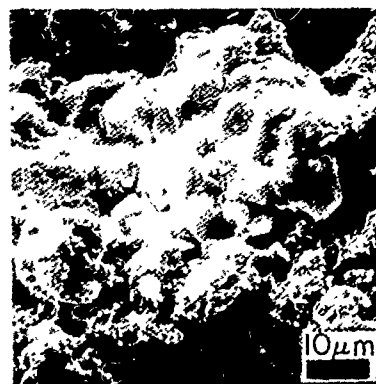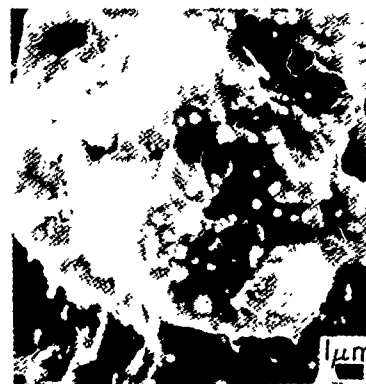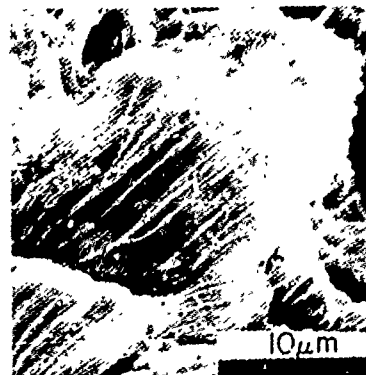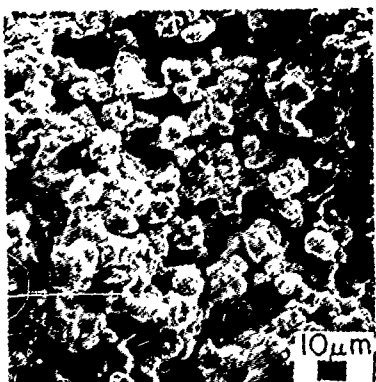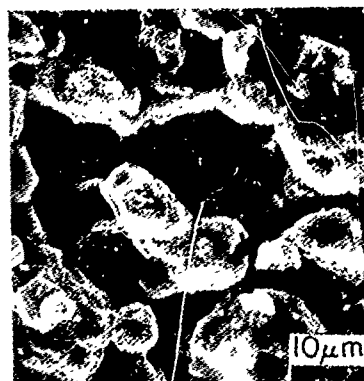
156

Fig. 16 Scanning electron micrographs of superplastic uniaxial
tensile fracture surfaces at 4.14 MPa confining pressure
(a) and (b), $T = 516°C$, $\dot{\varepsilon} = 2 \times 10^{-4}$ s^{-1}.
(c) and (d), $T = 490°C$, $\dot{\varepsilon} = 2 \times 10^{-4}$ s^{-1}.
(e) and (f), $T = 516°C$, $\dot{\varepsilon} = 1 \times 10^{-3}$ s^{-1}.

157

deformation. It seems likely that surface tension stresses cause gradual smoothing out of these ridges by diffusive flow as the cavity expands during the superplastic deformation. The high temperatures and long testing times would aid this process. The areas of fracture surface between the exposed cavities (fractured ligaments) are shown for the three cases in Figs. 15b, e and h. These surfaces all appear to show essentially intergranular failure but also show evidence (extensive ridges and cusps) of considerable plastic flow at or near the grain boundaries. The plastic flow ridges appear to be most marked in the case with the lower testing temperature (490°C).

As expected, none of the fracture surfaces of specimens tested with 4.14 MPa confining pressure (Fig. 16), showed significant coarse cavities. The fracture surfaces were all essentially intergranular in nature with varying degrees of plastic flow in evidence. The optimum superplastic deformation conditions, as shown in Figs. 16a and b, show rounded-off grain shapes in the fracture surface with many small protrusions. These protrusions appear to be of the size and frequency to be consistent with being associated with dispersoid particles. The lower temperature case (Figs. 16c and d) again shows the most marked plastic flow characteristics, both in terms of the microscopic ridges on the exposed grain surfaces and of the macroscopic fracture surface shape which was, as mentioned earlier, almost perfectly chisel-edge shaped. The higher strain rate case (Figs. 16e and f) showed the most markedly brittle intergranular fracture surface with little evidence of plastic flow. The apparent degrees of plastic flow shown by the fracture surfaces in Fig. 16 are consistent with the tensile specimen cross sections

shown in Figs. 14c, e and g. Thus, increasing the strain rate at a high temperature promotes brittle type intergranular failure, whereas decreasing the temperature at a slow strain rate increases the ductile nature of the fracture.

5.4.4 Effects on Ambient Temperature Tensile and Fatigue Properties

Figure 17 shows the effects of superplastic blow forming, with various positive back pressures, on the T6 tensile properties. As expected, the yield strength and tensile strength are unaffected due to the relatively low superplastic strains attainable with the female dies. Increasing back pressure did have a beneficial effect on ambient temperature ductility, however. It can be seen, by comparing the ductility data presented elsewhere in this document (1), Fig. 6 and Fig. 17 that the application of back pressure > 4 MPa restores the ductility to the levels of the unstrained material. Figure 18 shows that the fracture strain is more affected than the uniform strain, by the superplastic deformation, and is correspondingly more affected by the imposition of confining pressures during the superplastic deformation.

Figure 19 shows the effect of superplastic strain and confining pressure on fatigue life at a single maximum stress. The effect of superplastic strains up to 0.8 are not sufficiently large to show up in the i̶n̶ ble scatter that is obtained with the type of sheet fatigue specimens ̶ed in these tests. This is consistent with the data shown elsewhere in this document (1), from the superplastic uniaxial strained material. Thus the imposition of a confining pressure would not be expected to have any

159
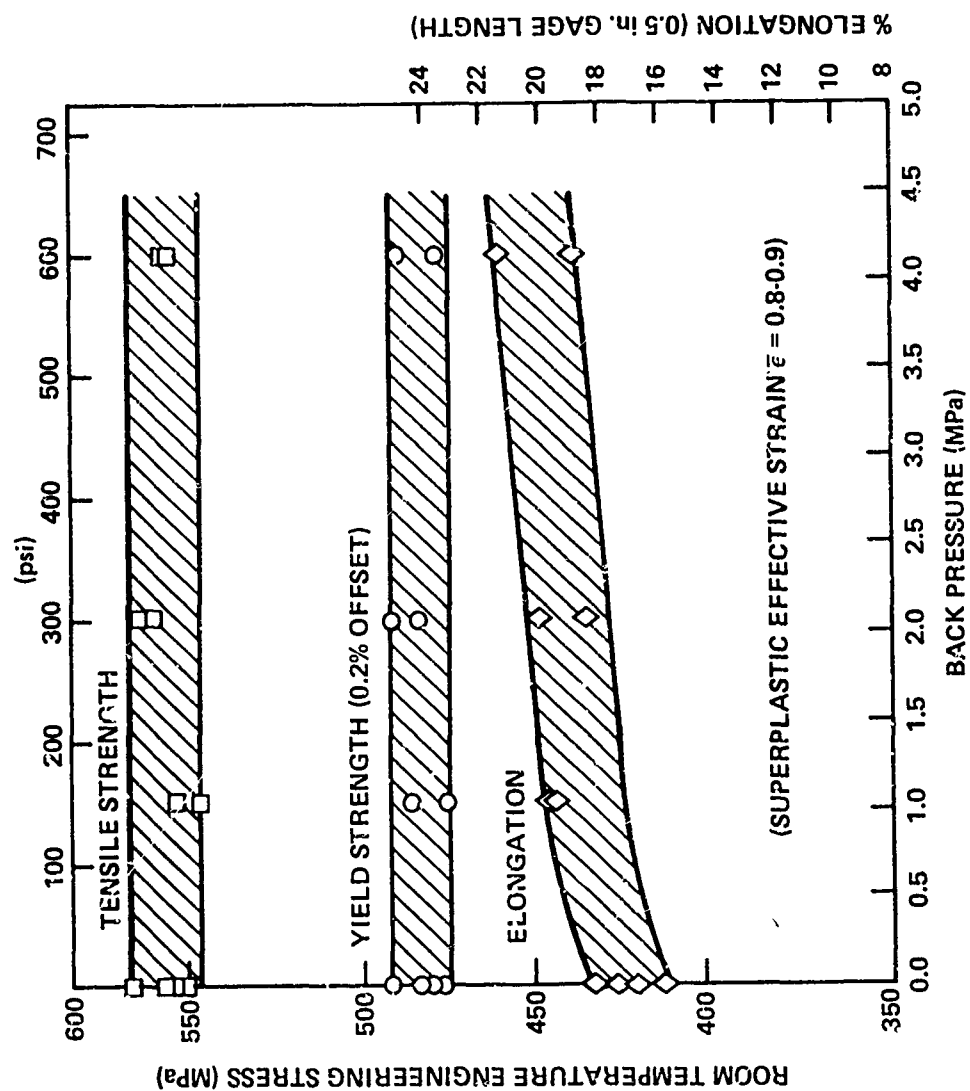
Fig. 17 Effect of superplastic plane strain deformation with confining pressures (T = 516°C, $\dot{\varepsilon}$ = 2 x 10⁻⁴S⁻¹) on the ambient temperature engineering tensile properties of fine grained 7475 Al (T6).
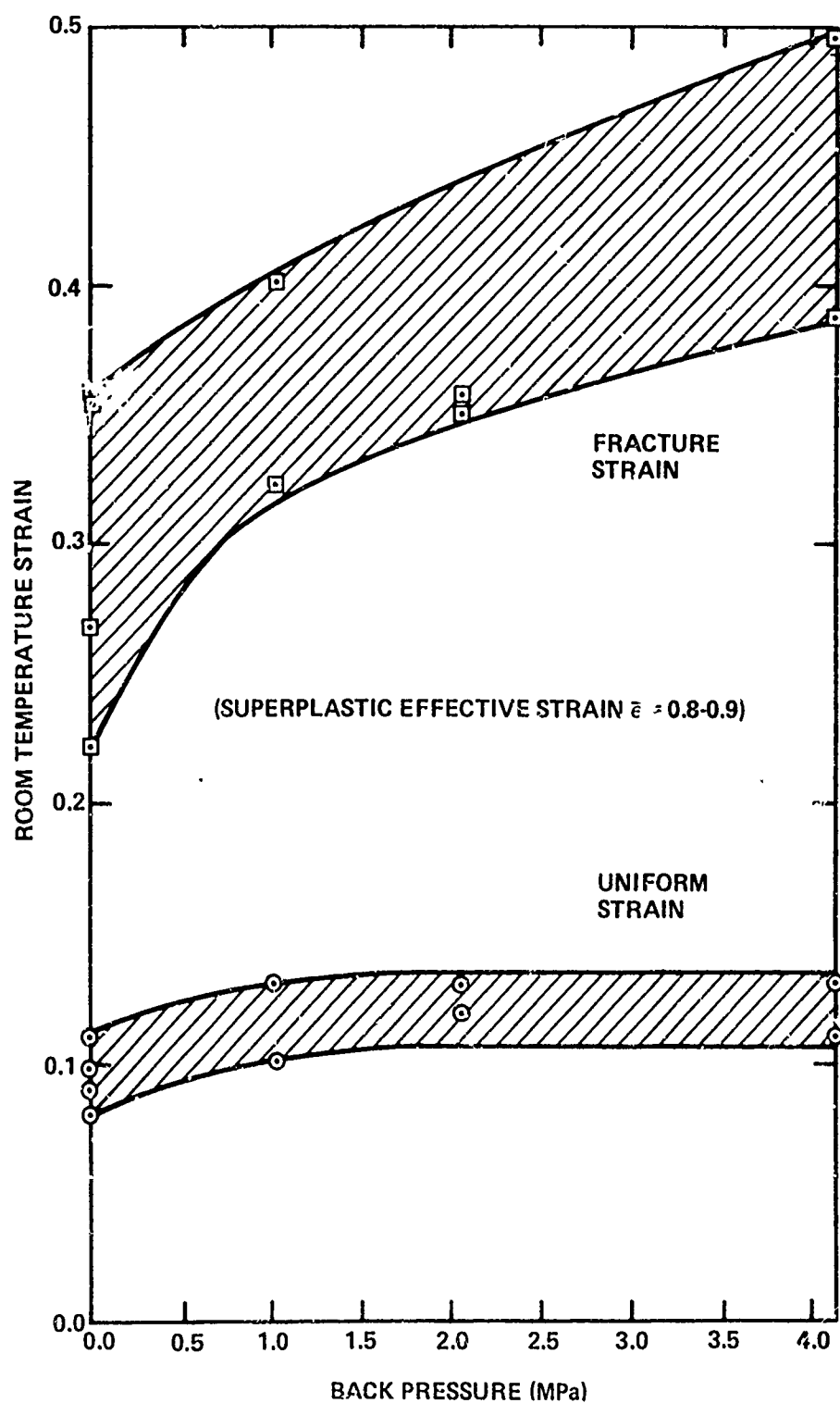
Fig. 18 Effect of superplastic plane strain deformation wi.h confining
pressures (T = 516°C, $\dot{\epsilon}$ = 2 x 10⁻⁴S⁻¹) on the ambient tempera-
ture uniform and fracture tensile strains of fine grained
7475 Al (T6).   161
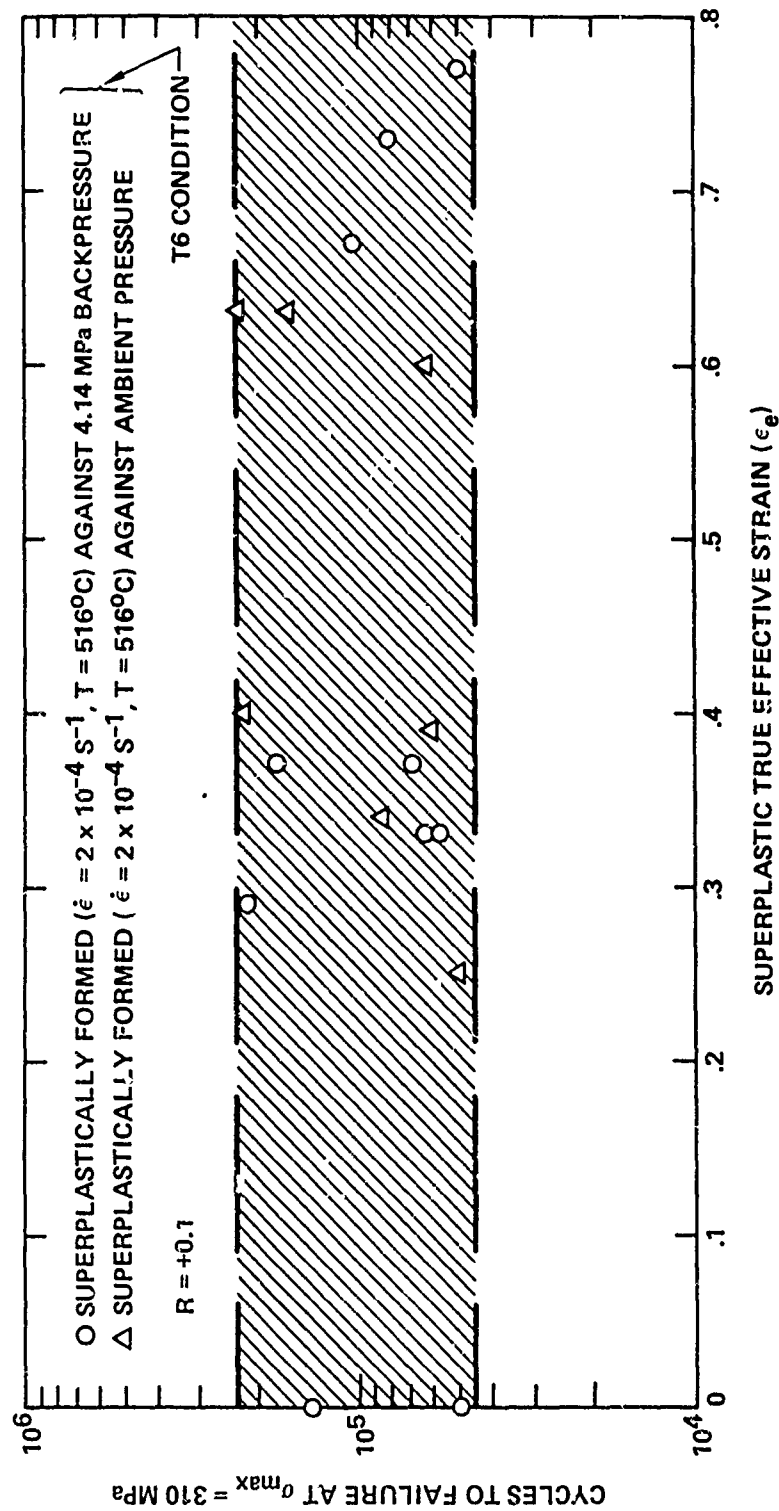
Fig. 19   Effect of superplastic strain deformation with confining pressures (T = 516°C, $\dot{\epsilon}$ = 2 x 10⁻⁴ S⁻¹) on the ambient temperature fatigue life of fine grained 7475 Al (T6).

162

noticeable effect on fatigue life, as is shown in Fig. 19. It would be necessary to devise a method of forming large, flat areas of sheet, with confining pressures, to strains in excess of about 1.0 in order to demonstrate the effect on fatigue life. Although it is possible to achieve very high strains with confining pressures in the uniaxial tensile apparatus, described earlier, Section 4.3.1, the samples are not large enough to provide room temperature tensile or fatigue specimens.

5.5 CONCLUSIONS

1. The application of confining gas pressures (compressive hydrostatic pressure) during superplastic deformation of fine grained 7475 Al may reduce, or entirely prevent, the intergranular cavitation encountered at ambient pressure. This effect is similar in all three of the main forming strain states (uniaxial, equibiaxial and plane strain) when related to equivalent true strain.

2. Superplastic flow characteristics (flow stresses and m values) are not affected by confining pressure. Flow stresses within the normal superplastic forming range, show essentially linear relationships with effective strains.

3. At the optimum superplastic deformation conditions, cavitation may be prevented almost entirely if $p/\sigma_e > 0.6$, where p is the confining pressure and σ_e is the maximum flow stress reached during the forming cycle. The critical value for p/σ_e to prevent cavitation does not change appreciably if the forming temperature is lowered by some 25°C, but increasing the strain rate by a factor of 5 reduces the critical ratio to $p/\sigma_e > 0.3$. In practice, however, significantly higher confining pressures are required to completely prevent cavitation at higher strain rates due to the much higher flow stresses.

165.

4.   At optimum superplastic deformation conditions, and at lower temper-
       atures, the superplastic ductilities and local fracture strains are
       improved by the application of confining pressures. This is a result
       of the corresponding decreases in cavitation, which plays a contribu-
       tory role in ultimate failure. Although the failure modes in these
       forming conditions are essentially intergranular, even in the absence
       of coarse cavitation, they have significantly ductile characteris-
       tics, especially at lower temperatures.

5.   At faster superplastic strain rates, the ductility and local fracture
       strains are not significantly improved by the application of confin-
       ing pressures, even though cavitation may be virtually eliminated.
       It appears that some form of catastrophic grain boundary embrittling
       mechanism dominates tensile failure at the faster strain rates.

6.   The detrimental effects of superplastic cavitation on service tensile
       properties may be eliminated by the use of suitable confining
       pressures during superplastic forming.

5.6 ACKNOWLEDGEMENTS

5.7 REFERENCES

1. C. C. Bampton and J. W. Edington, "The Effect of Superplastic Deformation on Subsequent Service Properties of Fine Grained 7475 Al," this document.
2. U. S. Patent Application No. 150471, 1980, C. H. Hamilton, "Method for Superplastic Forming."

3. J. A. Wert, N. E. Paton, C. H. Hamilton and M. W. Mahoney, submitted to Met. Trans. A., 1980.

4. A. K. Ghosh and C. H. Hamilton, Proc. ASM Materials & Processing Congress, Chicago, Fall 1979.

5. M. W. Mahoney, C. H. Hamilton and A. K. Ghosh "Forming Limits for Superplastic Formed Fine Grain 7475 Al," this document.

6. C. H. Hamilton, Science Center report for U.S. Army Armament Research and Development Command, No. ARSCOD-CR-8001, February 1980.

7. C. C. Bampton, unpublished research.

8. C. C. Bampton and J. W. Edington, "A Microstructural Study of Cavities Formed During Superplastic Deformation of Fine Grained 7475 Al," this document.

SECTION 6 THE EFFECT OF SUPERPLASTIC DEFORMATION ON SUBSEQUENT SERVICE PROPERTIES OF FINE GRAINED 7475 Al

C. C. Bampton and J. W. Edington

Rockwell International Science Center
Thousand Oaks, Ca 91360

and

University of Delaware
Newark, DE 91711

ABSTRACT

A preliminary investigation has been carried out to quantify the effects of superplastic deformation on the major ambient temperature service properties. It is shown that the properties most degraded, by the development of cavitation after large superplastic strains, are those that depend on the tensile overload stress (fracture stress). This affects, to varying extents, ductility, tensile strength, fatigue life and stress corrosion life. The effects are not, however, generally significant below superplastic effective strains of about 0.8 to 0.9 (120-150% elongation) with the optimum forming conditions ($T = 516°C$, $\dot{\varepsilon} = 2 \times 10^{-4}$ s^{-1}). Furthermore, since the fine grain processing has an initial beneficial effect on the ductility related properties compared to conventionally processed sheet, most superplastically formed components would suffer very little, if any, design penalties.

6.1 INTRODUCTION

The development of the Rockwell grain refining process (1) has enabled successful superplastic forming of complex structures in the high strength 7475 Al alloy. Significant cost and performance advantages may be gained by utilization of superplastically formed sheet aluminum components in aerospace structures. Since many of the potential uses involve load bearing structural components, the effects of superplastic deformation on the material's basic service properties must be fully characterized.

The major microstructural change which may occur during superplastic deformation of fine grained 7475 Al is development of intergranular cavities. This work is a preliminary investigation to quantify the effects of superplastic deformation and the associated cavitation on the major service properties (ambient temperature tensile, fatigue and stress corrosion) of fully heat treated (T6) 7475 Al.

An earlier study (2) investigated the influence of the fine grain processing (1) on the service properties of commercial 7075 Al type alloys. It was concluded that T6 tensile and fatigue properties are not appreciably affected by grain refinement typical of the Superaluminum process. Exfoliation corrosion is greatly reduced by grain refinement and stress corrosion crack propogation rates are slightly more rapid in the grain refined material.

The aim of this work was to provide preliminary data that would contribute to the determination of basic superplastic forming design

175

allowables for fine grained 7475 Al sheet as discussed elsewhere in this document (3). An alternative approach is to control the cavitation by means of confining gas pressures (4) so that the superplastic forming strain does not have to be included in the design allowables. Preliminary data have been obtained on the additional effect of simultaneously applied confining pressures during superplastic forming on the subsequent ambient temperature T6 tensile and fatigue properties and are reported elsewhere in this document (5).

6.2 MATERIALS

This work involved only 7475 Al. The compositional limits are shown in Table 1. The majority of the testing involved a single lot of sheet that was processed to hot rolled plate, 20 mm thick, by ALCOA Laboratories, followed by fine grain processing (1) at the Science Center. The tests to investigate the effects of confining pressures involved a second lot of sheet that was processed to warm rolled sheet, 2.5 mm thick, by ALCOA Laboratories, with the fine grain processing completed at the Science Center. The final grain sizes were ~ 14 μm diameter in the rolling plane and ~ 8 μm in the short transverse direction.

Table 1
Compositional Limits for 7475 Aluminum (wt %)

Si	Fe	Cu	Mn	Mg	Cr
0.10max	0.12max	1.2-1.9	0.06max	1.9-2.6	0.18-0.25

Zn	Ti	Others, each	Others, total	Al
5.2-6.2	0.06max	0.05max	0.15max	Remainder

6.3 EXPERIMENTAL

6.3.1 Superplastic Deformation

All superplastic deformation was carried out with the optimum forming conditions (6) ($\dot{\varepsilon}$ = 2 x 10^{-4} s^{-1}, T = 516°C), regarding total ductility and uniformity of thinning, since these are the conditions most likely to be used in commercial practice.

Uniaxial tensile straining was used for the majority of the testing material since this allowed very close control of sheet temperature and strain rate and also allowed relatively high superplastic strains to be achieved. Controlled strain rate blow forming into female dies was also used to provide testing material since this is the technique most likely to be used in commercial practice. Relatively large, flat areas of formed sheet are required for the service property test pieces, however, and the female die blow forming technique is limited to relatively low strains. Figure 1 shows typical uniaxial straining samples before and after superplastic deformation. The small ambient temperature tensile and fatigue specimens, which are cut from the superplastically strained samples, are also shown in Fig. 1. The gage lengths of the initial superplastic samples were dependent on the superplastic strain that was to be introduced so that the final sample dimensions (after interrupting the constant strain rate test at the appropriate time) provided the maximum amount of useful material. Superplastic strains were measured from the grids, as seen in Fig. 1.
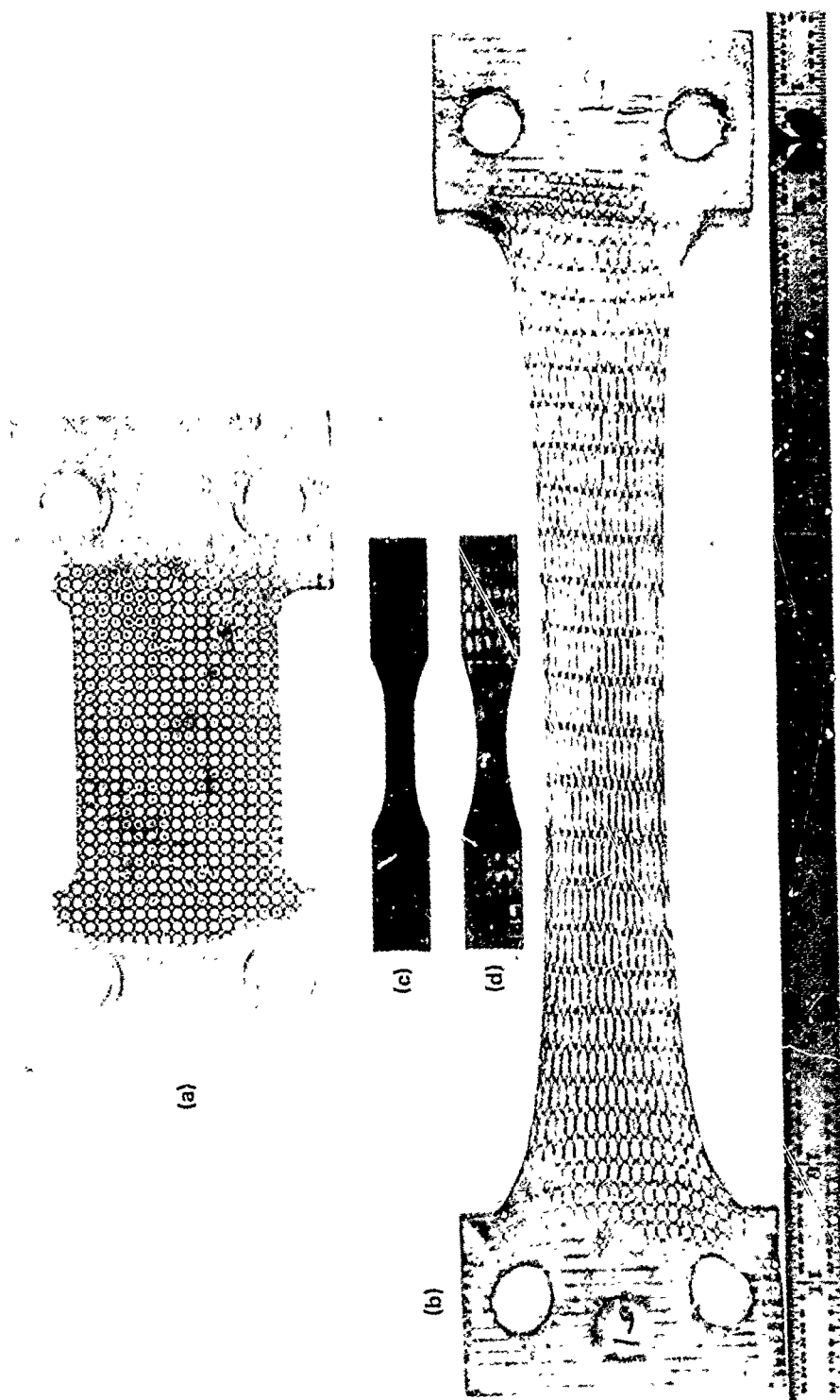
Fig. 1 Examples of the large superplastic uniaxial tensile specimens used to provide ambient temperature testing material. (a) As machined superplastic specimen, (b) superplastically strained sample, (c) ambient temperature tensile specimen, (d) ambient temperature fatigue specimen.

An example of a constant strain rate blow formed pan is shown in Fig. 2. This shows a rectangular pan, with high depth to width ratio that provides a relatively high plane strained region in the vertical walls. Ambient temperature specimens were cut from these pans as indicated in Fig. 2. Lower strained material was provided by similar blow formed pans which had a lower depth to width ratio. The pressure differential was controlled by calculated pressure/time profiles as described in Ref. 7 so that the critical regions of forming sheet are strained at the desired constant rate.

6.3.2 Ambient Temperature Tensile Testing

Figure 3a shows the specimen shape and dimensions used for all of the ambient temperature tensile testing. A non-standard specimen was designed which made economical use of the superplastically strained sheet. The specimen also has a sufficiently small gage length to avoid excessive changes in superplastic strain when cut from a sample which had an unavoidable thickness strain gradient.

The machined specimens were T6 heat treated by solution treating for one hour at 482°C in molten salt, water quenching to room temperature and aging for 24 hours at 121°C in oil

The specimens were tensile tested in air, at room temperature at a constant cross head speed of 0.5 mm/min. Yield stress (0.2% offset) was determined by means of an electrical extensometer connected to a servodriven
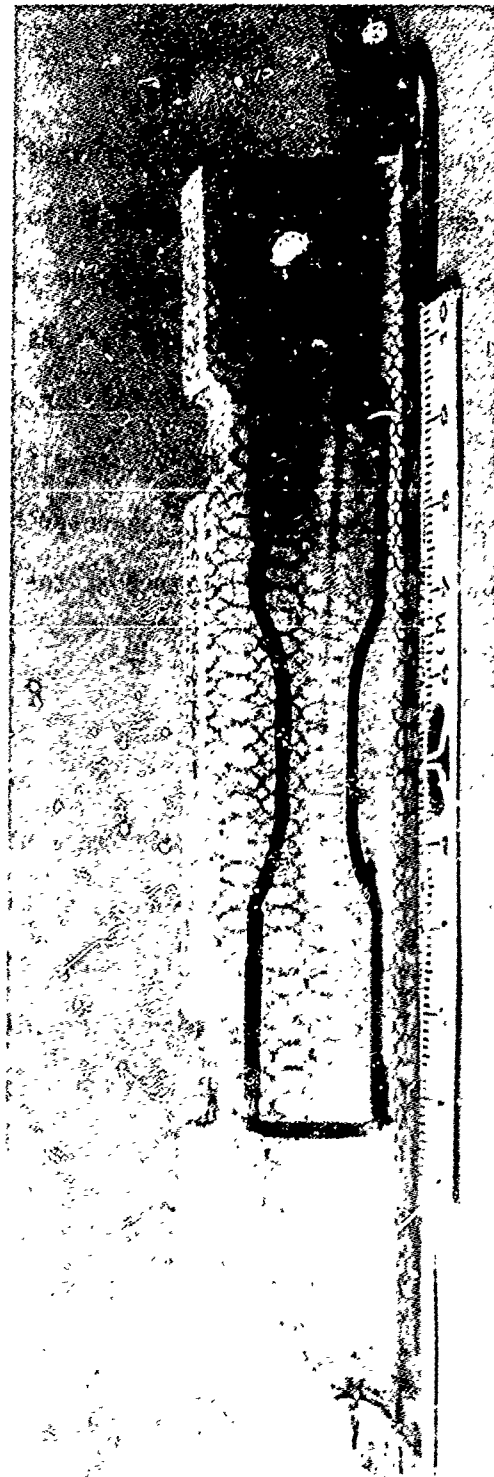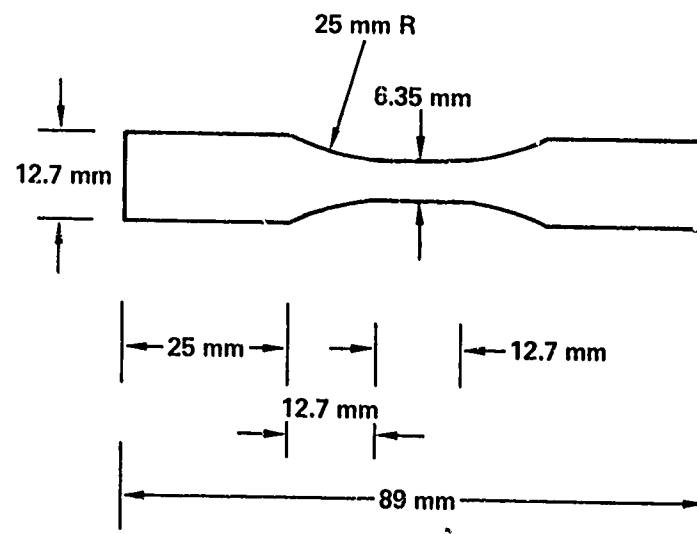
181

Fig. 2 An example of a superplastically blow formed rectangular pan from which ambient temperature tensile and fatigue specimens were cut, as indicated.

(a) AMBIENT TEMPERATURE TENSILE SPECIMEN

(b) AMBIENT TEMPERATURE FATIGUE SPECIMEN
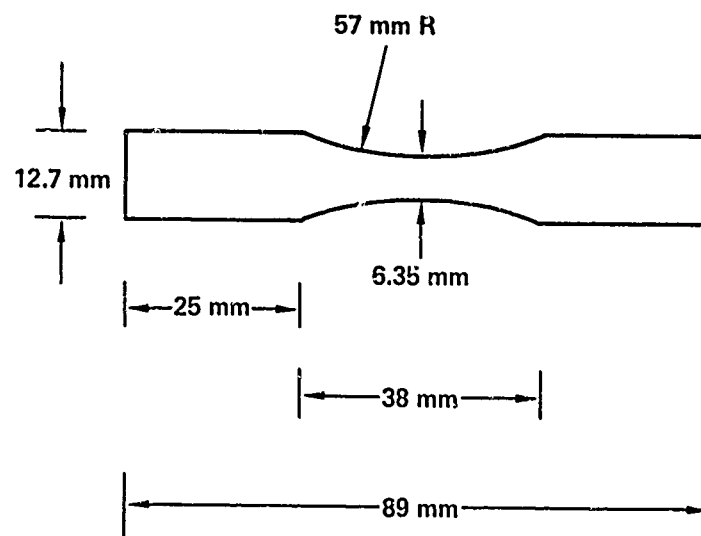
Fig. 3 Specimen dimensions.

chart recorder. Ultimate tensile strength and uniform strain were also
determined from the load/extension chart recording. Total elongation and
reduction of area at fracture were measured directly from the specimens using
a travelling microscope.

6.3.3 Ambient Temperature Fatigue Testing

Figure 3b shows the specimen shape and dimensions used for all of the
ambient temperature fatigue testing. The overall specimen dimensions were the
same as for the tensile specimens. An hour-glass shape was employed, hcwever,
rather than a parallel gage length, to induce fatigue failure in the specimen
centers rather than at the shoulder radii. It was also necessary to surface
grind the samples to 600 grade emery paper to remove the coarse surface
defects. TS treated 7000 series type alloys are notoriously sensitive in
tensile fatigue to notch-type surface stress raisers.

The fatigue tests were tension-tension cycled from a constant maximum
load to a constant minimum load, 0.1 of the maximum (R=+0.1). The number of
cycles to failure were counted and plotted against the maximum initial
stress. The tests were carried out in laboratory air at ambient temperature
at a frequency of 12.5 cycles/second.

184

6.3.4 Stress Corrosion Testing

The stress corrosion tests were conducted at the University of Delaware.

Small rectangular specimens 38 mm x 12.7 mm, were cut from the testing samples which had been T6 heat treated. The surfaces were ground to 600 grade emery paper. The specimens were sprung into small Teflon frames, as shown in Fig. 4 and these were periodically immersed, by moving racks, in 3.5% NaCl solution. The rack immersion cycles involved 10 minutes immersion followed by 50 minutes in air, all at ambient temperature. The Teflon frames were designed to promote bending stresses in the sheet samples of 75% yield stress in the outer fibers. A yield stress of 455 MPa was taken, so that the outer fiber stress was set at 340 MPa. The number of days to failure was recorded for each specimen.

The ASTM standards were not complied with in these tests (due to material limitations) in the following respects: (i) the specimens were too small, (ii) the specimen thicknesses varied, (iii) the specimens were not flat and (iv) the humidity and drying rate were not controlled. The tests thus provide a semi-quantitative assessment of the effect of superplastic strain on stress corrosion rate.

6.3.5 Measurement of Cavitation

When each of the ambient temperature test pieces was cut from the testing samples of sheet, a small sample, about 5 mm x 5 mm, was also cut from

185
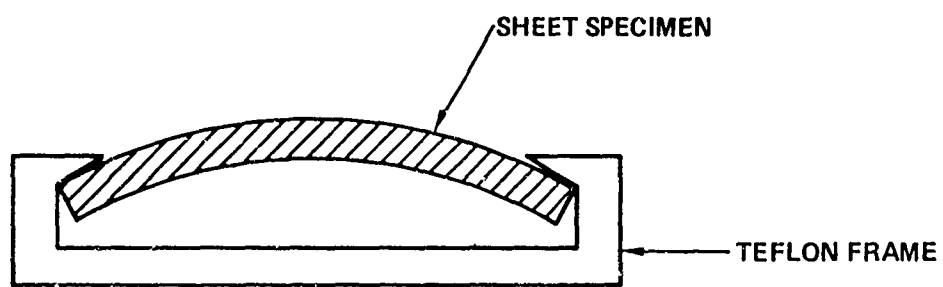
Fig. 4 Schematic drawing of the stress corrosion testing frames.

the sheet immediately adjacent to the test piece gage length. These pieces were retained for measurement of cavitation by density loss. The technique used was a variable density liquid flotation method which is more fully described elsewhere in this document (3). The heat treatment condition of the sheet was found to affect the measured density and an apparent material variablility of density was also found. The density of each cavitation sample was therefore measured in the solution treated and water quenched condition and compared with a standard non-cavitated sample in the same heat treated condition cut from the shoulder, or flange, (unstrained) of the superplastic formed sample.

187

6.4 RESULTS AND DISCUSSION

6.4.1   Ambient Temperature Tensile Properties

The engineering tensile data from material superplastically deformed in uniaxial tension is shown in Fig. 5. It can be seen that the yield strength is not greatly affected by superplastic strains up to at least 1.0 to 1.1. Tensile strength is similarly affected, although it tends to drop rather more rapidly than yield strength for superplastic strains above about 1.1. Ductility is most severely affected and appears to suffer a decline for superplastic strains greater than about 0.5 to 0.7. Figure 6 shows the corresponding data for material that has been superplastically deformed in plane strain. Here the highest superplastic strains achieveable with the dies used were lower than for the uniaxial tensile strained material. Again the yield and tensile strength show no significant deterioration up to superplastic strains of at least 1.0. The ductility, however, appears to drop slightly more rapidly in the superplastic plane strained material than in the superplastic uniaxial strained material.

The ductility results may be examined more closely by comparing the uniform strains and fracture strains. Figure 7 shows results for the superplastic uniaxial tensile case. Clearly the fracture strain, which includes a very large contribution from the final neck, is considerably more affected than the uniform elongation by the prior superplastic strain. The same can be seen to be true in Fig. 8, which shows the superplastic plane strain case, although there is more scatter in these results. Comparing these

189
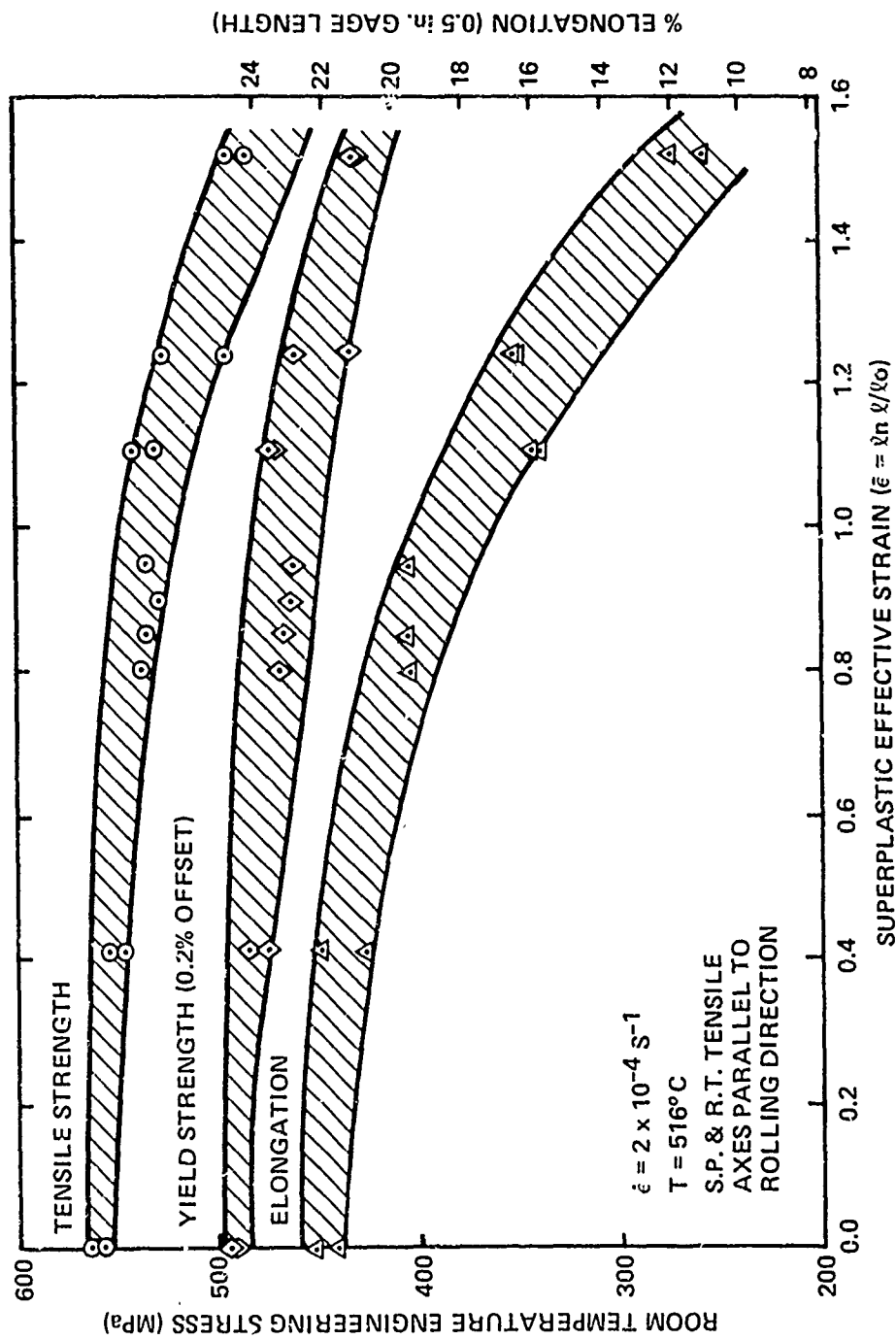
Fig. 5 Ambient temperature engineering tensile properties of fine grained 7475 Al (T6) after superplastic uniaxial tensile deformation.
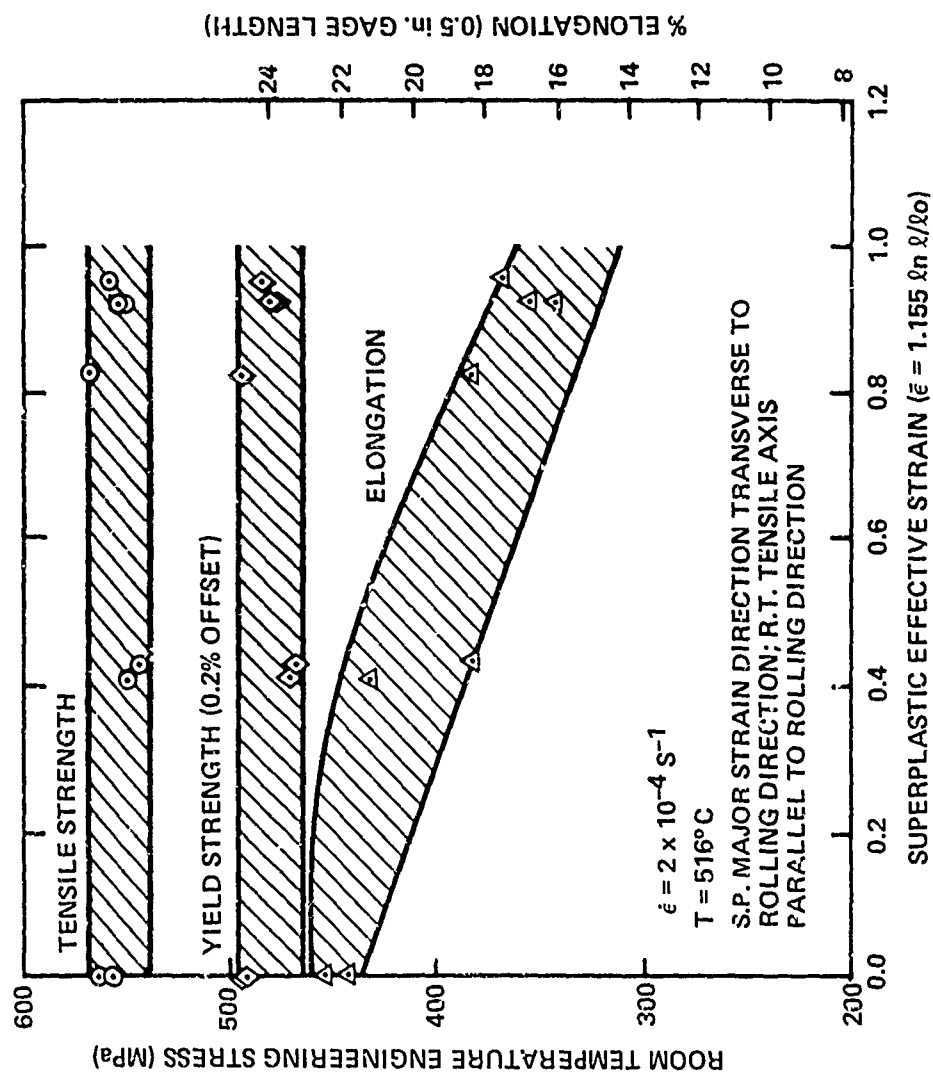
Fig. 6 Ambient temperature engineering tensile properties of fine grained 7475 Al (T6) after superplastic plane strain tensile deformation.

191

Fig. 7 Ambient temperature uniform and fracture tensile strains of fine grained 7475 Al (T6) after superplastic uniaxial tensile deformation (T = 516°C, $\dot{\varepsilon}$ = 2 x 10^{-4}S^{-1}).
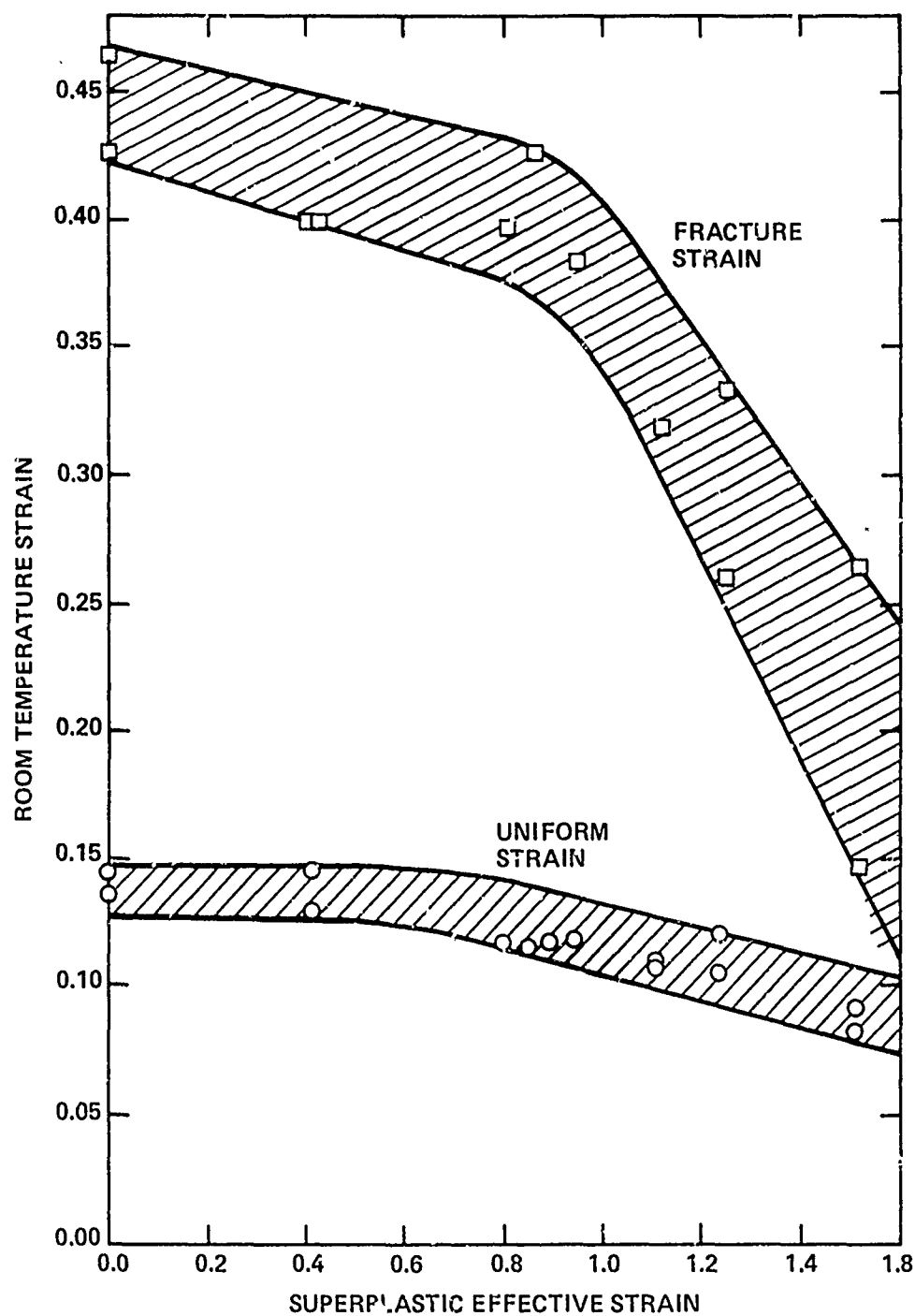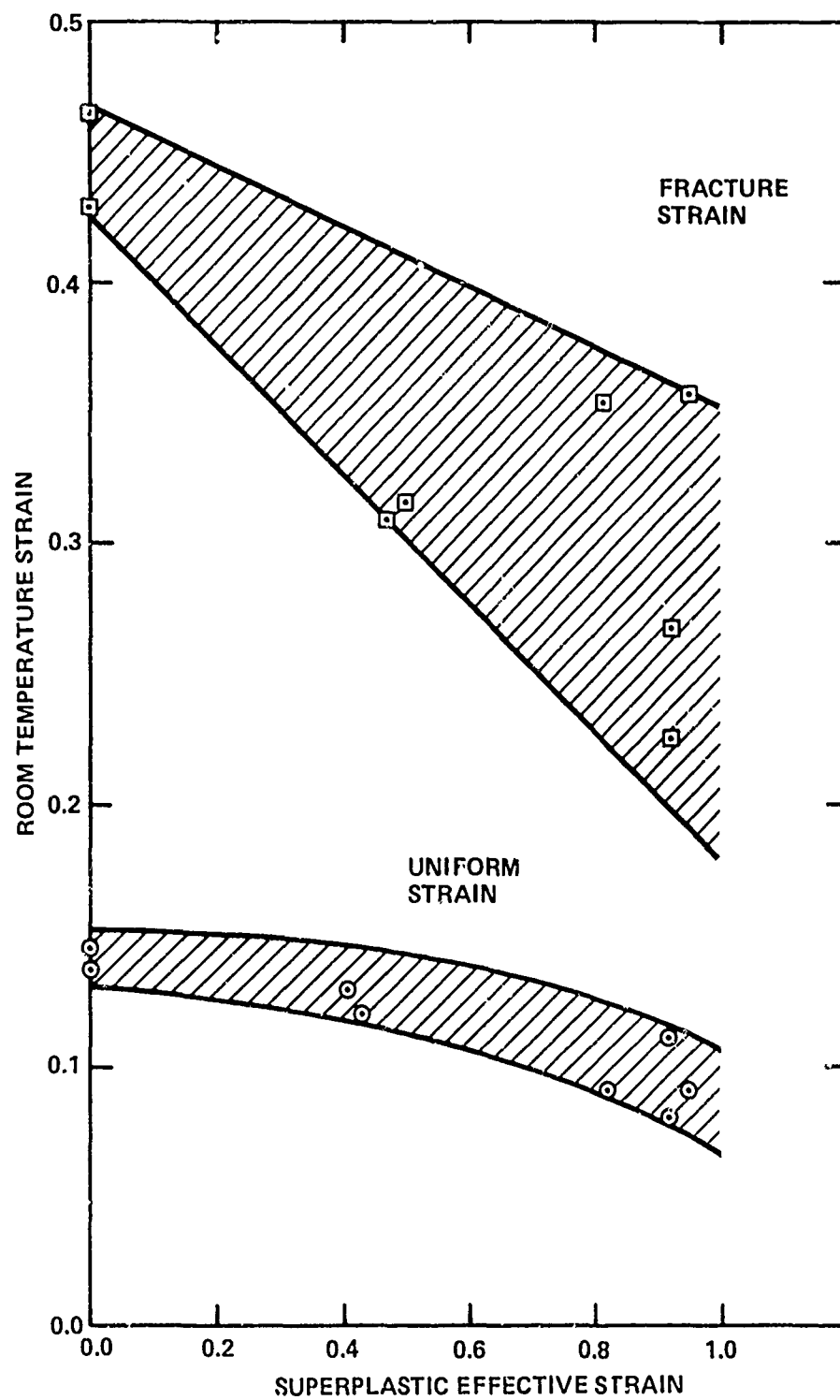
192

Fig. 8 Ambient temperature uniform and fracture tensile strains of fine grained 7475 Al (T6) after superplastic plane strain deformation (T = 516°C, $\dot{\varepsilon}$ = 2 x $10^{-4}S^{-1}$).

193

results with the measured cavitation from the superplastic uniaxial strained material shown in Fig. 9, there is a close qualitative correlation with the observed degradation of T6 tensile properties.

As would be expected, cavity development has the smallest effect on flow stress in the uniform elongation region, although the cavities do act as local stress raisers giving a small overall drop in flow stress with increasing cavitation. This same effect tends to initiate local necking at lower strains (i.e lower uniform strain) with increasing cavitation since the work hardening rates are effectively decreased with increasing cavitation. These two effects both tend to lower the tensile strength, as observed. The major effect of the cavitation, however, is on the final local necking and fracture. Scanning electron microscopy, such as shown in Figure 10, has shown that the fractures are essentially transgranular-ductile, even in specimens with the highest superplastic cavitation. The large intergranular superplastic cavities show no obvious tendency to enlarge and coalesce with each other by grain boundary cracking. It may be proposed that the local stress fields associated with large superplastic cavities develop much larger transverse components when the tensile specimens start to neck and the applied stress becomes increasingly triaxial. Thus the local stress fields of adjacent superplastic cavities may interact in the transverse direction, especially as the specimen cross section is reduced. The ligaments between superplastic cavities may then encounter additional transverse stresses, due to the presence of the superplastic cavities thus enhancing ductile hole

194
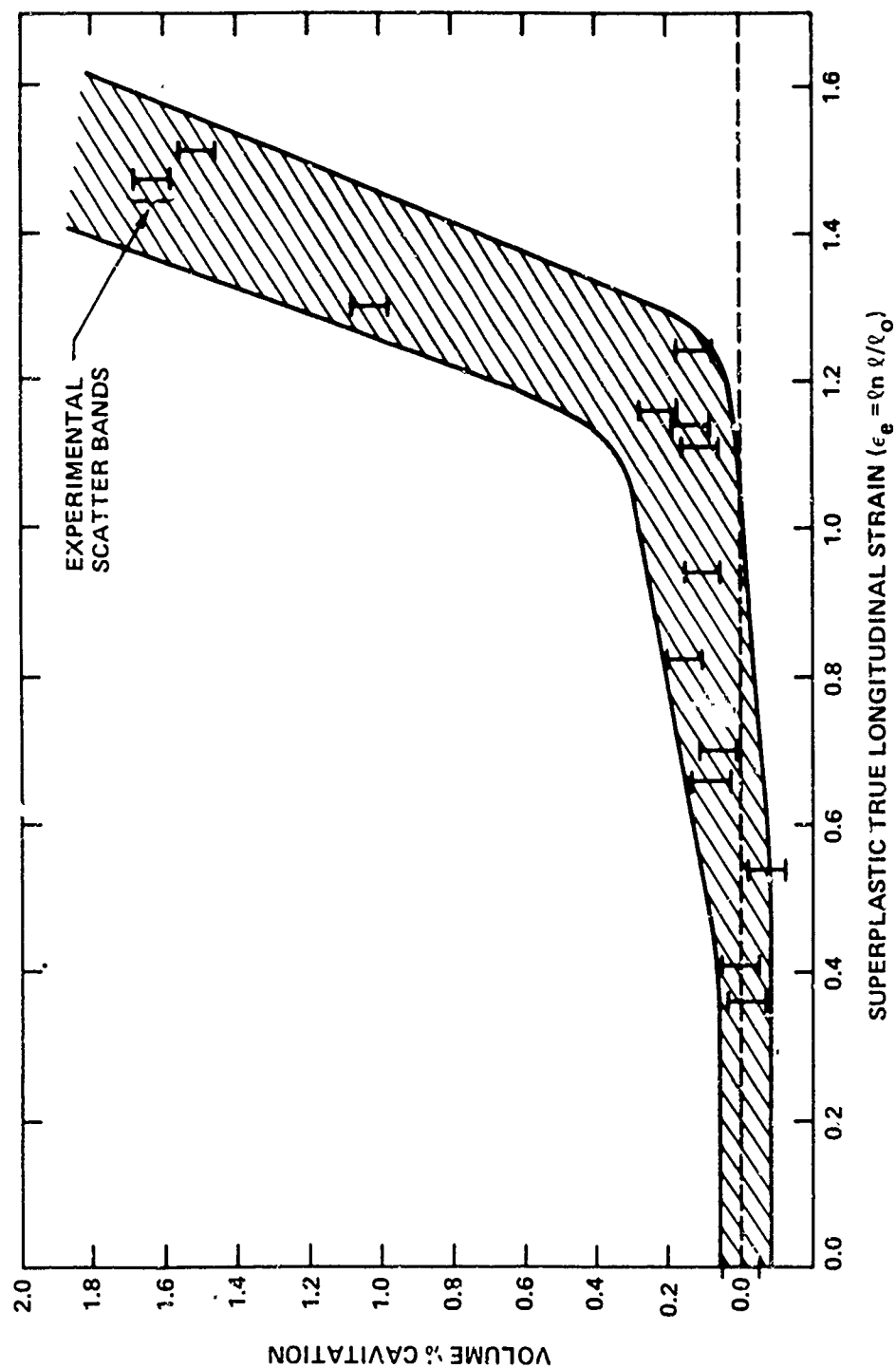
Fig. 9 Development of cavitation with superplastic uniaxial tensile deformation ($T = 516°C$, $\dot{\epsilon} = 2 \times 10^{-4}S^{-1}$) in the samples used for ambient temperature service property measurements.

Fig. 10 Scanning electron micrographs of T6 treated ambient temperature
tensile fracture surfaces. (a) Zero superplastic strain, (b)
superplastic strain, $\varepsilon_e = 1.49$ (T = $516°C$, $\dot{\varepsilon}$ = 2 x $10^{-4}S^{-1}$).

196

growth (at second phase particles and inclusions) and coalesence leading to failure by void sheeting.

The observation that ductility was more adversly affected by the superplastic plane strain deformation than superplastic uniaxial deformation may be due, at least in part, to the different directions of the major super-plastic strains in each case relative to the original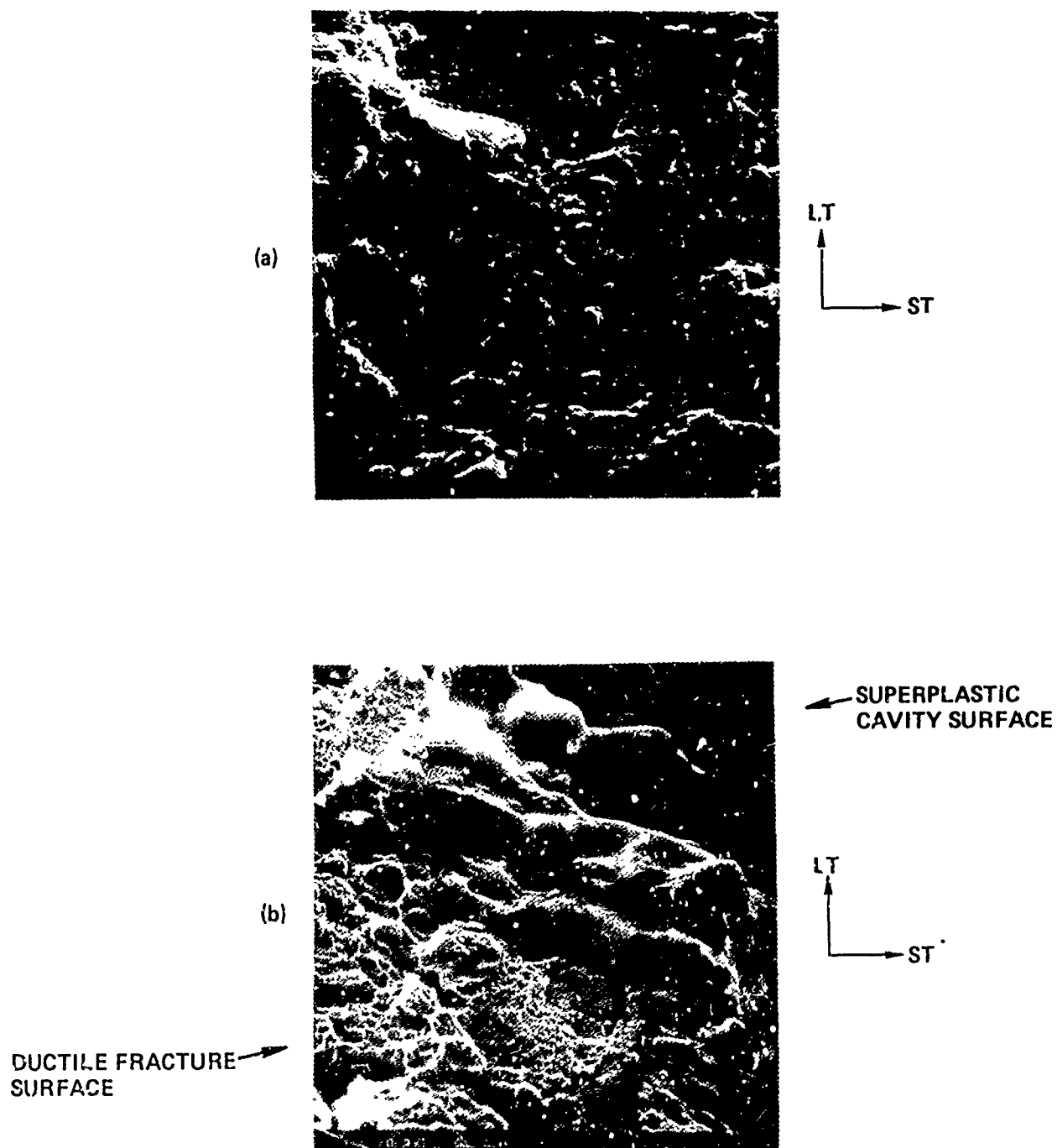 sheet rolling direction. All tensile testing directions at ambient temperature were parallel to the rolling direction. The major stain direction in the superplastic uniaxial case was, however, parallel to the rolling direction while the directions were transverse to each other in the superplastic plane strain case. Recent work (8) has shown that the rate of cavitation is generally greater in superplastic samples uniaxially strained transverse to the rolling direction than in those strained parallel to the rolling direction. The reasons for this anisotropy are not clear although they may be associated with a tendency for enhanced dynamic grain growth in the rolling direction and/or the alignment of inclusion particles with respect to the rolling direction. In any case, the anisotropy of cavitation rate, with respect to the relative orientations of major superplastic straining direction and rolling direction is directly reflected in the subsequent ambient temperature mechanical properties.

6.4.2   Ambient Temperature Fatigue Properties

The basic S-N curve of the fine grained T6 7475 Al is shown in Fig. 11. This compares well with the published data for conventionally processed commercial material (9). The superplastically strained material was
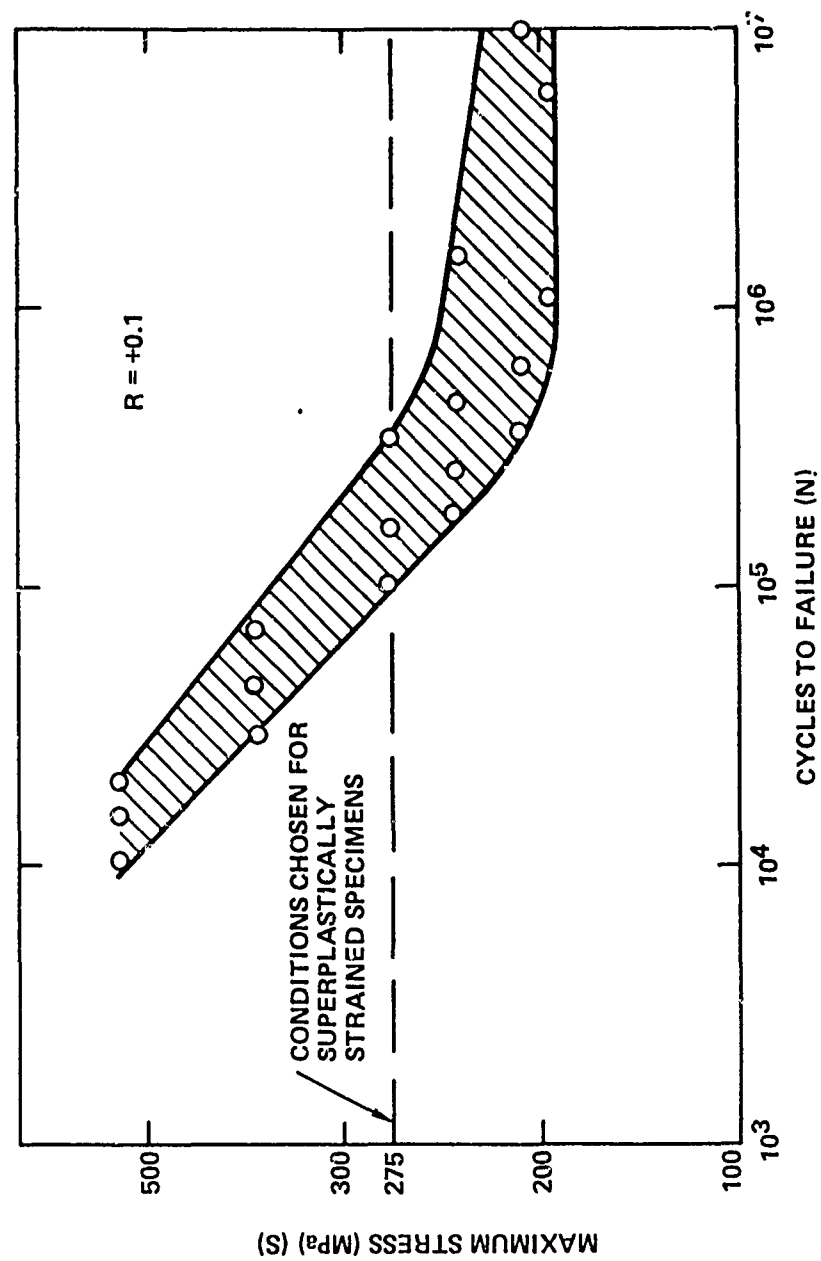
197

Fig. 11 Basic S-N fatigue curve for fine grained 7475 Al (T6) sheet.
Constant maximum load, tension-tension cycles.

198

fatigue tested all at the single maximum stress of 275 MPa (shown in Fig. 11).
The results are shown in Fig. 12. The fatigue lives decrease with increasing
superplastic strains above about 0.7 to 0.8. This corresponds closely with
the tensile ductility, especially the fracture strain. Although it is not
shown here, it was found that small superplastic strains actually improved
fatigue lives of specimens with as rolled surfaces. All data shown here is
from specimens surface ground to 600 grade emery. The grain boundary sliding
during superplastic deformation appears to effectively remove many of the
surface defects produced during rolling which may initiate fatigue cracks.

Examination of the fracture surfaces allowed the relative proportions
of fatigue to ductile failure areas to be measured. This is shown in Fig. 13.
The fatigued portions of the fracture areas clearly decrease with superplastic
strains in qualitatively the same way that fatigue lives decrease with super-
plastic strain. This suggests that the reduction of fatigue life with super-
plastic strain is due mainly to the same effects proposed to explain the
reduction of fracture strain, i.e. the local stress raising effects of large
superplastic cavities lead to early void sheeting-ductile failure, especially
in the presence of triaxial stresses. SEM examination has shown that super-
plastic cavities exposed at the machined specimen edges are generally the
initiating sites for the fatigue cracks in specimens with fairly large super-
plastic strains. This can be seen in Fig. 14. It seems, however, that in-
creases in fatigue crack initiation rate and growth rate are not as signifi-
cant, as regards the overall fatigue life, as is the reduction in tensile
fracture stress due to superplastic cavitation.

199

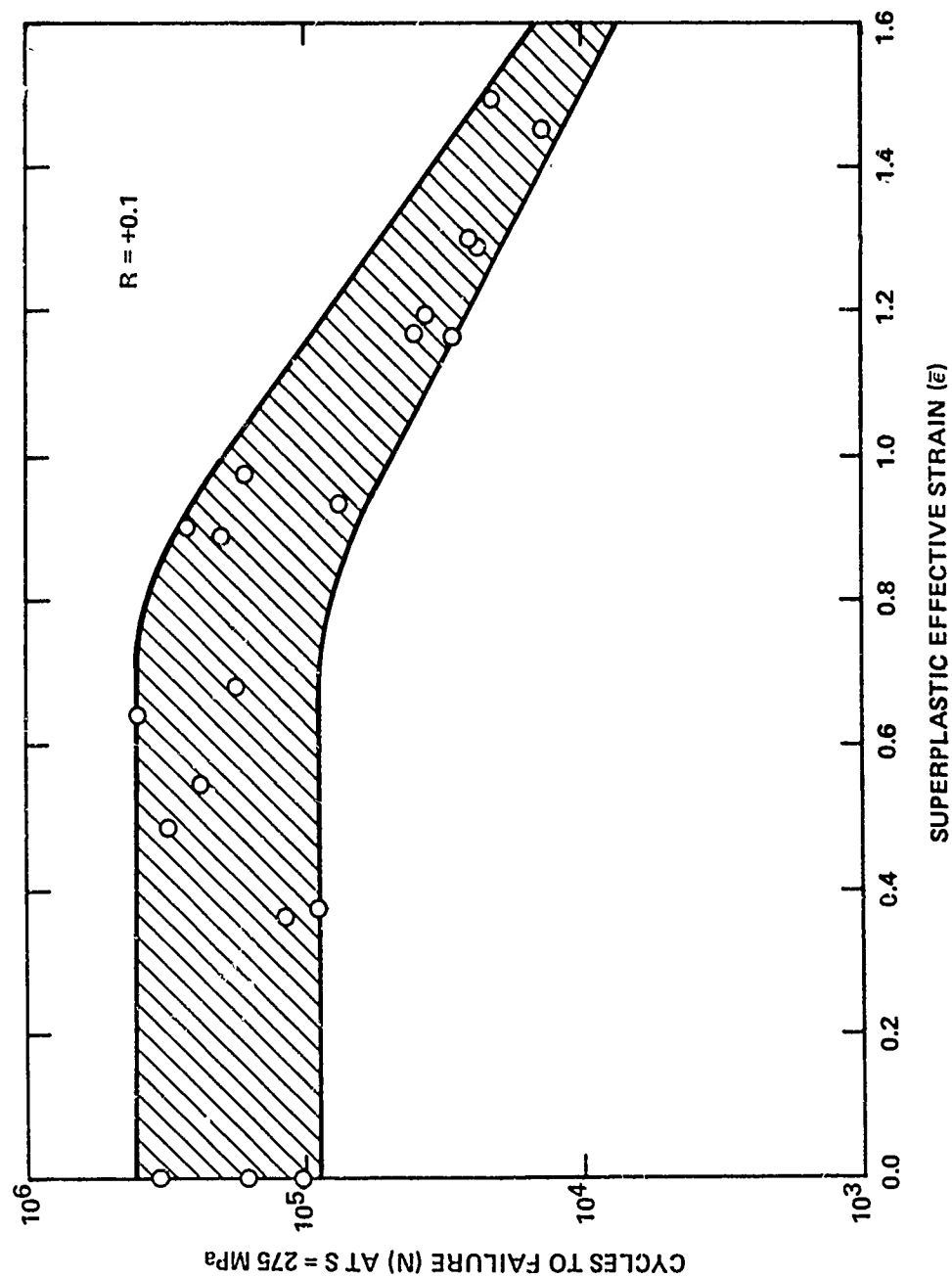Fig. 12 Effect of superplastic uniaxial tensile deformation ($T = 516°C$, $\dot{\epsilon} = 2 \times 10^{-4} S^{-1}$) on the fatigue life of fine grained 7475 Al (T6).
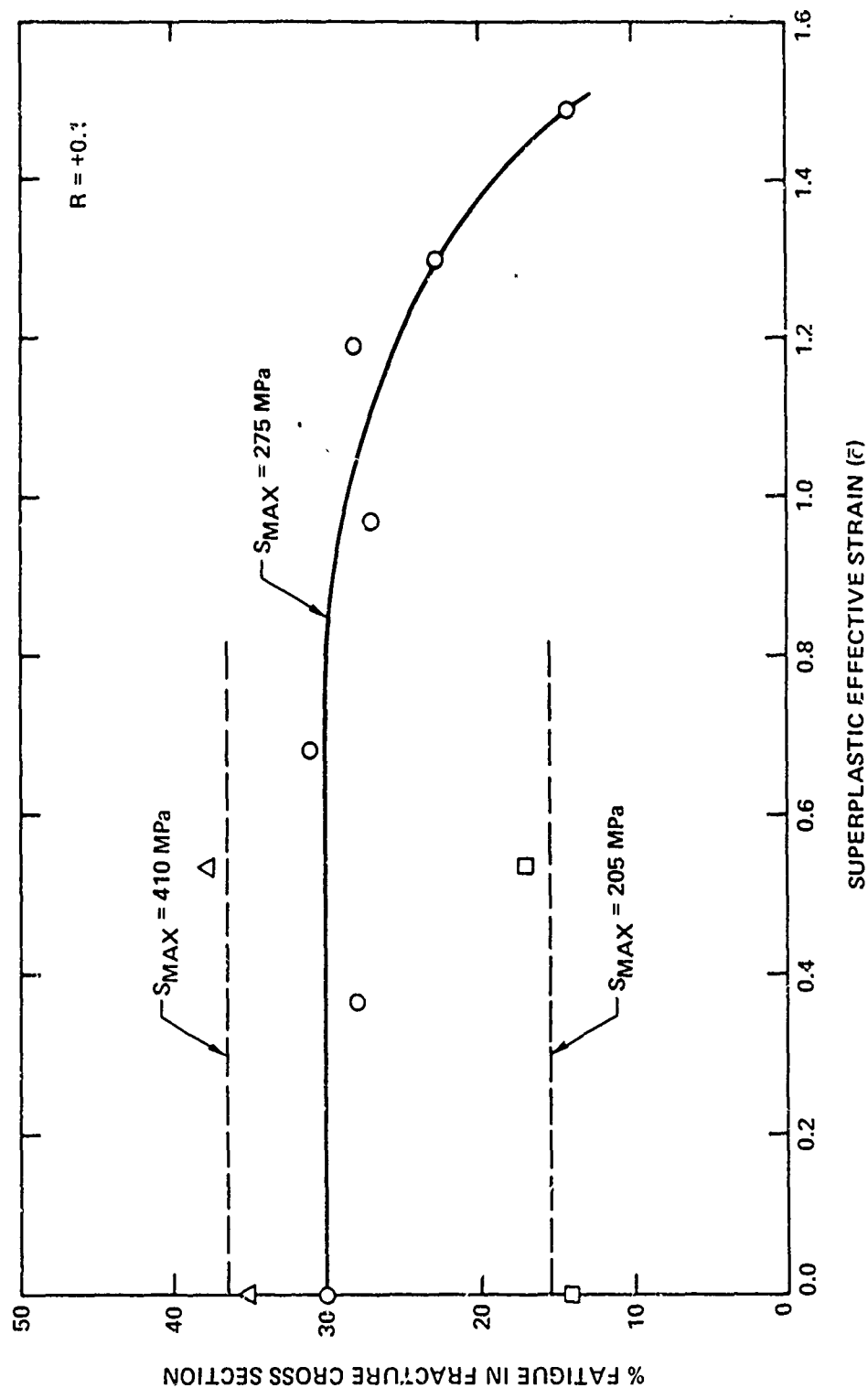
Fig. 13 Effect of superplastic uniaxial tensile deformation (T = 516°C, ε̇ = 2 x 10⁻⁴S⁻¹) on the ratio of fatigue crack area to tensile overload area in the fracture surfaces of ambient temperature fatigue specimens (c.f. Fig. 12).

Fig. 14 Scanning electron micrographs of a fatigue crack surface
showing the initiation at a superplastic cavity exposed
at the machined specimen edge (arrowed). ε_e = 1.16, S_{MAX} = 275 MPa.

6.4.3 Stress Corrosion Properties

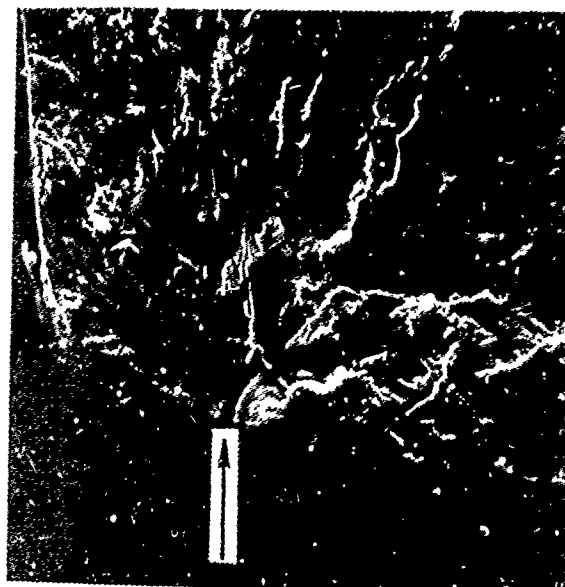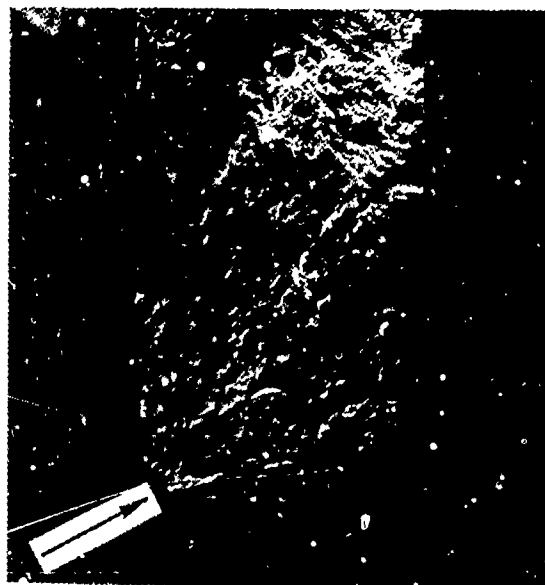Table 2 summarizes the stress corrosion results. The tests were not extended longer than 90 days since the ASTM standard uses this as the basic minimum life for good stress corrosion resistance in 7000 series aluminum alloys. The lifetimes shown in Table 2 provide a preliminary indication of the effect of superplastic strain. It appears that superplastic strain up to at least 1.3 does not have a significant effect on the stress corrosion life. Also, these tests did not show a significant difference in stress corrosion behaviors between the unstrained coarse and fine grained material. Clearly a larger number of tests would need to be conducted in order to provide sufficient data for a statistically reliable evaluation of the effect of superplastic strain on stress corrosion properties.

Table 2

Table 2

Stress Corrosion Results

Test Material Treatments	Grain Diameter at Sheet Center (μm)		Sheet Thickness (mm)	No. of Specimens Tested	Lifetimes (days) for Specimens failing <90 Days
	L&LT	ST			
As processed to fine grain size (1) + 1 hour at 516°C + T6 heat treatment	14.5	7.7	2.0	26	75,75,65,52,45,41,40 (19 survived)
"	11.1	6.0	1.0	16	70,53,50,41, (12 survived)
" + slow heat-up to recrystallization temperature	40	12	1.0	8	68,64 (6 survived)
As processed to fine grain size + superplastic uniaxial strain: $\varepsilon = 0.96$ $\dot{\varepsilon} = 2 \times 10^{-4}\ s^{-1}$ $T = 516°C$ +T6 heat treatment	19.5	8.8	1.0	2	69 (1 survived)
" $\varepsilon = 1.28$	20.4	9.2	1.0	2	--- (2 survived)

6.5 CONCLUSIONS

The service properties of fine grained 7475 Al may be degraded by the development of intergranular cavitation during superplastic deformation. These effects are not, however, generally significant below superplastic effective strains of about 0.8 to 0.9, with the usual forming conditions ($\dot{\varepsilon}$ = 2 x 10^{-4} s^{-1}, T=516°C).

The properties most affected by the development of cavitation, especially after superplastic strains greater than about 1.0, are those that depend on the tensile overload stress (fracture stress). The presence of high concentrations of large intergranular cavities, effectively embrittles the material in circumstances when the local stress concentration effects of the cavities become significant.

Cavitation, even after high superplastic strains, reduces tensile flow stresses only slightly but reduces localized necking strain more significantly. Thus elongations at failure may be reduced to the level of uniform elongation, which is about 10% after superplastic effective strains of 1.6. Reduction of fatigue lives by cavitation shows a strong relationship with tensile elongation. This is because cavitation induces earlier fatigue failure through a reduction in the tensile overload stress rather than by any significant increases in fatigue crack initiation or propagation rates. Superplastic cavitation does not significantly influence stress corrosion resistance of 7475-T6 except by virtue of its effect on the basic tensile properties.

The microstructural study of cavity initiation sites, described elsewhere in this document (10) has suggested that the cavitation rate at ambient pressure may be significantly reduced by appropriate prior treatments. If it is not found to be practically feasible, or desirable, to totally remove the tendency to form cavities by material processing techniques, then the cavitation rates may at least be reduced to consistent, predictable levels. The "forming limit" approach, discussed elsewhere in this document (3), may then be used as an alternative to cavitation control at the forming stage, such as by the confining pressure technique (5).

6.6 ACKNOWLEDGEMENTS

6.7 REFERENCES

1. J. A. Wert, N. E. Paton, C. H. Hamilton and M. W. Mahoney, Submitted to Met. Trans. A, 1980.

2. J. A. Wert, N. E. Paton and J. C. Chesnutt, Science Center report for AFOSR, No. SC5053.6FR, 1980.

3. M. W. Mahoney, C. H. Hamilton and A. K. Ghosh, "Forming Limits for Superplastic Formed Fine Grain 7475 Al," this document.

4. C. H. Hamilton, Patent Application No. 150471, 1980.

5. C. C. Bampton, M. W. Mahoney, C. H. Hamilton, A. K. Ghosh and R. Raj, "Suppression of Cavitation by the Application of Confining Gas Pressure During Superplastic Deformation of Fine Grained 7475 Al," this document.

6. C. H. Hamilton, Science Center report for U.S. Army Armament Research and Development Command, No. ARSCD-CR-8001, February 1980.

7. A. K. Ghosh and C. H. Hamilton, Proc. ASM Materials and Processing Congress, Chicago, 1979.

8. C. C. Bampton, Unpublished research.

9. P. L. Mehr, "ALCOA 7475 Sheet and Plate," ALCOA Green Letter, 1978.

10. C. C. Bampton and J. W. Edington, "A Microstructural Study of Cavities Formed During Superplastic Deformation of Fine Grained 7475 Al," this document.